Investigating the kinetic stability and transformation of vapor-deposited glasses with AC nanocalorimetry experiments

By

Michael Tod Tylinski

A dissertation submitted in partial fulfillment of

the requirements for the degree of

Doctor of Philosophy

(Chemistry)

at the

UNIVERSITY OF WISCONSIN-MADISON

2017

Date of final oral examination: 12/21/2016

The dissertation is approved by the following members of the Final Oral Committee

Mark D. Ediger, Professor, Chemistry

Gilbert Nathanson, Professor, Chemistry

Lian Yu, Professor, Pharmaceutical Sciences

James Skinner, Professor, Chemistry

Max Lagally, Professor, Materials Science and Engineering

Acknowledgements

I will start by thanking my parents Elaine and Randy for their constant love and encouragement throughout my life. Mom and Dad, I cannot overemphasize how important your support has been to me. To my brothers Tyler, Austin and Cody, thank you guys for always being a source of laughter, love, and enthusiasm in my life.

There are several teachers who are very important to me as learner and a scientist; their lessons still influence me today and will continue to do so for the rest of my career. At Napeville North High School, Mrs. Beverly George's chemistry classes built my self-efficacy through her high expectations and high belief in her students. Mr. Jim Effinger was the first to teach me that science is not a collection of facts, but a process of continually testing, improving and expanding our understanding of the world around us. About 12 years ago he told my classmates and I that the only fact we'd remember from his biology class was that his wife's name is Rose. He was right, and yet I still learned so much in his classes.

My time as an undergraduate student at Grinnell College is very important to me. My classmates, my professors, my coaches, and the staff all contributed to an incredibly supportive and creative learning environment. Professors Leslie Lyons, Andy Mobley and Elaine Marzluff, thank you for being encouraging mentors, advisors and instructors. My time learning and growing with your guidance has inspired me to pursue a career of teaching in academia. I want to thank Minna Mahlab who directs mentoring program through the Grinnell Science Learning Program. As a science mentor, I had hands on experience practicing and growing as a teacher of my peers. And also, thank you Professor Paul Hutchinson, your education courses are the inspiration for my continued learning about teaching philosophy and methodology.

Turning to my Ediger groupmates, Ben Bending, thank you for welcoming me to UW, and to the Ediger Group. Shakeel Dalal, thank you for your friendship, encouragement, and advice. You helped me grow a lot in my first few years. Ankit Gujral, Diane Walters, Josh Ricci, Kelly Suralik, Jing Jiang, Kelly Hebert, Yue Qiu, Trevor Bennin, Camille Bishop, Kushal Bagchi, Audrey Laventure, Noah Johnson, Niko Van den Brande, Ben Kasting and Marie Fiori, thank you all for being both groupmates and friends. I couldn't imagine a better set of coworkers! Katie Whitaker thank you for everything you've taught me and preparing me to do everything in this thesis. I could not have done any this work without your mentoring. Alfonso Speulveda, thank you for being a mentor and a friend. Your immense positivity still encourages me to "expect the best" every day. Jaritza Gomez, we met on visit weekend and now are defending within a week of each other after being friends and coworkers for five and a half years. It has helped me so much to have your support throughout this entire time. We did it! Maddy Beasley, thank you for being the best mentee I could ever hope for. It has been a joy to work with you so closely for the last few years. I really value our mentor/mentee relationship and our friendship. And of course, I know the project is being left in good hands. Whether it is for something silly or serious, you are free to call or email me whenever you want. I'm excited to hear about the great things you will do at UW and beyond. To my advisor Mark, thank you so much for all your advice and support. You helped me grow far more as a scientist than I ever thought possible.

Thank you Greg Eyer and Matt Holden for being incredible friends. Our runs and time together over the years have always been exactly what I needed whether I was facing a challenge or wanting to celebrate an accomplishment. Sue Martin-Zernicke, thank you of course for all

your help with navigating requirements and reimbursements and so on, but more importantly, thank you for always wanting to know that I was doing well. Bill Goebel, thank you so much for all your help with everything related to electronics; from spot-welding to sun spots. My trips to the electronics shop always put a smile on my face even in the midst of my most frustrating technical problems.

I want to think Professor Ranko Richert and Hai Bin Yu, my collaborators from Arizona State University. It's been a pleasure to work with and learn from you. Thank you for sharing your expertise.

I'm also incredibly grateful to Yeong Zen Chua, Mathias Arhenberg and Professor Christoph Schick form the University of Rostock. All of the work in this thesis is part of our collaboration with Christoph's research group. You all have been so helpful and patient with all my questions. It has been so much fun meeting you anytime you come to the states. Yeong Zen, we really enjoyed having you work with us in Madison over the summer. I wish I had the opportunity to visit Rostock during my thesis work, but hopefully I'll be able to visit in the future.

Table of Contents

Abstract

This thesis presents experiments and discussion that advance the understanding of vapor-deposited glasses. When vapor-deposited glasses exhibit high kinetic stability, they're known as stable glasses. Stable glasses are known to transform into the liquid state via a front mechanism. My first project introduced a quantitative evaluation of the uniformity of these fronts over time and space. I found that the front velocity varies by less than 4% over the duration of the transformation. For films 280 nm thick, the transformation rates at different spatial positions in the film differ by about 25%; this quantity may be related to spatially heterogeneous dynamics in the stable glass. In my second project, I established that vapor deposition could be used to prepare stable glasses of an alcohol molecule. It was previously unknown if this was possible. I also found that while at least one alcohol molecule can be used to prepare a stable glass, several other alcohol molecules formed glasses with minimal kinetic stability when using standard deposition conditions. The wide range of kinetic stabilities is useful for investigating the factors that control stable glass formation. I compared the kinetic stability of vapor deposited glasses prepared from 14 molecules and found a correlation with the value of τ_α at 1.25 T_g. In my final research project, I performed experiments that tested various hypotheses for why 2-ethyl-1-hexanol forms vapor-deposited glasses with limited kinetic stability when using standard preparation conditions. The experiments supported the hypothesis that the surface mobility is less than for other molecules that are used to prepare stable glasses. My analysis of the data led to the estimation that at the substrate temperature commonly used to deposit stable glasses, 2-ethyl-1-hexanol molecules at the surface move more than 10^4 times slower compared to molecules that do form highly stable glasses using typical preparation conditions. The thesis

concludes with proposed projects that would quantify the effect of hydrogen bonding on surface mobility in glasses, and explore the limit of kinetic stability in vapor-deposited glasses in order to learn about the supercooled liquid below the glass transition temperature.

Chapter 1

Introduction

My thesis work is in the field of supercooled liquids and glasses. Humans have been using and manipulating glass for a long time, but our understanding of the behaviors and properties of these materials is far from complete. The goal of this chapter is to present a perspective on supercooled liquids, glasses, and vapor-deposited glasses to provide context for my work. This perspective is targeted at introducing the ideas that are most relevant for this thesis. If you are interested in learning more about supercooled liquids and glasses, I direct you to references [1] and [2] for reviews of general phenomenology, and reference [3] for a perspective on the recent and future research in the field. Section 1.1 defines supercooled liquids and glasses, and describes the conventional method of preparing a glass. Section 1.2 introduces some of the behaviors of supercooled liquids that are important to the field and will be mentioned later in this thesis. Section 1.3 describes how some of the supercooled liquid and glass phenomena can be understood with a potential energy landscape model. Section 1.4 discusses motivations for research involving supercooled liquids and glasses. Section 1.5 introduces vapor-deposited glasses, demonstrates how these glasses can differ from liquid-cooled glasses, and presents a qualitative explanation for the properties of vapor-deposited glasses in the context of the potential energy landscape. Section 1.6 highlights the motivations for studying vapor-deposited glasses. Section 1.7 gives an overview of the experimental methods used in the thesis. Finally, Section 1.8 explains how this thesis contributes to our understanding of vapor-deposited glasses.

1.1 Supercooled liquids and glasses

I will begin by describing how a liquid is cooled to prepare a supercooled liquid, and cooled further to prepare a glass. Through these steps we will see that supercooled liquids are out of equilibrium with respect to the crystal, but act as metastable state until crystallization occurs. Glasses are out of equilibrium with respect the supercooled liquid and their properties continually change until they become the supercooled liquid. This is shown in Figure 1. We start with a liquid above the melting temperature (T_m), and consider the molar volume or molar enthalpy of our sample. As we cool the sample towards T_m it is true for most substances that the volume and enthalpy decrease. At temperatures below T_m the crystal is the equilibrium state because it has the lowest Gibbs energy. However, time is required for the atoms or molecules of our liquid to organize into the crystal structures. Thus, for fast enough cooling it is possible to cool below T_m and maintain the liquid. The cooling rate to maintain the liquid depends on the substance in question and can vary widely. With this fast cooling, we now have a supercooled liquid. The supercooled liquid is a non-equilibrium state because the crystal is favored at these conditions. However, until crystallization eventually happens, the supercooled liquid properties are a function of temperature and pressure and are constant over time; making the superercooled liquid metastable. As we continue to cool our sample, the volume and enthalpy continue to decrease. Since there is less thermal energy, molecular motions also slow down. Eventually, dynamics become so slow that when we continue to cool the sample, molecules cannot rearrange in the timescale of our observation and the volume or enthalpy deviates from the metastable supercooled liquid line. Since the molecules cannot make significant movement during our observation time, the entire sample now behaves like a solid, and is a glass. The temperature

when the sample falls off the supercooled liquid line is called the glass transition temperature (T_g). The slowing of molecular motion as temperature decreases is smooth and continuous. As the sample is cooled through T_g, there isn't any sudden change in molecular mobility. This behavior is demonstrated in Figure 2 which the structural relaxation time (τ_α) vs temperature for many supercooled liquids. The structural relaxation time is the characteristic time for how quickly the liquid flows. τ_α is proportional to the liquid viscosity. τ_α can be measured by applying a small perturbation to the sample (changing the temperature or applying an electric field) and determining how long it takes for the liquid properties to respond. The structural relaxation time is around 100 seconds at T_g. I'll discuss this convention in the following paragraph. In Figure 2 we see that τ_α changes by a massive 14 orders of magnitude from the high temperature limit to temperatures near T_g, and this change is continuous. I've not included data below T_g (because it is often difficult to acquire), but the τ_α data below T_g is continuous with the data above T_g. There also isn't a drastic change in the structure of the material as we transition from supercooled liquid to glass. A snapshot of a liquid and of a glass would look pretty much the same to the eye. There is a lot of work looking at higher order correlation functions between particles that have found some changes at the glass transition, but there is not yet a clear structural reason for the glass transition.[4]

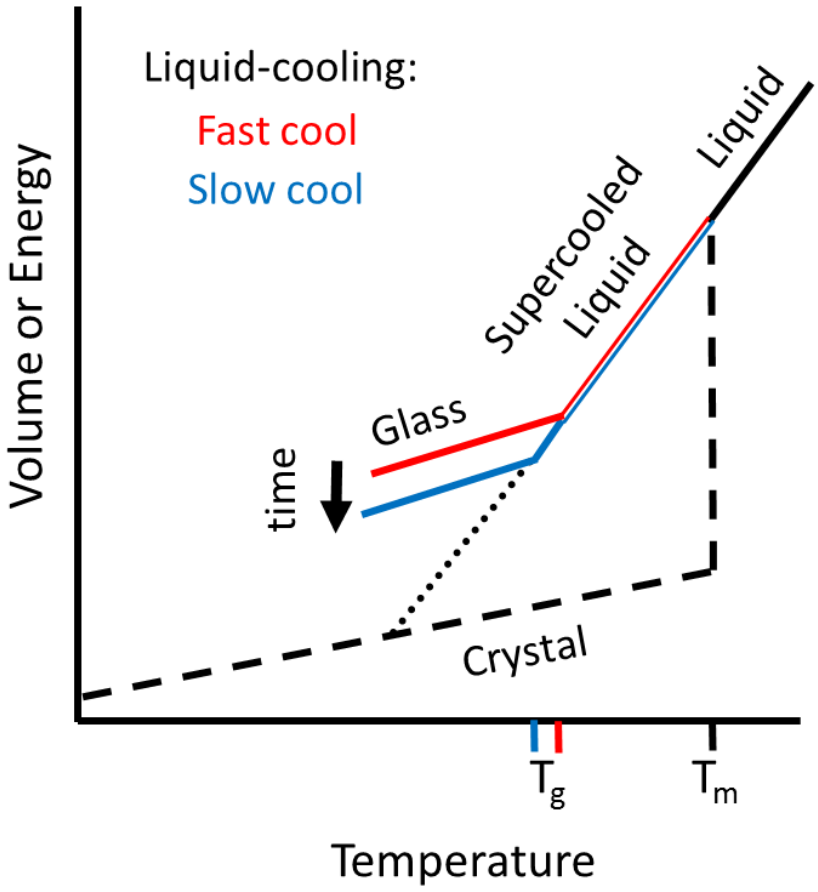

Figure 1: *A plot of the properties of a sample as it is cooled to become a glass. When the liquid is cooled below T_m and avoids a crystallization it becomes a supercooled liquid and is metastable. As the supercooled liquid is cooled, slowing molecular dynamics means the sample eventually falls out of the metastable equilibrium and becomes a glass. This happens at the glass transition temperature (T_g) and depends on the cooling rate. The glass properties also change over time in a process called "aging."*

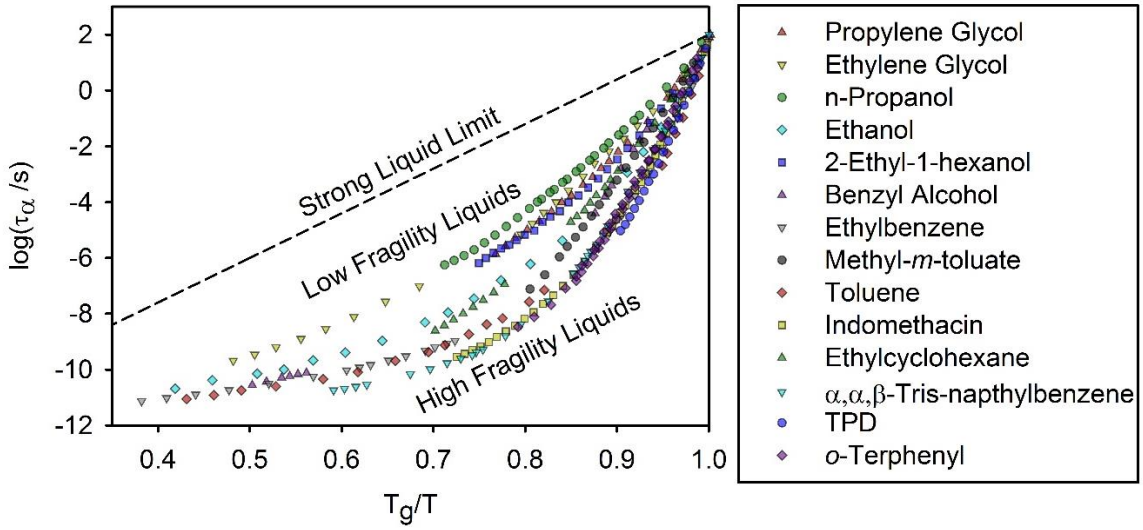

Figure 2: *A plot of structural relaxation time (τ_α) vs inverse temperature for 14 organic liquids. T_g is defined for each material as the temperature when τ_α = 100 seconds. The dashed line represents the behavior of a liquid with dynamics that follow the Arrhenius equation with a constant activation energy and a high temperature limit of $\tau_\alpha = 10^{-12}$ seconds. Liquids with behavior that deviate from the strong liquid limit are termed "fragile liquids" and have an apparent activation energy that increases with decreasing temperature. This data in this figure are compiled in reference* [5]*. TPD is the abbreviation for N,N′-bis(3-methylphenyl)-N,N′-diphenylbenzidine.*

While our glass sample below T_g acts as a solid over short times, its properties are continually changing to reach the supercooled liquid state. The slow evolution of glass properties is called aging. You may have realized that the temperature when the sample falls off the supercooled liquid line depends on the cooling rate that is used. This makes the "fall-off-the-

supercooled-liquid-line" definition of T_g more complicated. To avoid this issue, I and many other glass scientists prefer to define T_g as the temperature when the structural relaxation time (τ_α) is 100 seconds. This is roughly equal to the "fall-off-the-supercooled-liquid-line" temperature when using a cooling rate of 10 K/min.[6] I will use this definition throughout the thesis. I previously said that glass properties change with aging, and I should add that the rate of aging, or how fast the glass properties change, decreases for temperatures further below T_g.[7] So the instantaneous properties of a glass are a function of the cooling rate used to prepare it, the temperature(s) it has been aging at, the aging time at each temperature, and the molecular identity.

1.2 Important supercooled liquid behaviors

Supercooled liquids are often studied and discussed along with glasses because glass properties are related to the properties of the supercooled liquid state at the temperature just before falling out of metastable equilibrium. There are three phenomena of supercooled liquid dynamics that are important to this thesis. First, the apparent activation energy for structural relaxation increases with decreasing temperature. This non-Arrhenius behavior of τ_α is temperature is illustrated by the upward curving data in Figure 2. This phenomenon is called "fragility." Second, the rate of molecular motion varies spatially across the sample. There are fast regions and slow regions that make the sample dynamically heterogeneous. Finally, there can be a significant difference between the rate of molecular relaxation at the surface and in the bulk. A very nice description of bulk supercooled liquid dynamic phenomenology can be found in a book chapter written by Ranko Richert.[8] For further perspectives about the mobility at the

surface of supercooled liquids and glasses, Lian Yu reviewed how this topic related to vapor-deposited glasses and crystal growth,[9] while Mark Ediger and James Forrest have reviewed the research into polymer dynamics near the free surface.[10]

The concept of fragility can be visualized in Figure 2. Dynamics that follow the Arrhenius equation (with the high temperature limit of $\tau_\alpha = 10^{-12}$ seconds) are plotted as the dashed line. This line is called the strong liquid limit. When there is a constant activation energy for molecular motion, $\log(\tau_\alpha)$ vs T_g/T yields a straight line. However, many supercooled liquids have dynamics that do not follow the strong liquid limit and instead have an upward curving trend on the plot. The apparent activation energy for structural relaxation increases as temperature decreases. Fragility is the measure of how much a given supercooled liquid's dynamics deviate from Arrhenius behavior.[11] Liquids with dynamics that more closely follow the predicted Arrhenius behavior are called strong liquids and liquids that deviate significantly from that limit are called fragile.

It has recently been established that supercooled liquids exhibit dynamic heterogeneity.[8,12,13] The rate of relaxation varies with location in a supercooled liquid. Some regions relax faster than average, while others relax slower than average. Over time, the fast regions become slow, the slow regions become fast; any given region will have an average relaxation rate when averaged over long times. Within these regions, molecular motions are correlated, and they are called cooperatively rearranging regions. The cooperatively rearranging regions are small or even non-existent at high temperatures but grow as temperature decreases towards T_g. Experiments that were able to prove the existence of dynamic heterogeneity were

very important to the field.[14,15] Dynamic heterogeneity can be used to explain a number of odd features of supercooled liquid dynamics that have puzzled researchers for a long time. There is now a consensus that dynamic heterogeneity happens, and the field has characterized some generalized features of it. However, there is still much to learn about why this phenomenon happens and how it might vary from one supercooled liquid to another.

Supercooled liquids can have dynamics at the surface that are much faster than bulk dynamics and this topic has seen a lot of investigation in recent years. The surface that we will be concerned with in this thesis is the interface between the sample and vacuum or the sample and gas. Bell and coworkers have determined the viscosity as a function of depth in a liquid film of 3 methyl pentane, and found that the viscosity changes by 6 orders of magnitude from the surface to the bulk.[16] Their results are shown in Figure 3A. Zhang and coworkers have measured the surface diffusion constant of *o*-terphenyl glasses and found that surface molecules diffuse 10^8 times faster than bulk molecules at T_g.[17] Their results are shown in Figure 3B. There has been evidence of enhanced surface mobility for many organic molecules, but recent experiments show that for some molecules, surface mobility is quite limited and is similar to bulk mobility.[18] Enhanced surface mobility may be a common phenomenon, but the degree of enhancement can vary widely and more work is needed to understand what influences surface mobility.

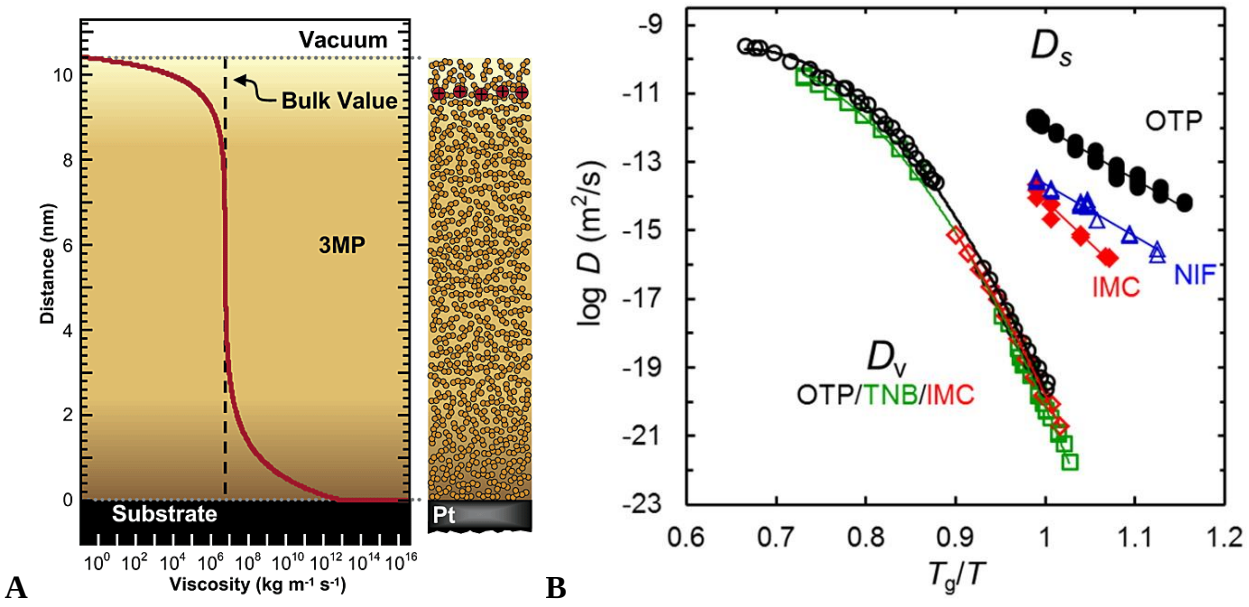

Figure 3: *Experiments that demonstrate enhanced surface mobility in organic liquids. Panel A: Viscosity as a function of thickness for a 3-methylpentante film determined by ion penetration experiments.*[16] *Figure reprinted with permission from reference 16. Copyright 2003 American Chemical Society. Panel B: Surface diffusion constants (D_s) compared to bulk diffusion constants (D_v) for o-terphenyl (OTP), nifedipine (NIF) and indomethacin (IMC).*[17] *Surface diffusion constants are determined by grating decay experiments. Figure reprinted with permission from reference 17. Copyright 2015 American Chemical Society.*

1.3 Supercooled liquids and the potential energy landscape

I want to briefly return to the idea of fragility in Figure 2. The increasing apparent activation energy is often discussed along with the potential energy landscape, or PEL.[2,11] The PEL describes the potential energy of a sample as a function of the coordinates of every atom or molecule in the sample. This is obviously a huge number of coordinates and often times the PEL is discussed in a qualitative way. However, for simulations of smaller numbers of particles, the

PEL can be actually be calculated.[19,20] PEL provides a framework for understanding supercooled liquid dynamics.[19] At a given moment in time, the liquid exists in a configuration that is a local minimum. This local minimum is surrounded by numerous other minima with similar configurations that are associated with very small changes in the atomic coordinates. The liquid rapidly and reversibly samples this collection of local minima that is called a metabasin. When a liquid leaves a metabasin, it finds a new configuration that is potentially very different form the previous one. Unlike sampling local minima within a metabasin, once the liquid leaves a metabasin it has an extremely low probability of returning. At higher temperatures, the sample visits minima that are high in the landscape and structural relaxation occurs when the sample leaves one metabasin and visits another. The amount of time it takes for structural relaxation is determined by temperature and the size of the barrier between metabasins in the PEL. As temperature decreases, the sample is driven to visit lower energy configurations in the PEL, and the low temperature dynamics are influenced by the size of the barriers around the low energy metabasins. In Figure 4, I've sketched one dimensional PEL cartoons that would belong to three types of liquids. For fragile liquids we see that the barriers surrounding lower metabasins are much larger than barriers around the metabasins that are higher in the landscape. This is shown in Figure 4A. The larger barriers for metabasins that are low in the PEL give rise to increasing apparent activation energy characteristic of fragile liquids. For a stronger liquid, or one with less fragility, the barrier heights do not increase as much when moving down the landscape. This is shown in Figure 4B. Finally if a supercooled liquid displays dynamics that are in the strong liquid limit, the apparent activation energy is constant. It has been found in simulations that these type of liquids have found the bottom of the amorphous part of the PEL.[20] Once the liquid is at a

low enough temperature to be sampling the bottom of the landscape, it won't find any lower minima at cooler temperatures. So as the sample is cooled, thermal energy decreases but the barrier height to relaxation stays the same, and the activation energy is constant. A strong limit PEL is shown in Figure 4C. You may notice that at high temperatures this liquid can have fragile behavior. Such liquids are said to go through a fragile to strong transition at temperatures when they start sampling the bottom of the landscape. Simulations of liquid silica have found that the fragile to strong transition in this material is indeed the result of bottoming out the landscape.[20]

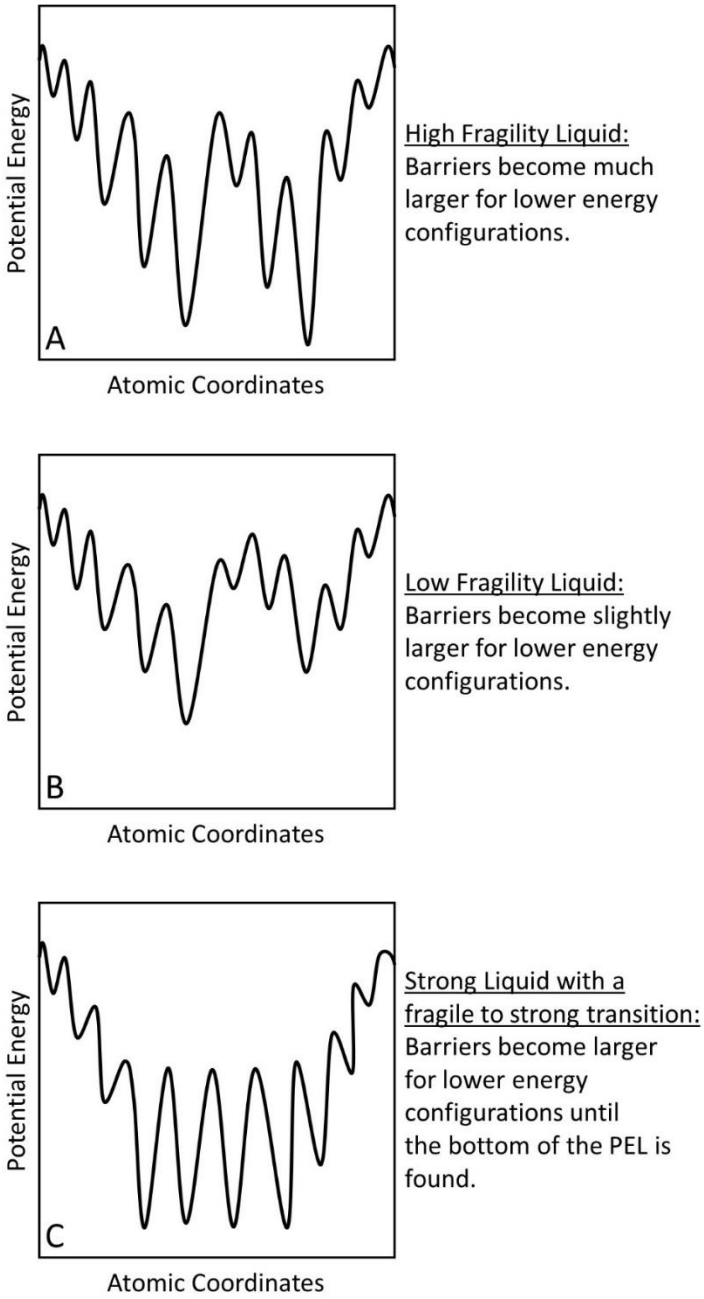

Figure 4: *Cartoons of potential energy landscapes (PEL) for liquids displaying different dynamical behaviors. The sketched minima and barriers are for individual metabasins, the local minima within each metabasin have been omitted for clarity.*

1.4 Motivations for supercooled liquid and glass research

The motivations for research in the field can crudely be split in two; improving our fundamental understanding of supercooled liquids glasses and improving the performance of glass materials for societal applications. The work in this thesis falls in to the category of fundamental study. Researchers in the field have measured and characterized many phenomena in supercooled liquids and glasses but the understanding of many phenomena is incomplete. For example, I'll show in Chapter 4 that the leading theoretical descriptions of surface mobility do a poor job of explaining some behaviors that are observed in experiments. Further experiments and analysis are required to improve the theoretical understanding of supercooled liquids and glasses. Better theories of these materials should ultimately help us manipulate these materials in applications.

Perhaps the most famous problem in the study of supercooled liquids is the long standing Kauzmann entropy crisis. The Kauzmann entropy crisis can be seen when plotting the entropy of supercooled liquids as a function of temperature, as done in Figure 5.[21] For some substances, the extrapolation of the liquid entropy intersects the entropy of a perfect crystal and then intersects zero entropy at a temperature above 0 K. This second feature is a violation of the 3rd law of thermodynamics which is a problem. We can't cool a supercooled liquid to these low temperatures because the glass transition intervenes. But it is important to remember that the observed glass transition is a kinetic phenomenon. So it is fair to ask, if we could wait long enough, would we get a liquid with entropy less than the crystal? Or even less than zero? Given the robustness of thermodynamics, the consensus is that something must happen before the liquid violates the 3rd law. Actually, it is thought that something must happen at or before the liquid

entropy meets the crystal entropy. This is because the S vs T lines have a slope given by c_p/T, and there are few examples of amorphous materials with lower heat capacity than the corresponding crystal heat capacity. Therefore, to avoid violating the 3rd law, something must happen at or before the supercooled liquid entropy meets the crystal entropy. The observation of this crisis and the proposal that something must happen by the temperature when the liquid and crystal entropies meet was put forth by Kauzmann in 1948.[21] Thus, we call the temperature of that intersection that Kauzmann temperature. Since 1948 there have been plenty of ideas of how nature might resolve the Kauzmann Entropy Crisis, but there is no consensus on what would happen if we could wait long enough.[1,22]

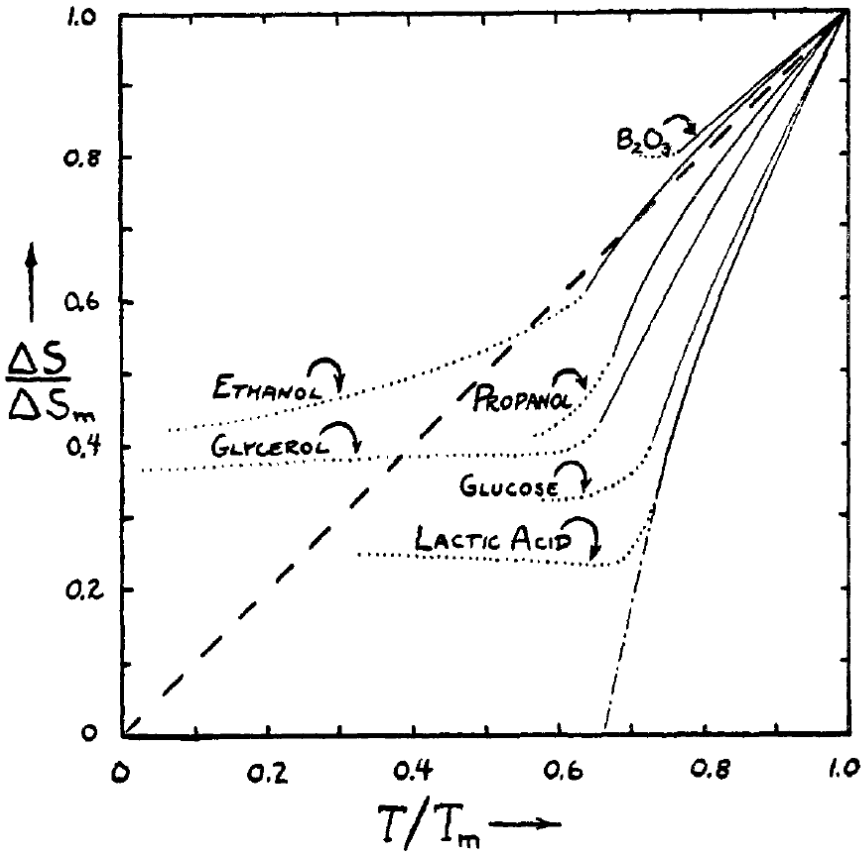

Figure 5: *Plot of the difference between liquid and crystal entropy vs temperature for a number of liquids.*[21] *For propanol, glycerol, glucose and lactic acid the extrapolated liquid entropy intersects the perfect crystal entropy significantly above 0 K. Because the perfect crystal entropy decreases to zero at 0 K, the possibility of a liquid with an entropy less than the perfect crystal seems extremely unlikely, despite the extrapolation. Figure reproduced with permission from reference 21. Copyright 1948 American Chemical Society*

Even when setting aside the Kauzmann entropy crisis, the theoeritical understanding of supercooled liquids and glasses is incomplete. Biroli and Berthier began a 2011 summary of

various supercooled liquid and glass theories[22] by saying: "It is impossible to cover all of them in this review, simply because there are too many of them. This is perhaps the clearest indication that the glass transition remains an open theoretical problem." There are lots of ideas, and even lots of good ideas, but the field hasn't yet been won over by any particular theory. Therefore, an important aspect of current and future experimental work is to expand upon the things that we know happen in supercooled liquids and glasses. More experimental knowledge allows theories to be tested, and then either improved or abandoned. Phenomena such as dynamic heterogeneity and enhanced surface mobility of supercooled liquids are recent discoveries that should be part of complete theories of supercooled liquids and glasses. However, it's important for experiments to explore the details of such phenomena. For example recent work by Lian Yu's group has demonstrated a wide range of surface diffusivities at T_g.[18] Enhanced mobility at the surface of glasses and supercooled liquids may be a general feature, but the degree of enhancement at the surface can vary significantly between glass-formers.[18,23] A complete theory of supercooled liquids and glasses will need to be able to account for nuance like this.

Research is also very important to improve the applications of glasses in society. In many applications the value of a glass over a crystal is the ability to almost arbitrarily change chemical composition, and the lack of grain boundaries in glasses. Silicate based glasses used for windows and display screens are still improving. The process of ion exchange has been used to strengthen silicate glasses, which are traditionally considered to be mechanically fragile materials.[24] Perhaps the highest profile commercial realization of ion exchanged glass is Gorilla Glasses developed by Corning.[25] Gorilla Glass is used in many phones and tablets. Many polymer materials are glasses and as plastics become used more as structural materials, it is important to understand

their mechanical properties.[26] Some pharmaceutical molecules are not soluble as a crystal, and drug manufacturers must work to keep these molecules in an amorphous state.[27,28] Fiber optics are made of glass.[29] Glasses can be made from mixtures of nearly arbitrary composition, which allows one to tune the index of refraction for optical applications. Metallic glasses have properties that are very promising for engineering applications.[30,31] However, many metallic glasses suffer from crystallization, or brittleness after aging. Current research is seeking ways to make these metallic glasses more viable for applications. Finally, the active layers of organic electronics are often glasses, and the ability to control glass properties is important to improving device performance.[32]

I think it is important to note that many research topics are important for both fundamental understanding and for glass applications. One example is the study of what makes a good glass-former. There is a poor understanding of whether a molecule will be a great crystallizer and therefore hard to make into a glass, or if it will be easy to make into a glass.[33] This can be a fundamentally interesting question, but also a practically important question for keeping amorphous pharmaceuticals from crystallization and for finding metallic glass alloys that don't need to be made with extremely fast cooling rates which limits their size. We will discuss vapor-deposited glasses next which also straddle the line between fundamental and applied. In my thesis, I study fundamental topics; quantifying the front mechanism of how stable glasses transform and trying to understand the variation in kinetic stability of vapor-deposited glass. However, vapor-deposited glasses are also used in organic electronics and some of my coworkers perform research that is aimed at improving our ability to manipulate the properties of vapor-deposited glasses for use in devices.[34]

1.5 Vapor-deposited glasses

Glass properties depend on how they are prepared. It's useful to quickly review the process of preparing a glass. The most common method of preparing a glass is to cool the liquid fast enough to avoid crystallization. By changing the cooling rate, the sample falls out of meta-stable equilibrium at different temperatures and thus has different properties. Liquid cooling is not the only method of preparing a glass. Vapor-deposition is the procedure of condensing a gas into a solid. The solid sample is built in a layer by layer manner. You can vapor-deposit a crystal, but we're interested in cases where we prepare a glass. During vapor-deposition the main variables we can change are substrate temperature during deposition, and deposition rate. To understand how these variables can affect the properties of the glass we are preparing, we will return to the topic of surface mobility.

1.5.1 Theoretical explanations of surface mobility

I mentioned in Section 1.2 that supercooled liquids and glasses can have surfaces that move much faster than the bulk. Some molecules have surface diffusion coefficients that are 10^8 times faster than the bulk value at the same conditions (Figure 2B).[17] Viscosity measurements have found similar sized differences between the surface and bulk (Figure 2A).[16] So how can we think about these huge increases in mobility at the surface? As supercooled liquids are cooled closer to T_g, they become so dense that a molecule can't make any significant movement without hitting one of its neighbors. At these low temperatures and high densities, movement of a molecule can only be accomplished if there is cooperative motion of the neighboring molecules.

Molecules at the surface have far fewer neighbors than in the bulk; therefore they can make significant movements without needing cooperation.

We've just described a molecule that is on the surface of the liquid, but the experiments like the 3 methyl pentane viscosity determinations,[16] as well as simulations of glass surfaces[35,36] there is evidence from experiments[16] (Figure 2B) and simulations[35–37] that dynamics are still enhanced for a few layers into the film. There are two theoretical approaches that help us understand what this is. One is the Random First Order Transition (RFOT) theory.[38] Briefly this theory says that at lower temperatures molecular motion requires a collective repositioning of more molecules. Rearrangement of the larger groups of molecules is slower because the probability of finding a new arrangement that still fits inside the surrounding liquid becomes smaller. However, by being near a surface, the size of the group required for rearrangement is smaller, there is higher probabilities of finding a suitable new arrangement and thus motion is faster.[39] A cartoon of the smaller relaxing region at the surface compared to the larger relaxing region in the bulk is shown in Figure 6. The other useful theory for understanding dynamics near the surface is the Elastically Collective Nonlinear Langevin Equation (ECNLE) theory.[40] For the motion of a given molecule, this theory considers a cage of immediately neighboring molecules that must cooperate for the movement and then treats the surrounding material as an elastic continuum. The local cage must expand to accommodate a rearrangement, and thus pushes against the elastic medium. A molecule at the surface will have a smaller, incomplete local cage, and thus move faster.[41] A molecule near but below the surface will have a complete local cage, but because it is near the vacuum surface, the force required to deform the material outside the local cage is less. Thus the rearrangement is easier and happens faster. A cartoon of this theory is

shown in Figure 7. Both of these theories are useful ways to rationalize the enhanced mobility that has been shown to exist at and near the surface of some supercooled liquids and glasses.

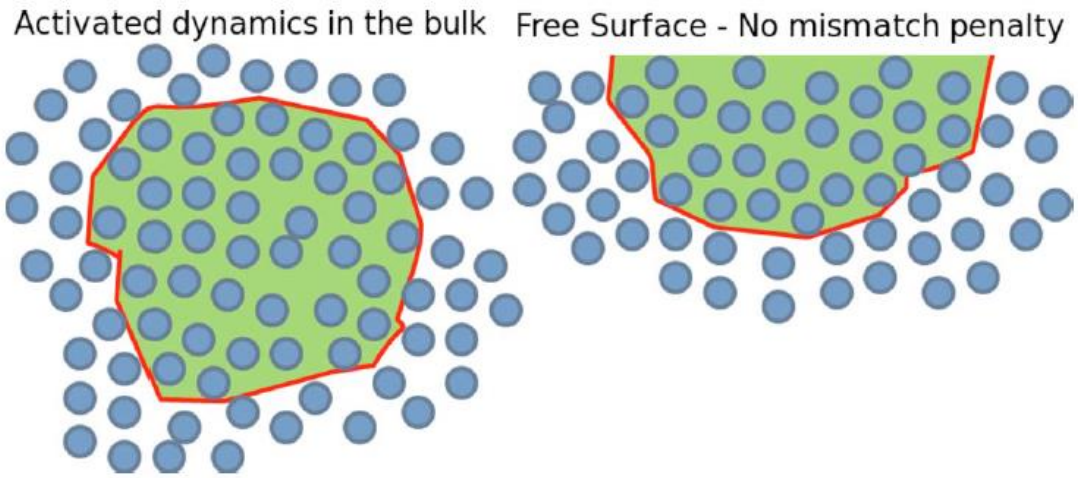

Figure 6: *Random First Order Transition (RFOT) theory cartoon of bulk (left) vs surface (right) relaxation.*[39] *In RFOT theory, relaxation in supercooled liquids and glasses requires cooperation from a large enough group of particles (red outline and green fill) in order for the new configuration to fit within the surrounding material. At the surface, there is no surrounding material to constrain the configurations of the rearranging group. Thus the number of particles required for cooperative relaxation is smaller and relaxation occurs faster at the free surface. Figure reprinted from reference 39, with permission of AIP Publishing.*

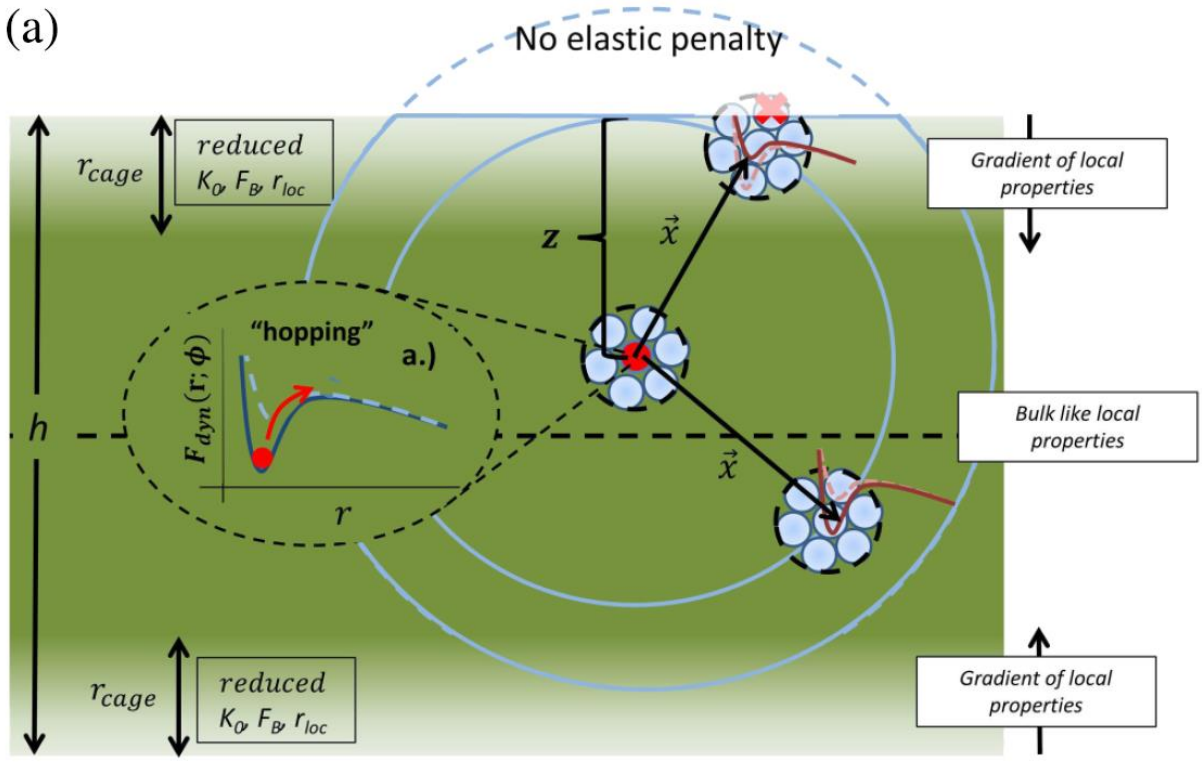

Figure 7: *Elastically Collective Nonlinear Langevin Equation (ECNLE) theory cartoon of relaxation near a free surface.*[41] *ECNLE theory treats relaxation in supercooled liquid and glasses by imagining the relaxation of a local cage (blue cirlces) that must deform a surrounding elastic continuum (green shading). At the free surface, the local cage for a given particle has fewer members which reduces the barrier to relaxation. For particles near the free surface, the local cage is complete, but the force needed to deform the surrounding material is less, and relaxation is still faster than deep in the bulk. Figure reprinted from reference 41 with permission of AIP Publishing.*

1.5.2 A hypothetical deposition

Let's now return to the process of vapor-deposition and see the consequence of the mobile surface. We build up our film in a layer-by-layer like fashion on the substrate. We're going to pick a substrate temperature a little bit below T_g. It turns out about 0.85 T_g is often a good choice.[42] At this temperature, a bulk sample would be a glass and the relaxation of the molecules is much longer than the afternoon it takes us to prepare the vapor-deposited glass. Molecules near the free surface are mobile and are able to sample low energy packing configurations. Since the entire sample is prepared by deposition, every molecule got a chance to be close to the surface and to find low energy configurations. So the whole vapor-deposited glass ends up in a low energy metabasin in the PEL. The metabasin that the vapor-deposited glass inhabits is much lower in energy than a metabasin inhabited by a liquid-cooled glass. This description is supported by calorimetry measurements that show that the enthalpy of the vapor-deposited glasses is lower than the enthalpy of a liquid cooled glass of the same composition.[43,44] The lower energy metabasin inhabited by the vapor-deposited glass has higher barriers around it compared to a liquid cooled glass metabasin. (We are assuming that our molecule is a somewhat fragile glass-former, see Section 1.2) Thus, there is are larger barriers to relaxation for the vapor-deposited glass compared to the liquid-cooled glass. Experiments demonstrate the effect of the higher barriers for the vapor-deposited glasses. When a vapor-deposited glass is heated, it often transforms into the supercooled liquid at a higher temperature than the liquid-cooled glass.[42] Another way to probe the effect of higher barriers is to perform a sudden temperature increase of a glass followed by isothermal annealing. In this experiment a vapor-deposited glasses often take longer times to transform into the supercooled liquid compared to a liquid-cooled glass.[5] Glasses

with these kind of behaviors are said to have kinetic stability. Both phenomena are demonstrated in Figures 8 and 9. Vapor-deposited glasses with exceptional kinetic stability are called stable glasses. What counts as exceptional kinetic stability? Stable glasses often have transformation temperatures that are about 1.05 T_g or higher,[42] which is compared to a liquid-cooled glass that transforms at T_g. During high temperature annealing experiments, stable glasses can take up to 10^5 times longer than a liquid-cooled glass to transform into the supercooled liquid.[5,45]

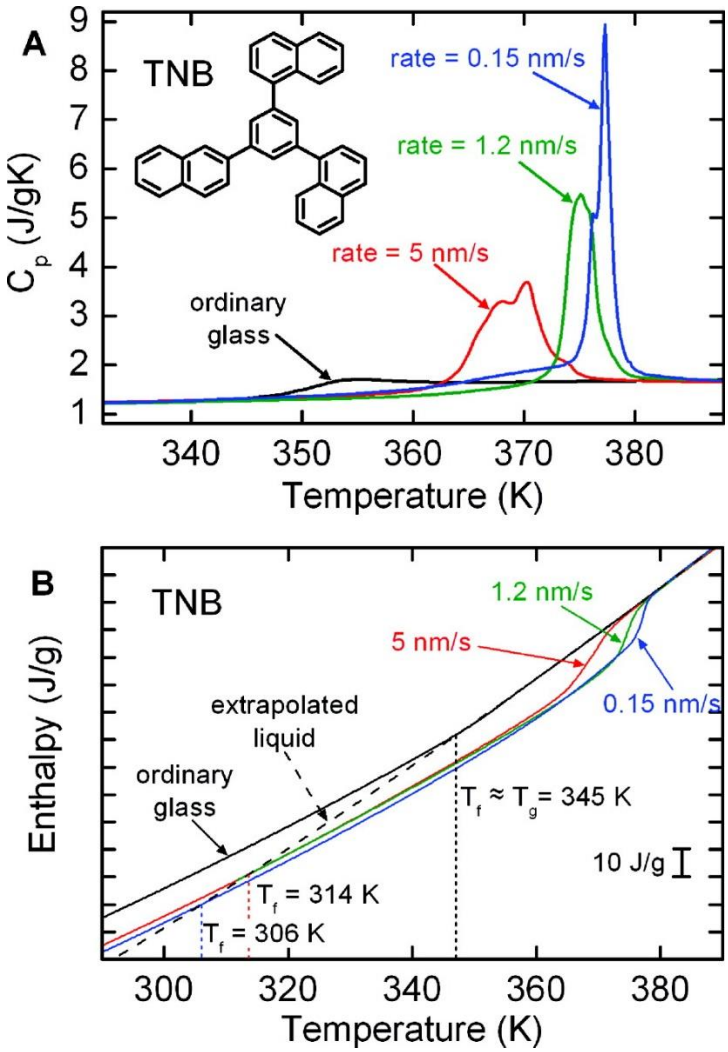

Figure 8: *Differential Scanning Calorimetry data at 40 K/min of α,α,β (tris)napthylbenzene (TNB) glasses.*[43] *Vapor deposited glasses prepared at* $T_{substrate} = 0.85\ T_g$ *and at different deposition rates are shown in red, green and blue traces. The black trace is a liquid-cooled glass ("ordinary glass") prepared by cooling at 40 K/min. Vapor-deposited TNB glasses prepared at 0.15 nm/s don't transform into the supercooled liquid until 30 K above* T_g *which is 1.09* T_g*. Figure reprinted with permission from reference 43. Copyright 2008 American Chemical Society.*

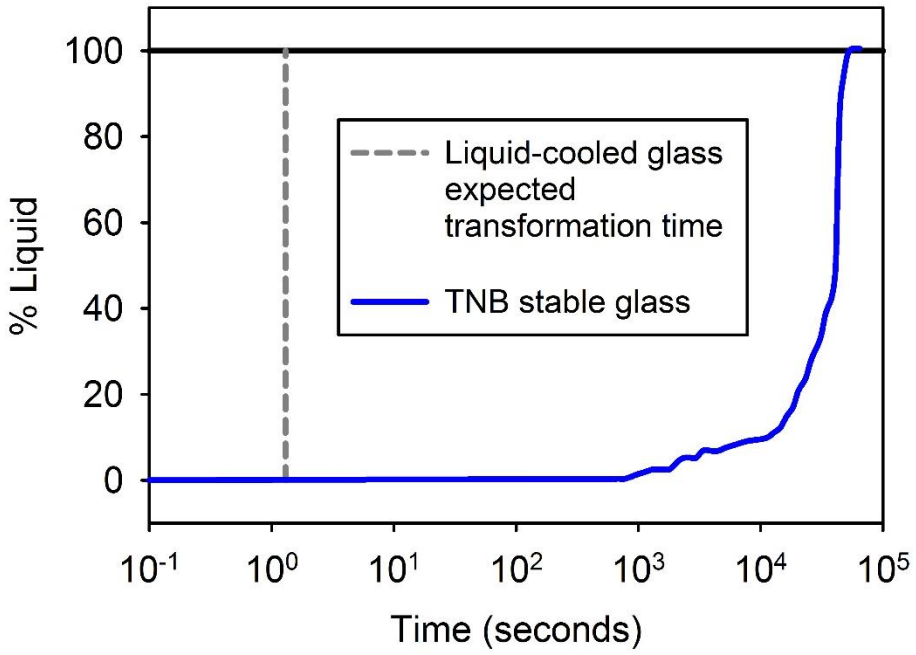

Figure 9: *Re-production of AC nanocalorimetry isothermal annealing data for a TNB stable glass at T_g + 8 K.*[45] *The y-axis of % Liquid is the percentage of the sample that has transformed from the glass into the supercooled liquid as calculated by the heat capacity change. The stable glass samples transform in about 50,000 seconds. At this annealing temperature the liquid structural relaxation time (τ_α) is about 1.3 seconds. A conventionally prepared glass will transform in about τ_α, so the transformation times of these stable glasses are $10^{4.6}$ times longer than that of a conventionally prepared glass. The TNB stable glass was prepared at $T_{substrate}$ = 0.85 T_g with a rate of 0.2 nm/s.*

1.5.3 The role of substrate temperature

The first important variable for vapor-deposited glasses is the substrate temperature. It's been found that the kinetic stability increases when the substrate temperature decreases until about 0.8 T_g, and then the kinetic stability decreases for lower substrate temperatures. This trend can be explained by the competition between metabasins with higher barriers being available at lower temperature and surface mobility decreasing with lower temperatures. If we were to deposit at $T_{substrate} \geq T_g$, the molecules may have quite high mobility near the surface, and sample lots of configurations, but the lowest energy configurations sampled during deposition are also accessible and sampled by the bulk supercooled liquid. Really, we're just depositing a supercooled liquid. If the sample is cooled after the deposition, the resulting material is just a liquid-cooled glass, and gets stuck in the same metabasins as any other liquid-cooled glass. If we deposit *just* below T_g, the configurations that the vapor-deposited glass can access are only slightly lower in energy than the configurations that the liquid-cooled glass gets stuck in. Therefore the metabasin the vapor-deposited glass is inhabiting has barriers only slightly larger than the barriers for the liquid-cooled glass metabasin. We have to move $T_{substrate}$ to lower temperatures for there to be the possibility of sampling much lower energy configurations, and thus preparing a glass that is much lower than a liquid-cooled glass in the PEL. However, there is a practical limit to lowering the substrate temperature. Eventually, the surface mobility, which decreases with decreasing temperature, is too slow to allow for significant sampling over any practical time scale. So, at very low substrate temperatures, say 0.50 T_g, there may be possible configurations that are quite low in energy but the surface mobility is so low that we can't practically do a slow enough deposition to allow molecules enough time to find those

configurations. In fact, by using practical deposition rates (around 0.2 nm/s) and depositing at 0.6 T_g or lower, the resulting glasses tend to be higher in the potential energy landscape than even a liquid-cooled glass,[44] and often go through some irreversible change upon heating before T_g.[42] These glasses are kinetically unstable, and are the result of the fact that at low temperatures, surface mobility might still be quite fast compared to bulk mobility but it is slow compared to practical deposition rates. So concerning deposition temperature, there is a tug of war between the available configurations in the PEL and the surface mobility. The "Goldilocks" temperature for many molecules is around 0.85 T_g, as demonstrated by Figure 10.

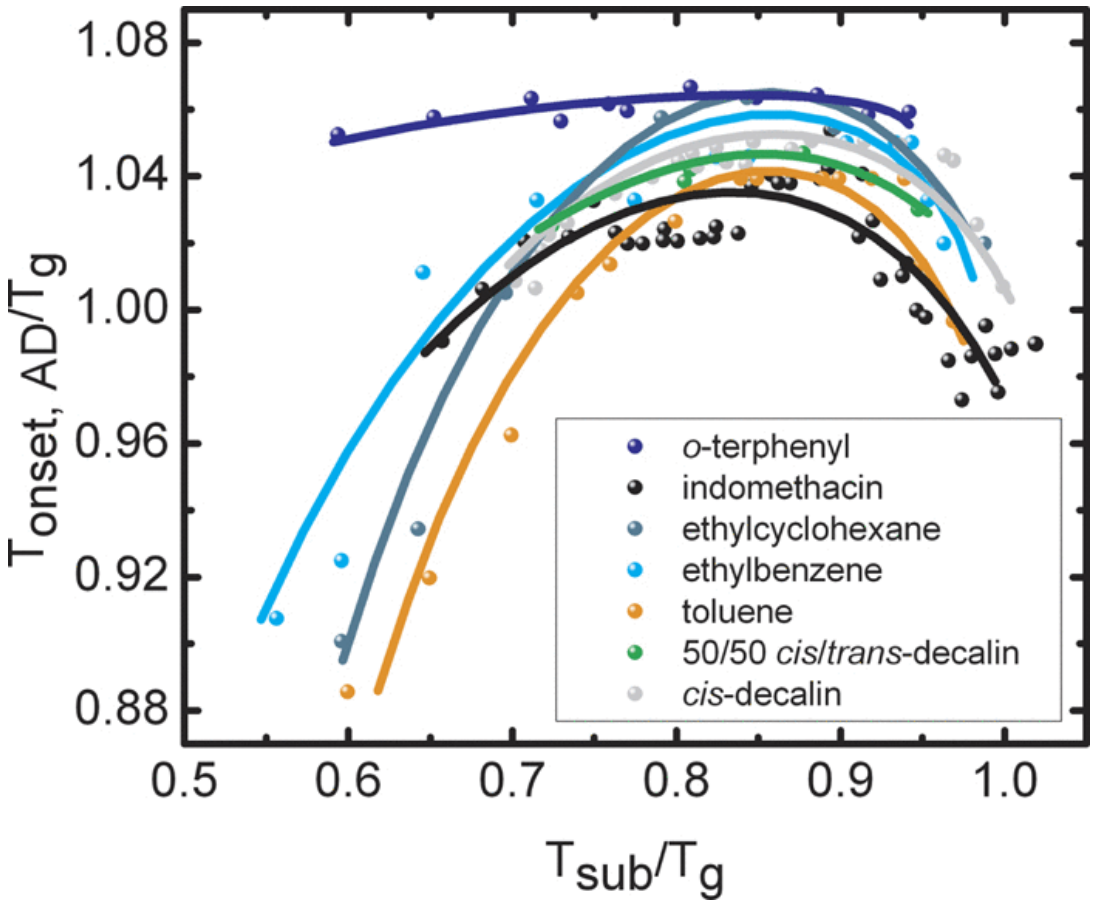

Figure 10: *The onset temperature (T_{onset}) for transformation into the supercooled liquid as a function of substrate temperature during deposition (T_{sub}) for several vapor-deposited glasses.*[42] *T_{onset} is a measure of kinetic stability, and increases with decreasing T_{sub} because there are configurations available at lower temperatures that correspond to metabasins with higher barriers. The T_{onset} decreases for lower values of T_{sub} because the surface mobility becomes slow with respect to the deposition rate. The deposition rates are between 0.15 and 0.2 nm/s. Figure reprinted from reference 42, with permission of AIP Publishing.*

1.5.4 The role of deposition rate

We'll now explore the influence of the deposition rate on our vapor-deposited glass. When preparing a stable glass using a substrate temperature of 0.85 T_g a typical deposition rate is about 0.2 nm/s. For a small molecule like ethylcyclohexane this corresponds to a complete new layer every 3 seconds or so.[46] This is called the free surface residence time. At 0.85 T_g, the characteristic time for structural relaxation at the surface for ethylcyclohexane is about 0.2 seconds. This is the surface τ_α, which is usually called "$\tau_{surface}$". When depositing at 0.2 nm/s, the free surface residence time (3 seconds) is much longer than $\tau_{surface}$ (0.2 seconds) and each molecule is able to sample low energy configurations while on the surface. Thus, the entire sample is in a low energy metabasin surrounded by high barriers that result in high kinetic stability. However, if we were to deposit at 200 nm/s, the free surface residence time is about 0.003 second, which is much less than $\tau_{surface}$. During the fast deposition, the molecules do not have enough time at the free surface to sample low energy configurations before being buried by further deposition. This fast-deposited glass gets stuck in a high energy metabasin that has low barriers around it, and the glass does not have high kinetic stability. The kinetic stability of vapor-deposited glasses increases as the deposition rate decreases (equivalent to the free surface residence time increasing). The increase of kinetic stability continues until a critical deposition rate. For depositions slower than the critical rate, the kinetic stability is a constant. This critical deposition rate depends on temperature because surface mobility is temperature dependent. The deposition rate needed for maximum kinetic stability over a range of substrate temperatures was determined for ethylcyclohexane by Chua and coworkers in reference [46] and their results are

shown in Figure 11. In this work, at $T_{substrate}$ = 0.85 T_g, the critical deposition rate is around 0.5 nm/s. This critical rate corresponds to a free surface residence time of 0.2 seconds, which is equivalent to $\tau_{surface}$.

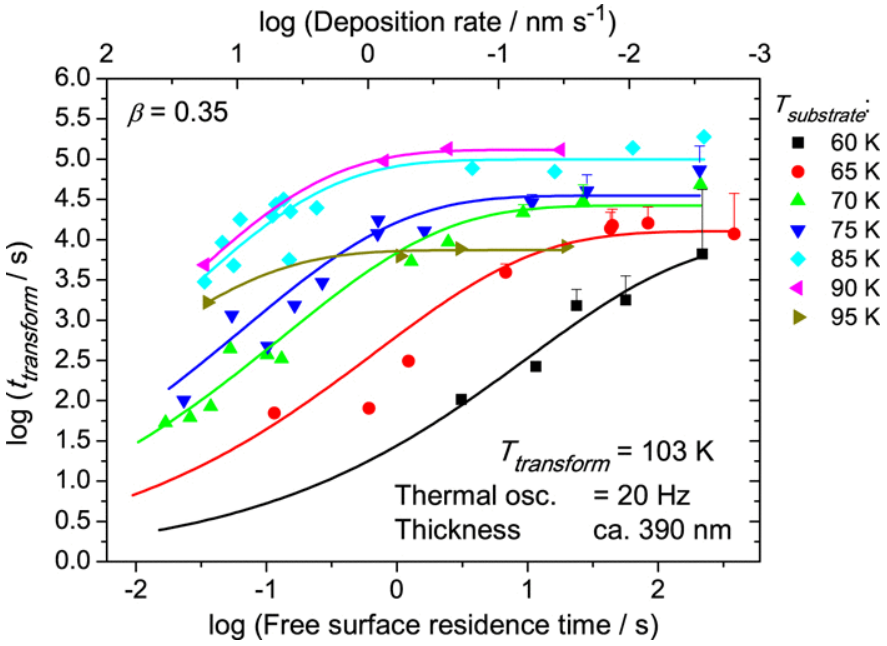

Figure 11: *Isothermal transformation times of ethylcyclohexane vapor-deposited glasses as a function of deposition rate (x-axis) and $T_{substrate}$ during deposition (symbol shape and color).*[46] *For a given $T_{substrate}$ the transformation times increase with slow deposition rate and eventually reach a plateau. The most likely interpretation of the plateau is that the molecules have found the lowest minima available (with the highest barriers) at that $T_{substrate}$. Figure reprinted from reference 46 with permission of AIP Publishing.*

1.5.5 Requirements to prepare a stable glass

There are three important assumptions I made in explaining the phenomena of vapor-deposited glasses with high kinetic stability. I'm actually going to present them as material requirements for preparing a stable glass. The first requirement is that our molecule of choice has enhanced surface mobility. For a while, researchers attempting to make stable glasses were luckily selecting molecules that did have enhanced surface mobility. However, it is becoming evident that some molecules have limited surface mobility. Lian Yu's group has reported a few molecules so far that have limited surface diffusion.[18] Vapor-deposition experiments by Madeleine Beasley, Yeong Zen Chua, and myself have found that ethanol, propanol, 2-ethyl-1-hexanol, propylene glycol, ethylene glycol, 1-pentene, triethyl phosphate, tripropyl phosphate, and tributyl phosphate do not form stable glasses when prepared with deposition rates and temperatures that are expected to yield stable glasses.[5,47] Instead, vapor-deposited glasses of these molecules have only a small amount of kinetic stability, or are even unstable. We hypothesize that these molecules have limited surface mobility.

The second requirement for preparing a stable glass is that there must be lower energy configurations available at temperatures below T_g. This is not true for extremely strong liquids.[20] The simulations of silica that I mentioned above are useful for imagining the deposition of an extremely strong liquid. For silica, the sample has already found the bottom of the amorphous portion of the PEL at temperatures well above T_g. This means any liquid-cooled glass already exists in one of the lowest possible minima. When preparing a vapor-deposited glass, the sample will end up in a minima quite similar to the one inhabited by the liquid-cooled glass, and thus we

won't get a stable glass. These first two requirements were important points of the discussion section for the paper presented in Chapter 3.

The third requirement is that the molecule cannot be "too good" of a crystallizer. The issue of unavoidable crystallization of the vapor-deposited glass was demonstrated by Katherine Whitaker in her attempts to prepare stable glasses of *trans*-decalin.[48] These samples crystallized during deposition or before they could be transformed into the supercooled liquid. I won't discuss the crystallization issue further since it was not an obstacle in this work, but it is an important possible hurdle to making stable glasses with physical vapor deposition.

1.5.6 Transformation mechanism of stable glasses

The mechanism for the transformation of stable glasses is distinct from liquid-cooled glasses, and is an important topic in this thesis. Thin films of stable glasses (less than ~ 1 μm) tend to transform via a front mechanism.[49–52] When the temperature is raised above T_g, the first molecules to transform into the supercooled liquid are those at the free surface. After top layer has transformed the next layer just below the free surface is then able to transform, and then layer below that, continuing through the film. This front transformation mechanism can be understood with the idea of kinetic facilitation. The molecules in the bulk of the stable glass are packed so well that they cannot move enough to transform even when the temperature is above T_g. However, molecules at the free surface don't have neighbors above them, so they have enough space to relax and transform. Once this top layer of molecules are mobile, it relives some of the packing constraints on the second layer which is then able to relax into the supercooled liquid. This front transformation mechanism of stable glasses is surprising because liquid-cooled

glasses appear to transform homogeneously.[49] However, in the short time since they were discovered, the transformation fronts have been characterized by multiple techniques,[49,51–54] explained by theory,[55,56] reproduced in simulations,[57] and researchers have even learned to manipulate the fronts.[58,59] My work in Chapter 2 provided the first quantitative description of how the front velocity varies during the time of a transformation (~ 4 % variation over time) and how the velocity varies for different locations in the sample (~ 26 % variation across space).

I'll briefly note that the transformation behavior of thicker stable glass films is different than for thin stable glass films, and is not well understood. A thick stable glass film (thicker than ~ 1 μm) will still possess a transformation front propagating from the free surface. However, after some amount of time, the bulk of the sample transforms on its own even though the front hasn't reached it yet.[60,61] For thin stable glasses when the transformation is dominated by the front mechanism, isothermal transformation times increase with film thickness. For thick stable glasses, the transformation is dominated by the bulk mechanism and isothermal transformation times are constant with respect to film thickness. There is not an explanation at the moment for how the bulk mechanism initiates or how it propagates.

1.6 Why study vapor-deposited glasses?

The study of vapor-deposited glasses contribute helps advance the overall understand of supercooled liquids and glasses. The issue of enhanced or limited surface mobility is important determining the properties of a vapor-deposited glass, so researchers in this particular field put a lot of effort in to measuring or deducing surface mobility. There are three glass transition theories that have been able to predict enhanced surface mobility (the Coupling Model, RFOT

and ECNLE).[39,41,62] As experiments continue to find molecules with limited surface mobility,[18,23] these theories will hopefully be improved to explain the wide variation of surface mobility for different molecules.

Vapor-deposited glasses also provide insight into what the potential energy landscape looks like at temperatures below T_g.[43] There has been much debate over what would happen to hypothetical equilibrium supercooled liquids at temperatures below T_g.[63] Experiments to measure τ_α of supercooled liquids even slightly below T_g are difficult to perform and the interpretation of these experiments is not always straight forward.[64–66] When we vapor-deposit molecules with enhanced surface mobility, those molecules explore portions the PEL that is otherwise inaccessible to bulk experiments. For example, calorimetry experiments on vapor-deposited ethylbenzene and ethylcylcohexane glasses have found that glasses prepared at $T_{substrate} = 0.92\ T_g$ have the enthalpy expected by extrapolating the supercooled liquid behavior.[44,67] An example of this data is in Figure 12. These data allow for the estimation of the supercooled liquid enthalpy for temperatures that would likely take years for a bulk sample to equilibrate. It may be the case that a fragile to strong transition occurs slightly below T_g for fragile supercooled liquids.[68,69] This transition would allow the equilibrium liquid to avoid the Kauzmann entropy crisis. If the PEL does bottom out just below T_g for a give molecule, there could be evidence of this in the behavior the vapor-deposited glasses. For temperatures below a fragile to strong transition, the material has found the bottom of the amorphous PEL, and the barriers to relaxation are constant with respect to temperature.[20] (Section 1.3) In such a scenario, the kinetic stability of vapor-deposited glasses would not increase for decreasing substrate temperatures

below the transition, even in the limit of low deposition rates. This behavior is actually seen in the ethylcyclohexane transformation time vs deposition rate data in Figure 11.[46] In the limit of low deposition rates, the kinetic stability increases as the substrate temperature is lowered to about 0.90 or 0.85 T_g, but the low deposition rate kinetic stability stops increasing for lower substrate temperatures (it actually begins to decrease). The data does not prove a fragile to strong transition, and such a transition wouldn't explain the decreasing plateau values for temperatures below 0.85 T_g. However, the data could reflect a change in the amorphous PEL at low temperatures, and deserves further consideration. I'll propose experiments related to this observation in Chapter 5.

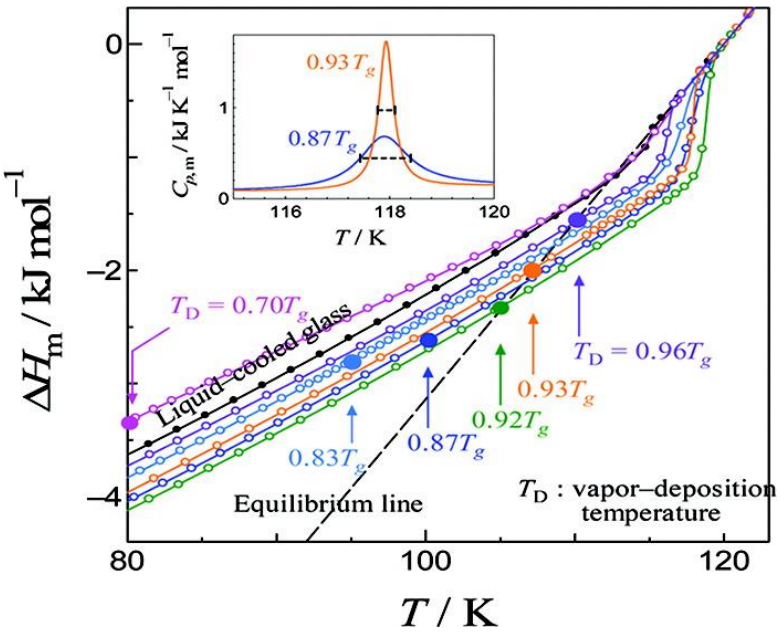

Figure 12: *The enthalpy of ethylbenzene glasses prepared by vapor deposition at 2 nm/s (colored symbols) and by liquid cooling at 10 K/min (black symbols).*[44] *The dashed line is an extrapolation of the supercooled liquid enthalpy. The solid colored circles plot the enthalpy of the vapor-deposited glass at the substrate temperature during deposition (T_D). From these colored solid circles we can see that the researchers were able to prepare a vapor-deposited glass at 0.92 T_g that has the expected enthalpy of the equilibrium supercooled liquid at 0.92 T_g. Figure reprinted with permission from reference 44. Copyright 2011 American Chemical Society.*

Vapor-deposited glasses are also important in current applications. Organic light emitting diodes are often prepared by vapor-deposition into the glass.[32] Having glassy materials avoids the issue of high electrical resistances at grain boundaries that exist in polycrystalline materials. Vapor-deposition is a good method for preparing glassy thin films and has been found to allow

for the control of molecular orientation in the glassy film. Recent experiments and simulations have led to a hypothesis of how molecular orientation can be tuned by vapor deposition.[34,70] Glasses with preferred molecular orientation can have greater performance in OLED devices by having improved electron and hole mobility and improved light output. The control of molecular orientation may also prove to be important for future types of thin film organic electronics.[32]

1.7 Experimental techniques used in this work

The characterization technique used in this thesis is alternating current nanocalorimetry. These devices are calorimeters built on a small chip. On the chip there is a small active area that is suspended above the device body and subject to measurement. Figure 12 provides photos of the device. By measuring a calorimetric signal for a small, suspended area, the heat capacity contribution of the device is very small, and allows us to measure the heat capacity of thin films with small masses (as small as nanograms). On the active area there are small resistors that can be used to heat the substrate and any sample that is present. There is also a series of thermocouple junctions that measure the difference between the temperature of the active area and of the frame of the device. During alternating current measurements, an AC voltage is provided to the resistive heaters which creates an oscillating heat input to the active area. The temperature on the active area oscillates, while the frame temperature remains constant. The applied power is small enough and the frame is far enough away that there is negligible change to the frame temperature as a result of this AC heating of the active area. The thermocouples will then produce an AC voltage that is proportional to this oscillating temperature difference. This temperature oscillation is on the order of 0.3 K.[71] The exact size of the temperature oscillation is

inversely proportional to the heat capacity of the active area and any film present on it. In order to improve the sensitivity of the technique, the AC heating voltage is provided to two nearly identical calorimeters in series. One of the calorimeters will have a sample on it while the other is kept empty as a reference. We then measure the difference between the thermocouple signals from the two calorimeters to remove the contribution from the device heat capacity. Since the two devices are not perfectly identical, we also measure the differential signal of the two empty calorimeters in order to correct for the slight difference between the devices.

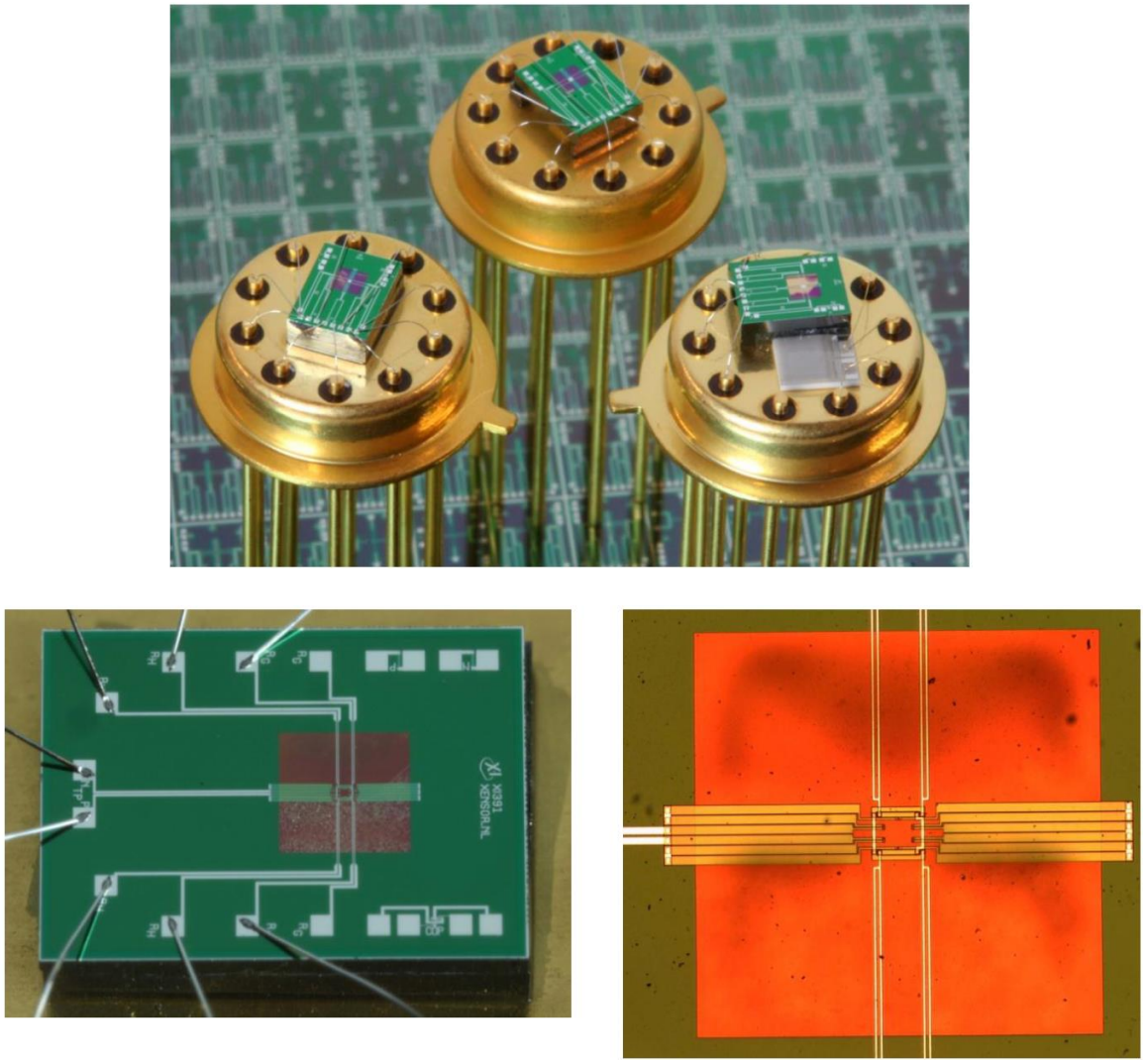

Figure 12: *Images of AC nanocalorimeter devices produced by Xensor Integration (The Netherlands).*[72] *The active area of the devices are the small square seen in the middle right of the lower left figure, and in the center of the lower right figure. In the lower left figure: The vertical leads are for the resistive heaters on the top and bottom of the active area. The horizontal leads are for the series of thermocouples with hot junctions on the left and right of the active area. The cold junctions of the thermocouples are just outside the orange square. Images are the copyright of Xensor Integration 2016.*

The advantage of doing an AC measurement is that it allows us to measure heat capacity quasi-isothermally. The measurement is quasi-isothermal because of the ~ 0.3 K temperature oscillation. This means that I can track the changing heat capacity during annealing experiments above T_g as a vapor-deposited glass transforms into the supercooled liquid. The one disadvantage of the AC technique is that it is not sensitive to irreversible changes to the heat capacity, which means my colleagues and I do not observe the heat capacity overshoot when a low enthalpy glass transforms into the supercooled liquid. Thus, the AC technique cannot measure the enthalpy of glasses.

The absolute temperature of the device can be measured by using the temperature dependent resistance value of the active area heater as a thermometer. As the temperature increases, the resistance of the active area heater also increases. The resistance values can be calibrated by measuring known phenomena in organic samples. My colleagues and I measure τ_α as a function of temperature for previously studied supercooled liquids, or measure first order phase transitions like plastic crystal phase transitions. Further discussion of the calorimeter construction, operation of the calorimeters, and temperature calibration can be found in references [71] and [54] and in the experimental sections of Chapters 2, 3 and 4.

The sample and reference calorimeters are held together in a copper housing with a cartridge heater and platinum RTD and attached to a copper liquid nitrogen reservoir to allow for temperature control. The liquid nitrogen cools the copper housing and temperature is then modified by using the cartridge heater to heat against the liquid nitrogen reservoir. Because of the location of the calorimeters, RTD, and cartridge heater with respect to the liquid nitrogen

reservoir, there exists temperature gradients (as large as 30 K) between the RTD and calorimeter. This is why it is best to use the resistance of the heaters on the calorimeters to determine absolute temperature. Despite the size of the temperature gradient, it is quite consistent, and the RTD can still be monitored to control the copper housing temperature.

The calorimeters in their housings are inside an ultra-high vacuum chamber that enables vapor deposition. The low base pressure of the chamber (~10^{-9} torr or better) ensures that during deposition, any contaminants in the film are kept to a minimum. The chamber is pumped by a turbomolecular pump that is in series with a scroll pump. The turbo pump exhausts to the scroll pump inlet and the scroll pump exhausts to atmosphere. Pumping in series is necessary because turbomolecular pumps are not able to exhaust to atmosphere. Both of these pumps are lubricant free to avoid diffusion of pump oils into the chamber that can occur with lubricated pumps. Under good conditions, my own experiments have shown that the deposition of contaminants onto the nanocalorimeters occurs at a rate of 10^{-5} nm/s or slower. This allows me to prepare films using very slow deposition rates and be confident that there is a high degree of sample purity.

For deposition, the molecules of interest are introduced into the chamber via a leak valve. The molecules in this work are all volatile liquids at room temperature, so they are kept as liquids in crucibles attached to the leak valves. An ion gauge is used to monitor the relative deposition rate. The absolute thickness can be determined by ellipsometry. There is a silicon wafer that is held in a temperature controlled copper housing and positioned next to the calorimetry devices. A special calorimeter housing has been made such that calorimeter receives the same deposition flux as the wafer. Then, an ellipsometry light source and detector can be attached to the chamber. Elliptically polarized light is directed onto the sample, interacts with the

film and wafer, and is reflected into the detector. The intensity and polarization state at each wavelength can be used to determine the index of refraction and thickness of the sample. The magnitude of the nanocalorimetry thermocouple signal is also measured during this deposition. In this way the nanocalorimetry signal can be calibrated for thickness. The development of the ellipsometery apparatus and procedures, and the performance of the measurements and analysis used in this work were done by my coworkers Shakeel Dalal and Diane Walters. Shakeel and Diane are experts in this technique. These in-situ ellipsometry experiments and analysis can be tedious, and I am very thankful for their efforts.

1.8 Contributions to the field from this work

This section will provide an outline of the following chapters in the thesis and briefly explain how each project contributed to the knowledge of vapor-deposited glasses. During the time that I've been working on this thesis, I think the fundamental study of vapor-deposited glasses has begun to make a significant transition. When I started studying the field, it seemed that the formation of stable glasses by organic molecules might be universal.[73] Scientists were working to understand how stable glasses form and understand why the exhibit the properties they do. Five or so years ago the major advancements in the field were: surface diffusion measurements of multiple molecules,[74,75] computer simulations that qualitatively replicate the creation and properties of a stable glass,[57,76] theoretical understanding of stable glass formation,[39,55] theoretical understanding of enhanced surface mobility,[39,41,62] and understanding why stable glasses transform via a front mechanism.[52,55,58,77] Stable glasses were being treated as a general phenomenon. The work in my thesis pioneered making deeper quantitative descriptions

of the front mechanism,[54] and brought to light the fact that some organic molecules can be vapor-deposited into a glass, but will not form a stable glass using standard preparation conditions.[5,23] I think the field is moving towards understanding the differences in properties between stable glasses, and understanding why some molecules struggle to form stable glasses.

Chapter 2 describes my work in analyzing the front mechanism during the transformation of methyl-*m*-tolutate stable glasses.[54] Previous work studying this front mechanism in stable glasses had described the front as propagating with a constant velocity,[49] but this had not been assessed quantitatively. In my work, I analyzed the front velocity as a function of time, and as a function of position. I found that the front velocity is constant over time with a variation of 4% or less. I was also able to analyze the spatial uniformity of the front velocity. The idea of spatial variation in the front is quite plausible given the established dynamic heterogeneity that is known to exist in supercooled liquids and glass.[8,12,78] However, this had not yet been connected to stable glass transformation fronts. I found that the front velocity varies by 26% or less across the area of the sample. Using a simple mathematical model, I connected the measure of spatial uniformity with the expected size of cooperatively rearranging regions in a typical glass. In future experiments, researchers could use this type of analysis to determine the size of cooperatively rearranging regions in a stable glass. My determinations of the growth front velocities as a function of temperature using AC nanocalorimetry experiments were in very good agreement with pervious work with methyl-*m*-toluate from the Ediger group that utilized dielectric spectroscopy. The agreement between techniques demonstrated our ability to accurately determine temperature and thickness in these experiments.

Chapter 3 describes my work characterizing the kinetic stability of vapor-deposited glasses of alcohol molecules.[5] There was a question if alcohol molecules could be used to prepare stable glasses, and we answered that question by showing at least one alcohol could form stable glasses when prepared with a typical deposition rate of 0.2 nm/s, while others alcohols formed glasses with limited kinetic stability at this deposition rate. This was the first paper to demonstrate a very wide range of abilities to form kinetically stable glasses. Benzyl alcohol could be used to prepare glasses with comparable kinetic stability to any other stable glass, while vapor-deposited glasses of propylene glycol had kinetic stabilities that were only slightly better than liquid-cooled glasses. I discussed the connection between the stable glass forming ability of the alcohol molecules with what is known from literature about the intermolecular hydrogen bonding of the bulk liquids. I then showed that there is a correlation between the kinetic stability of 18 vapor-deposited glasses with the supercooled liquid fragility of the same molecules. Authors have looked for this correlation before,[79,80] but with a smaller number molecules and only one measure of fragility. I showed a much better correlation with alternate measures of fragility and a larger number of molecules. This work concludes with an explanation of why supercooled liquid fragility could be expected to correlate with kinetic stability of vapor-deposited glasses.

Chapter 4 is recent work that performs a deposition rate study on a molecule that only makes a moderately kinetically stable glass when using typical deposition rates.[23] In the paper associated with Chapter 3 we hypothesized that 2-ethyl-1-hexanol did not form a stable glass with high kinetic stability because of limited surface mobility.[5] However, there are other possible explanations. The potential energy landscape may bottom out soon after T_g, or the preferred

surface configurations may not correspond to bulk configurations with high barriers to relaxation. I designed experiments to test these three hypotheses for why 2-ethyl-1-hexanol does not form a highly stable glass when deposited at 0.2 nm/s. The results are consistent with the hypothesis that stable glass formation for 2-ethyl-1-hexanol is inhibited by limited surface mobility. I was able to estimate the surface relaxation times ($\tau_{surface}$) for this molecule and found that they can be 4 orders of magnitude greater than $\tau_{surface}$ of molecules commonly used to prepare stable glasses at the typical deposition rate. I also found that some features of the $\tau_{surface}$ vs temperature data for several molecules are not described by theory, which invites further examination of our understanding of surface mobility in supercooled liquids and glasses.

The 5th and final chapter proposes future experiments that build on important topics from my work. I suggest experiments and glass-forming systems that will help develop quantitative predictions of hydrogen bonding influences surface mobility. I also advocate for a study to measure the kinetic stability of more stable glasses prepared at low deposition rates in order to learn about how the potential energy landscape evolves at temperatures below T_g.

I think the most important takeaway from this thesis is the demonstration that the ability to make a stable glass with high kinetic stability is not universal for organic molecules, and discussions that propose hypotheses for why some molecules can and cannot form stable glasses. For the first 5 years of stable glass research, it seemed that stable glass formation was universal, and there was a solid explanation for the phenomenon. There was even a paper published in 2010 called "Generality of forming stable organic glasses by vapor deposition."[73] The discovery of molecules that will not form stable glasses means that we must build nuance into our

understanding and explanation of vapor-deposited glasses. This work may also have implications for the applications of vapor-deposited glasses. Vapor-deposited glasses are used in organic electronics,[32] and work is ongoing to demonstrate and understand the ability for vapor deposition to tune the orientation of the molecules.[34,70] The work in this thesis suggests that functional groups may play a role in determining if there is enhanced surface mobility which allows molecules to explore configurations that are preferred at the surface and thus yield an oriented glass.

Chapter 2

Vapor-deposited glasses of methyl-*m*-toluate: How uniform is stable glass transformation?

M. Tylinski[A], A. Sepúlveda[A,B], Diane M. Walters[A], Y.Z. Chua[C], C. Schick[C], M.D. Ediger[A]

[A] Department of Chemistry, University of Wisconsin – Madison, Madison, Wisconsin 53706, USA

[B] Present address: Imec, Kapeldreef 75, 3001 Leuven, Belgium

[C] Institute of Physics, University of Rostock, Wismarsche Str. 43-45, 18051 Rostock, Germany

As published in The Journal of Chemical Physics, Volume 143, Article 244509, 2015

DOI: 10.1063/1.4938420

2.1 Abstract

AC chip nanocalorimetry is used to characterize vapor-deposited glasses of methyl-*m*-toluate (MMT). Physical vapor deposition can prepare MMT glasses that have lower heat capacity and significantly higher kinetic stability compared to liquid-cooled glasses. When heated, highly stable MMT glasses transform into the supercooled liquid via propagating fronts. We present the first quantitative analysis of the temporal and spatial uniformity of these transformation fronts. The front velocity varies by less than 4% over the duration of the transformation. For films 280 nm thick, the transformation rates at different spatial positions in the film differ by about 25%; this quantity may be related to spatially heterogeneous dynamics in the stable glass. Our characterization of the kinetic stability of MMT stable glasses extends previous dielectric experiments and is in excellent agreement with these results.

2.2 Introduction

Over the past 8 years, physical vapor deposition (PVD) has been used to prepare amorphous solids with properties that cannot be achieved with any other preparation method. These exceptional materials are called stable glasses because of their high kinetic stability in comparison with conventional liquid-cooled glasses.[34,42,44,46,48,61,67,73,81–90] Kinetic stability can be observed in two types of experiments. When the temperature of a stable glass is increased at a constant rate, it maintains glassy properties until higher temperatures than liquid-cooled glasses.[34,42,44,46,48,67,73,81–88,90] Alternately if a stable glass is held isothermally at an elevated temperature, the transformation into the supercooled liquid can take up to 10^5 times longer than the transformation of a liquid-cooled glass.[42,46,48,52,61,81,86,89] In addition to kinetic stability, stable

glasses have lower heat capacity,[42,45,46,48,86,91] lower enthalpy,[44,57,67,73,76,81,82,85,87,92–95] and lower molar volume in comparison with liquid-cooled glasses.[34,57,76,81,83,84,88,96] Stable glasses also often exhibit anisotropic packing.[34,70,76,87,88,96,97]

Perhaps the most surprising feature of stable glasses is the process by which they transform into the supercooled liquid when heated above the glass transition temperature T_g. While liquid-cooled glasses soften everywhere at once (at least when averaged over a scale of ~ 5 nm),[49] stable glasses have been shown to transform via propagating fronts.[45,49–52,57,58,60,61,89,93,94] The stable glass transformation is qualitatively similar to the melting of a crystal via a constant-velocity melting front.[98] For both crystals and stable glasses, the thermodynamically favored liquid state is achieved by a propagating front because the barriers for rearrangement inside the material are much higher than the barriers at a surface or interface. When thick stable glasses are annealed at high temperatures, a bulk-initiated process also contributes to the transformation.[45,60,61,93]

Experiments,[45,49–52,58,60,61,89,94] simulations,[57,93] and theory [55,56,59,77] have combined to provide a partial understanding of the propagating transformation fronts of stable glasses. Free surfaces and the interface between a stable glass and a liquid always initiate a transformation front. This behavior is qualitatively described by the idea of kinetic facilitation;[55,58,59] a molecule in the stable glass escapes its local packing environment only when neighboring molecules have high mobility, such as those in a liquid or at the free surface. It has also been observed that propagating fronts can initiate at interfaces with solid materials such as an underlying substrate;[51,89] for a given molecule, these substrate-initiated fronts may occur only for certain deposition conditions and this behavior cannot yet be predicted. Once a front is propagating

through a stable glass, it appears to move with approximately constant velocity at a given temperature. However, the uniformity of the front velocity over time has not been quantified. It is also unknown how uniform the front velocity is at different locations in the stable glass. Given that supercooled liquids and glasses are known to have spatially heterogeneous dynamics,[99] we would expect that front propagation cannot be completely uniform. Determining the variation of front velocities in a stable glass sample may inform us about the spatial heterogeneity present in stable glasses.

Here we investigate the temporal and spatial uniformity of propagating fronts that transform stable glasses. We used PVD to prepare stable glasses of methyl-*m*-toluate (MMT). MMT is a low fragility supercooled liquid and dielectric relaxation experiments recently demonstrated that it forms a stable glass via PVD.[61] The dielectric work showed that MMT stable glasses transform directly into the equilibrium supercooled liquid via propagating fronts and that surface-initiated fronts dominate the transformation for films thinner than 5 μm. We use AC nanocalorimetry in the current work to measure the reversing heat capacity of MMT stable glasses during transformation. The fast data acquisition rate of the AC nanocalorimetry technique provides detailed information about the propagating fronts during annealing experiments above T_g. We are able to control the number of propagating fronts during the transformation with a bilayer film geometry of a stable glass deposited on top of a liquid-cooled glass. This control allows us to quantitatively analyze the uniformity of the stable glass transformation.

For the 280 nm thick films of MMT stable glasses studied here, we find that the front velocity varies by less than 4% over time and we estimate that the spatial distribution of velocities has a FWHM of about 25%. The spatial distribution of velocities is consistent with our expectation of a stable glass that transforms via cooperatively rearranging regions with a size of 5 molecular diameters. We characterized the kinetic stability of the vapor-deposited glasses as a function of substrate temperature during deposition and obtain good consistency with previous dielectric spectroscopy experiments. The front velocities for transforming MMT stable glasses are also in excellent agreement with the previous measurements. We find that vapor-deposited MMT glasses have heat capacities that are up to 2.5% lower than the heat capacity of the liquid-cooled glass.

2.3 Experimental Methods

2.3.1 Materials

MMT with 98% purity was purchased from Alfa Aesar and used as received. The temperature dependence of the structural relaxation time (τ_α) of the supercooled liquid of MMT has been characterized by dielectric spectroscopy.[61,100,101] In this paper, we define T_g as the temperature where τ_α is 100 seconds. By this definition, T_g = 169 K.[61]

2.3.2 Apparatus

MMT films were prepared by physical vapor deposition in an ultra-high vacuum chamber. The chamber is pumped by an Edwards STP 1003 turbomolecular pump and backed by an Edwards XDS35i scroll pump. Typical base pressure is 1 x 10^{-9} torr. Nanocalorimeter devices and a silicon wafer for *in situ* ellipsometry are held in copper housings containing a cartridge

heater and Resistive Temperature Device (RTD). The housings are attached to a copper reservoir filled with liquid nitrogen. The temperature of the nanocalorimeters and the silicon wafer are controlled by using the cartridge heaters to heat against the cooling of the liquid nitrogen reservoir. MMT molecules are introduced into the chamber via a fine leak valve.

2.3.3 Nanocalorimeter devices

Vapor-deposited MMT glasses were studied using AC nanocalorimetry, a technique that has characterized other stable glass formers.[42,45,46,48,71,86,91] We use XEN-39391 chip nanocalorimeters by Xensor. The devices are similar to the calorimeters described in detail in reference 44. The membrane contains a resistor and a series of thermocouples integrated into a thermopile. The thermopile measures the difference in temperature between the active area of the membrane and the TO-5 housing that holds the chip. A 10 Hz AC voltage is applied to the device heater by the internal oscillator of a Signal Recovery 7265 DSP lock-in amplifier, creating a 20 Hz thermal oscillation on the membrane (amplitude ~ 0.3 K). The temperature oscillation is sensed by the thermopile and the amplitude and phase is determined by the lock-in amplifier. We measure a differential thermopile signal between a nanocalorimeter with a sample on it and a reference device. Since the two devices aren't identical, we also subtract a background measurement of the two empty devices. The resulting background-subtracted differential thermopile signal is closely related to the reversing heat capacity of the films. Determination of the absolute reversing heat capacity requires modeling and knowledge of the mass of the film that interacts with the device. In this paper, we only present the background-subtracted differential thermopile signal. Ahrenberg et al. compared the thermopile signal and reversing

heat capacity data of toluene glasses.[71] Based on their comparison, we do not expect any inaccuracy in our determinations of relative heat capacities, transformation onset temperatures, or quasi-isothermal transformation times. We also perform a 4-wire measurement of the resistance of the device heater. This resistance measurement is used to determine the temperature of the membrane as described below. Further details of the thermopile and heater resistance measurements can be found in reference 44. Recent publications have shown that the difference in thermal expansion coefficients of the organic glass and the silicon nitride substrate can create strain on the calorimeter surface.[42,48] In the experiments presented here, no strain correction was applied as the films are thin enough that any influence on the measured signals is negligible.

2.3.4 Nanocalorimeter temperature calibration

In order to determine the sample temperature during an experiment we measure the resistance of the nanocalorimeter heater and use a set of calibration experiments to calculate temperature from this resistance. To calibrate the heater resistance we cool the apparatus to the lowest achievable temperature. The source of liquid nitrogen is then turned off and the reservoir, housing and nanocalorimeter are allowed to slowly warm to ambient temperature while the cartridge heater is off. During this passive heating experiment the temperature gradient between the RTD and device membrane is minimized and the RTD value can be used to calibrate the heater resistance. We performed this passive heating experiment in vacuum and in a 220 torr nitrogen gas environment; these experiments agree to better than 1 K. These results are shown in Figure 1. We also checked the accuracy of the temperature calibration against the 20 Hz nanocalorimetry relaxation of ethylbenzene, toluene, isopropyl benzene, and propylene glycol.

We determined the membrane heater resistance value at the phase minima and plot the results in Figure 1 at the expected temperature of the 20 Hz structural relaxation based upon literature measurements.[102,103] We assume for ethyl benzene, toluene and isopropyl benzene that the relationship between dynamics and temperature is the same for measurements by dielectric spectroscopy and by AC nanocalorimetry. The 20 Hz relaxation data are in good agreement with the temperature calibration line. Thus we are confident that the reported temperature of the membrane is accurate to within 1 K.

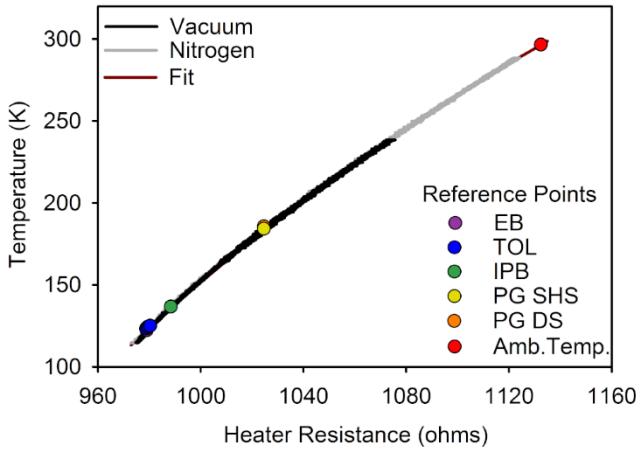

Figure 1: *Temperature calibration of a nanocalorimeter. Black and grey lines are passive heating experiments performed in vacuum and a 220 torr nitrogen atmosphere, respectively. The dark red line is a fit to the passive heating data and is behind the grey and black lines. The reference points plot the resistance of the 20 Hz phase minima from calorimetry vs the expected 20 Hz relaxation temperature from literature dielectric spectroscopy measurements of ethyl benzene (EB), toluene (TOL), isopropyl benzene (IPB).*[103] *We compare our 20 Hz phase minima to the 20 Hz relaxation temperature of propylene glycol as studied with specific heat spectroscopy (PG SHS), and with dielectric spectroscopy (PG DS).*[102] *The last reference point*

(Amb. Temp.) plots the heater resistance and RTD temperature at ambient temperature. We find good agreement between the reference points and the data from the passive heating experiments.

2.3.5 Determination of film thickness

We used *in situ* ellipsometry to calibrate the film thickness during deposition onto the nanocalorimeter. MMT molecules were deposited on a silicon wafer and a nanocalorimeter that are receptive to the same deposition angles and thus receive the same flux. We monitored the differential thermopile signal of the nanocalorimeter and measured the film thickness on the silicon wafer using ellipsometry. The results of this experiment are shown in Figure 2.

2.3.6 Ellipsometry Measurements

In situ ellipsometric measurements were made using a J. A. Woollam M-2000U spectroscopic ellipsometer. Measurements were made through windows on the vacuum chamber at an incident angle of 70 degrees. A silicon wafer with a 25 nm oxide layer was used as the substrate and was held in the vacuum chamber using a temperature-controlled copper housing, as described above. MMT was vapor deposited with the substrate held at 144.5 K. The thickness of the vapor-deposited organic film was determined by fitting the ellipsometric data in the wavelength range of 500 – 1000 nm using an anisotropic Cauchy model to describe the organic layer.[104] The MMT stable glasses have a birefringence of 0.014; this is within the range reported for other stable glass materials.[34,88,96,104,105]

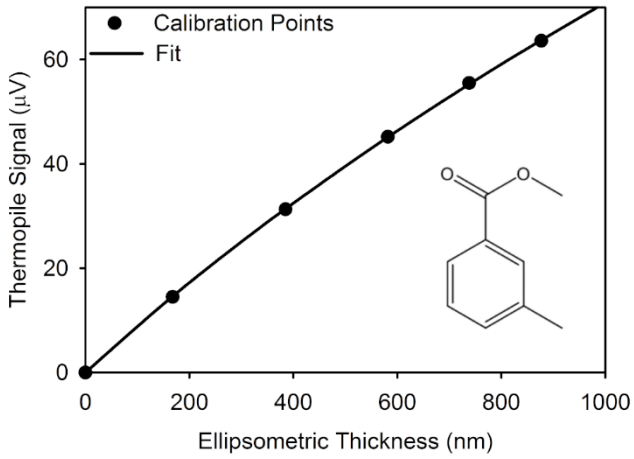

Figure 2: *Calibration of film thickness for AC nanocalorimetery by ellipsometry. The structure of methyl-m-toluate is included in the lower right.*

2.3.7 Deposition

Vapor-deposited MMT glasses were prepared using depositions at rates of 0.09 nm/s and 0.2 nm/s. During deposition the relative rate is monitored by the ion gauge pressure. Adjustment of the fine leak valve ensures a constant deposition rate. The absolute deposition rate is determined by the deposition time and final film thickness as calibrated by the ellipsometry measurements shown in Figure 2.

2.3.8 Temperature-ramping and quasi-isothermal annealing nanocalorimetry experiments

We performed temperature-ramping experiments and quasi-isothermal annealing experiments on vapor-deposited MMT glasses. After deposition and prior to these experiments, the chamber was filled with dry nitrogen at 220 torr to prevent desorption of the MMT. Films used in the temperature-ramping experiments were deposited at a rate of 0.09 nm/s. Their

thicknesses ranged from 130 nm to 250 nm. The temperature-ramping experiments were performed at a heating and cooling rate of 5 K/min. Thus the "liquid-cooled glass" mentioned throughout this paper is prepared by cooling the supercooled liquid at 5 K/min. Quasi-isothermal annealing experiments were performed on stable glasses deposited at 0.2 nm/s and at a substrate temperature at 0.84 T_g. These are the same conditions used in previous work.[61] The AC nanocalorimetry annealing experiments are quasi-isothermal because of the 0.3 K temperature oscillation used in the technique. We used two film geometries for the annealing experiments. Single layer films were prepared by depositing 250 nm of stable glass directly onto the calorimeter device. Bilayer films were prepared by depositing 280 nm of stable glass on top of a 250 nm thick liquid-cooled glass of MMT. For the quasi-isothermal measurements, films were heated at 8 K/min to the annealing temperature with a temperature overshoot of 0.1 K or less. During isothermal annealing, a data point was recorded every second. This acquisition time is 2 – 4 orders of magnitude faster than the stable glass transformation times in our experiments.

2.4 Results

2.4.1 Temperature-ramping experiments

Using temperature-ramping experiments, we observe that vapor deposition can prepare MMT stable glasses with lower heat capacities and higher onset temperatures than liquid-cooled glasses. The thermopile signal for a MMT stable glass is shown as the green line in Figure 3 while the black line is the signal for a 5 K/min liquid-cooled MMT glass. The thermopile signal measures the response of the sample to a 20 Hz temperature oscillation and is approximately proportional to the reversing heat capacity of the film. At low temperatures, both materials are

glasses and only vibrations (and any secondary relaxations) contribute to the reversing heat capacity. The reversing heat capacity of the stable glass is 2.1% lower than the liquid-cooled glass as shown by the blue arrows in Figure 3, indicating diminished contributions from vibrations, secondary relaxations, or both. As the liquid-cooled glass is heated above 170 K, the thermopile signal increases as a growing fraction of MMT molecules participate in structural relaxation at 20 Hz. The temperature at the midpoint of this step is in good agreement with the expected value from dielectric spectroscopy (183.2 K).[61] When the stable glass (green line) is heated, the heat capacity eventually increases when the stable glass packing is disrupted. As molecules transform from the stable glass into the supercooled liquid, they contribute to the 20 Hz reversing heat capacity via structural relaxation. The red dashed lines define the onset temperature for the stable glass transition. The stable glass in Figure 3 has a T_{onset} = 182 K which is 13 K above T_g. This elevated onset temperature quantifies the ability of the stable glass to retain solid-like packing and is a signature of kinetic stability.

The heat capacity and onset temperature of vapor-deposited MMT glasses depend on the substrate temperature during deposition. Figure 4A plots the fractional heat capacity decrease of the vapor-deposited glasses as a function of substrate temperature. The largest change in the heat capacity is obtained when MMT is deposited at substrate temperatures in the range of 0.75 – 0.85 T_g. A similar trend is seen in Figure 4B which plots the onset temperature (red circles) as a function of substrate temperature. A maximum onset temperature of 182 K is obtained by depositing MMT glasses at temperatures between 0.75 and 0.85 T_g.

Figure 4B shows that the kinetic stability of vapor-deposited MMT glasses depends on the substrate temperature during deposition in a manner that qualitatively agrees with previous

work. Dielectric spectroscopy experiments on vapor-deposited MMT glasses used a different measure of kinetic stability,[61] and those data are plotted as black squares in Figure 4B. That work measured the transformation time of 1 μm thick MMT films during isothermal annealing experiments at 177 K. While the quantitative relationship between the datasets is dependent on our choice of y-axis scaling, the overlapping datasets illustrate that both measures of kinetic stability have a very similar dependence on substrate temperature during deposition.

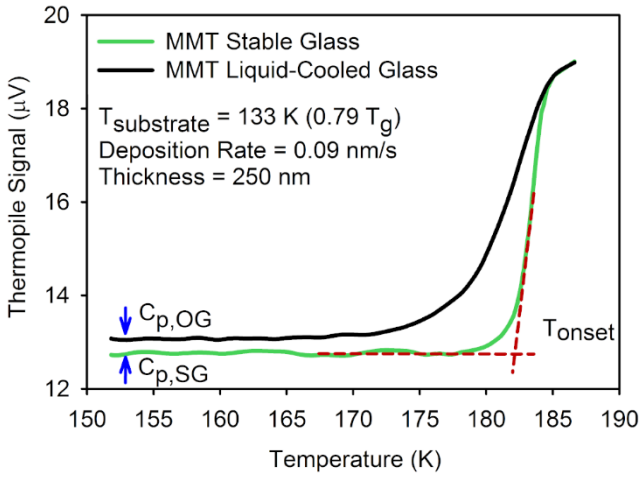

Figure 3: *Thermopile signal (proportional to reversing heat capacity at 20 Hz) of a stable glass (green) and liquid-cooled glass (black) during a temperature-ramping experiment. The stable glass has a decreased heat capacity compared to the liquid-cooled glass (blue arrows) and a delayed onset temperature for transformation into the supercooled liquid (red dashed lines).*

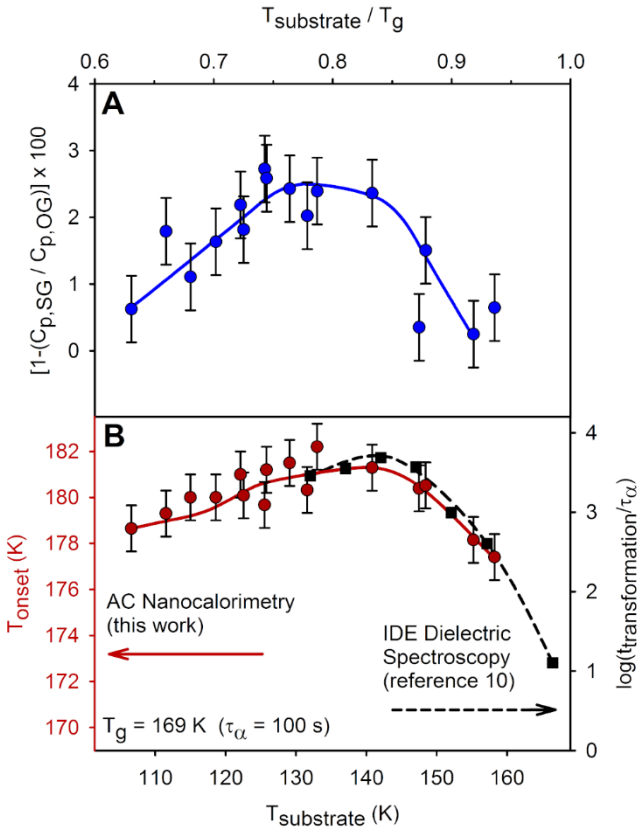

Figure 4: *The fractional heat capacity decrease (4A) and onset temperature (4B, red circles) of vapor-deposited MMT glasses depend on the substrate temperature during deposition. Both characteristics are maximized with deposition near 0.8 T_g. Black squares in Figure 4B plots $\log(t_{transform}/\tau_\alpha)$ vs $T_{substrate}$ data for isothermal transformations of 1 μm films measured by dielectric spectroscopy.*[61] *The two data sets in Figure 4B show very similar relationships between kinetic stability and substrate temperature during deposition.*

2.4.2 Single layer annealing experiments

We performed quasi-isothermal annealing experiments to provide a detailed view of the propagating fronts responsible for the transformation of MMT stable glasses into the supercooled liquid. Quasi-isothermal transformations of single layer stable glass films are shown in Figure 5; these MMT glasses were vapor-deposited at 0.84 T_g at 0.2 nm/s. The thermopile signal increases as an increasing fraction of the sample is transformed into the supercooled liquid and then plateaus when the transformation finishes. Larger increases in the thermopile signal are observed for films annealed at higher temperatures because the 20 Hz reversing heat capacity of the MMT supercooled liquid increases over this range of annealing temperatures. The transformation times are determined by the intersection of the black lines (shown for two annealing temperatures) and decrease with increasing annealing temperature. The transformation times indicate high levels of kinetic stability. For example, the transformation time at 172.5 K is about 10000 s while τ_α for the supercooled liquid at this temperature is about 7 s;[61] the transformation of a liquid-cooled glass is expected to occur on the timescale of τ_α.

Unexpectedly, the data in Figure 5 show an increase in slope during the transformation. As we discuss below, we interpret this result to mean that the film initially transforms by one front initiated from the free surface. After an induction time a second transformation front is initiated from the substrate and the film finishes transforming via these two fronts.

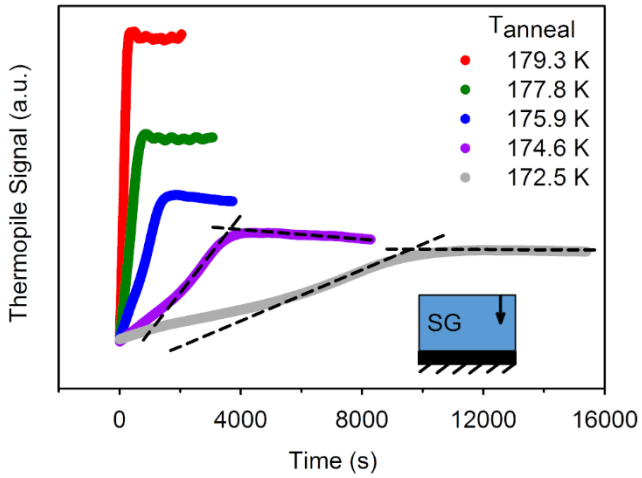

Figure 5: *Quasi-isothermal annealing experiments of 250 nm thick MMT stable glasses deposited directly onto the nanocalorimeter. The intersection of the black dashed lines defines the transformation time and is shown for select annealing temperatures. The illustration suggests a stable glass transforming via a single front, but the nonlinear shape of the data suggests a second front initiated at the substrate after an induction time.*

2.4.3 Bilayer annealing experiments

In order to control the number of propagating transformation fronts in MMT stable glasses, we have prepared bilayer samples by depositing a stable glass on top of a liquid-cooled glass. Upon annealing at temperatures above T_g, the liquid-cooled glass layer transforms into the supercooled liquid almost instantaneously (at least a thousand times faster than the stable glass layer). The interface of supercooled liquid and a stable glass is known to initiate a propagating front without any induction time.[58] Thus we interpret the data on bilayer films in terms of the two front mechanism illustrated in Figure 6.

Quasi-isothermal annealing experiments on bilayer MMT films yield constant transformation rates as seen in Figure 6. The constant slope in the data is consistent with two fronts of constant velocity that are both present throughout the transformation. The transformation rates for the single layer films are about 35% slower than for the bilayer films, which is consistent with our interpretation of the transformation mechanisms. We make a quantitative analysis of the front uniformity below.

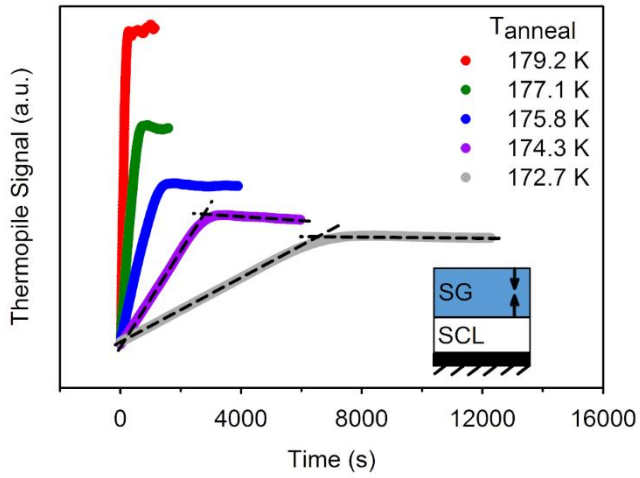

Figure 6: *Quasi-isothermal annealing experiments of bilayer MMT films. The films consist of a 280 nm stable glass on top of a 250 nm liquid-cooled glass. The intersection of the black dashed lines defines the transformation times and is shown for two annealing temperatures. These films transform via two fronts as indicated by the illustration.*

2.5 Discussion

2.5.1 PVD glasses of MMT as a function of substrate temperature

The data in Figures 3 and 4 demonstrate that vapor deposition can prepare MMT glasses with low heat capacity and high kinetic stability. The stable glasses prepared by depositing at a substrate temperature of 0.8 T_g have a reversing heat capacity that is 2.5% lower than the liquid-cooled glass. When this stable glass is heated at 5 K/min it maintains glassy properties well beyond the conventional glass transition temperature and doesn't transform into the supercooled liquid until 13 K above T_g. These results are in good agreement with those obtained for other vapor-deposited organic molecules. The largest onset temperature observed here for MMT is about 1.075 T_g. Data for PVD glasses of 7 other organic molecules show maximum onset temperatures from 1.05 to 1.07 T_g.[42,46,48,86,96] We used a slower deposition rate and faster temperature-ramping rate compared to other works; these variables will slightly increase T_{onset} and thus the maximum onset temperature for an MMT stable glass is similar to other systems. The maximum heat capacity decrease of 2.5% observed for MMT is typical for stable glasses.[42,45,46,48,86,91]

The properties of MMT stable glasses (and those of other organic molecules) can be rationalized with the hypothesis that enhanced surface mobility[43,75,81] at temperatures below T_g allows the PVD film to access minima low in the potential energy landscape. During deposition, this mobility allows each molecule to attain a near-equilibrium packing configuration before it is buried by subsequent deposition. These low energy configurations, which otherwise could not be attained except by extended physical aging, have high barriers for rearrangement and thus

PVD glasses can have high kinetic stability. At low substrate temperatures, there is insufficient surface mobility for this equilibration process and thus kinetic stability will be maximized for some substrate temperature not too far below T_g. The two data sets in figure 4B show that the optimal substrate temperature for producing highly stable MMT glasses is similar when measured by different experiments. The most stable PVD glasses also exhibit reduced heat capacity when compared to the liquid-cooled glass. The heat capacity of glasses can be attributed to vibrational frequencies, vibrational anharmonicities, and secondary relaxations.[106] A recent publication found that secondary relaxation is suppressed in stable glasses and this may be generally responsible for the reduced heat capacity.[107]

2.5.2 Bilayer films provide control over stable glass transformation behavior

Isothermal annealing experiments on stable glasses can reveal detailed information about the mechanism by which a stable glass transforms into a supercooled liquid. Prior work has shown that thin stable glass films transform via fronts that propagate at approximately constant velocity,[45,49–52,57,58,60,61,89,93,94] and this transformation mechanism can be rationalized with the concept of kinetic facilitation.[55,58,59] The molecules in the stable glass are packed so well that an average molecule cannot gain mobility until some of its neighbors become mobile. Molecules at the free surface have fewer neighbors and have been found to be more mobile than molecules in the bulk.[17,37,57,74–76,108] Thus the free surface acts as a source of mobility and always initiates a front during stable glass transformation. Other interfaces such as the substrate can also initiate fronts, but we do not understand what conditions give rise to substrate-initiated fronts.[51,89] When thick stable glasses are transformed, an additional transformation process initiates in the bulk of

the film.[45,60,61,93] Previous work on MMT stable glasses determined that the front mechanism dominated the transformation of films as thick as 5 microns.[61] Since the quasi-isothermal experiments done in this work used 250 nm and 280 nm thick stable glass films, we do not further consider the bulk mechanism.

The single layer annealing experiments in Figure 5 suggest transformation initially controlled by a front at the free surface with a second front (initiated at the substrate) contributing at later times. Such a scenario has been observed with ellipsometry for stable glasses of TPD.[89] Since the AC nanocalorimetry technique cannot directly detect the location or number of propagating fronts in the sample, we cannot be certain of this hypothesis. However, we can show that the observed transformation data are reasonably consistent with such a scenario. The transformation rate near the end of the single layer experiments are within about 25% of the bilayer film transformation rates in Figure 6.

The data in Figure 6 are consistent with the view that there are two growth fronts in bilayer annealing experiments and that both are present throughout the transformation. The bilayer geometry consists of a stable glass that has been deposited on top of a liquid-cooled glass. When the bilayer film is heated above T_g to the annealing temperature, the liquid-cooled glass transforms much faster than the stable glass. The resulting layer of supercooled liquid is a source of mobility and will initiate a propagating front without any measureable induction time, as has been shown in secondary ion mass spectrometry experiments of indomethacin stable glasses.[58] Since we are confident that we know how the bilayer films transform, we will use the data in Figure 6 in further analysis. This data provides access to the average velocity of the two

propagating fronts; for indomethacin stable glasses, fronts moving in opposite directions have velocities that differ by a factor of about two.[58]

2.5.3 Uniformity of the propagating transformation fronts

We can use the variation in the value of the first derivative of the thermopile signal with respect to time to determine the extent to which the stable glass transformation proceeds at a constant velocity. Figure 7A plots the first derivative for select data from Figure 6. The x-axis has been normalized by the value of $t_{transformation}$ determined from Figure 6. The values of the first derivatives have also been normalized for the purpose of plotting the data sets together. The variation of the first derivatives (and thus the variation in front velocity) is less than 4% at times up to 0.63 $t_{transformation}$. This very small variation indicates that the structure of the vapor-deposited film is uniform throughout its thickness and is consistent with previous qualitative statements that propagating fronts transform stable glasses at constant velocity.[45,49–52,57,58,60,61,89,93,94] It would be interesting to compare this temporal uniformity in melting rate with analogous data for organic crystals.

We are also able to investigate the uniformity of the propagating front velocity from location to location across the stable glass. We determine the spatial distribution of the transformation times by measuring the width of the second derivative of the thermopile signal with respect to time. The rounded transition from the linearly increasing to constant thermopile signal (as seen in Figure 6) creates the minimum in the second derivative in Figure 7B. The width of this feature is due to a range of finishing times across the sample and thus characterizes

the distribution of transformation times. The full width at half maximum (FWHM) values are 39% and 43% of $t_{transformation}$ for the two experiments shown.

The distribution of transformation times shown in Figure 7B is partially due to spatial variations in the front velocity but also reflects experimental factors such as thickness or temperature differences across the sample. We can estimate the contribution of temperature and thickness gradients as follows. We determined the size of the temperature gradient across the sample to be about 0.5 K by observing the width of the change in thermopile signal during a first order phase transition. Given the temperature dependence of the transformation rate shown in Figure 6, this would explain a 20% variation in finishing times. The thickness gradient in our sample can be estimated by considering the experimental geometry. The calorimeter used for these experiments receives molecular flux during deposition through a hole in its copper housing. Using conservative estimates of the calorimeter position and effective sample area, the thickness gradient could explain a 5% variation in finishing times. By assuming that the thickest regions of the sample are also at the lowest temperature, the widest distribution of finishing times due to these experimental factors would have a FWHM of 25%, which is less than what we observe in Figure 7B.

Even in the absence of temperature and thickness gradients, we expect that some spatial variation in finish times will be an intrinsic feature of transforming stable glasses. In a very simple model, we could treat a 280 nm film as being constructed of independent columns of MMT molecules, each ~ 430 molecules thick (taking the molecular size as 0.65 nm). We imagine a Poisson process that controls the time required to transform every column, with the distribution of times required to transform each layer being determined by the average front

velocity from the experiments. In this scenario, the Poisson distribution gives the distribution of finishing times across all the columns. For a process involving 430 steps, the FWHM will be 11%. This model is certainly oversimplified in many respects but we will improve upon one particular aspect. It has been suggested that molecules in supercooled liquids are part of cooperatively rearranging regions (CRRs);[99] in this case, it is likely that the front in a stable glass actually propagates as entire groups of molecules transform together. The diameter of a CRR in a supercooled liquid at T_g has been estimated to be 5 molecular diameters by Random First Order Transition theory.[78,109] If we re-envision the transformation from this perspective, the Poisson process would involve only 86 steps and the expected FWHM in Figure 7B would be 25% (dashed line). If we apply our earlier estimates of thickness and temperature gradients to this revised Poisson model with 5 molecules per layer, we calculate a distribution of finish times that matches the experimental data (solid line in Figure 7B).

The primary purpose of our analysis of the second derivative data is to demonstrate how close inspection of annealing experiments might teach us about the nature of spatial heterogeneity in stable glasses. Clearly there are important assumptions in the calculations presented in the previous two paragraphs, e.g., the assumption that neighboring columns of stable glass molecules transform independently. Future work with more precise control over thickness and temperature should be able to better quantify the spatial distribution of transformation velocities.

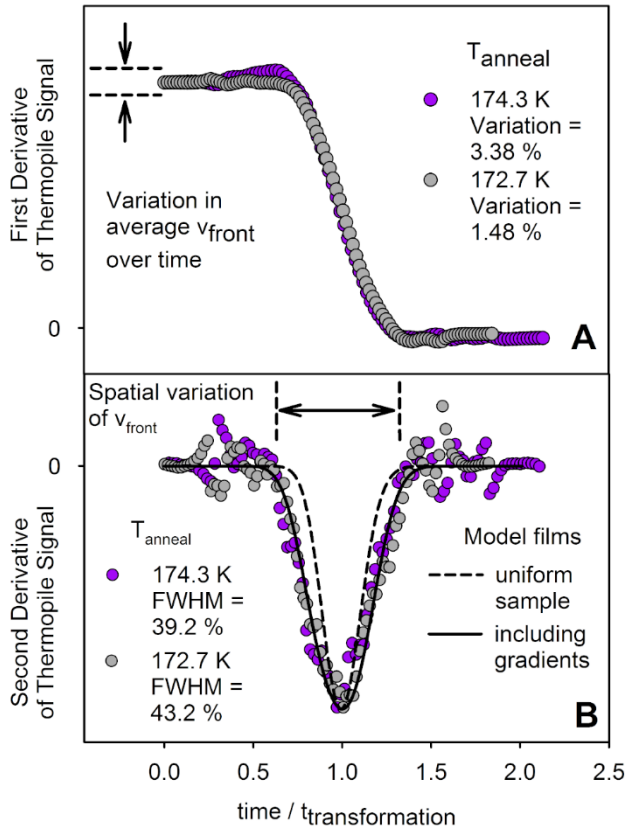

Figure 7: *First and second derivatives of the bilayer film transformation data from Figure 6. A: The first derivative of the transformation data shows a very small range of values up to* $t_{transformation} = 0.63$*, indicating that the front velocity is nearly constant during transformation. B: The second derivative of the transformation data shows a negative peak with the width indicating a distribution of transformation times across the film. The observed width is controlled both by the material response and experimental factors. The dashed line is for a model film with uniform sample thickness and temperature. The solid line is for a model film that contains a gradient in temperature and thickness similar to what is present in our experiments. In both cases, it is*

assumed that a cooperatively-rearranging group of molecules transforms as one unit. In both panels, the experimental first and second derivatives are normalized in order to plot the data sets together.

2.5.4 Consistent kinetic stability as measured by different techniques

The kinetic stability of vapor-deposited MMT glasses reported here is consistent with previously reported dielectric measurements.[61] One comparison was shown in Figure 4B and discussed above. A more direct comparison is shown in Figure 8. Here we observe excellent agreement between the transformation front velocities determined by nanocalorimetry (from Figure 6) and dielectric spectroscopy. The front velocity is a function of annealing temperature, with faster moving fronts at higher temperatures. The agreement between the two techniques is highly gratifying and supports the accuracy of the independent temperature and film thickness determinations utilized in these experiments. Assuming that each technique accurately determines thickness, the relative error in annealing temperatures is 0.8 K or less.

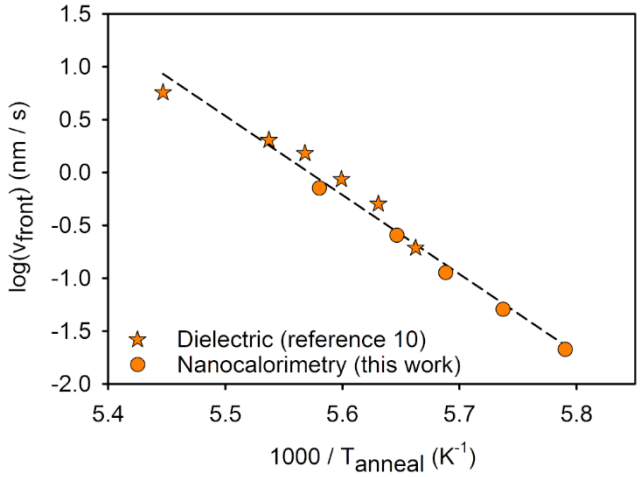

Figure 8: *Transformation front velocities from quasi-isothermal annealing experiments as a function of annealing temperature. Stars are from dielectric spectroscopy experiments in reference 10 and circles are nanocalorimetry experiments from the current work. These samples were all deposited at 0.84 Tg and 0.2 nm/s.*

2.5.5 Comparison of transformation velocities for stable glasses of different organic molecules

The propagating front velocities and their dependence on annealing temperature for MMT stable glasses are similar to those of stable glasses of other molecules. We plot front velocities as a function of structural relaxation time of the supercooled liquid at the annealing temperature (τ_α) for seven stable glasses in Figure 9. The nearly consistent negative slopes of the data sets reveal that supercooled liquid dynamics influence the propagating transformation fronts. If the process of structural relaxation directly controlled the front velocity, we would expect the front velocity to scale with τ_α^{-1} (a slope of -1 in Figure 9). The data in Figure 9 is not

quite consistent with this view as the stable glasses have slopes between -0.7 and -0.9. As discussed previously, it is possible that the self-diffusion coefficient provides a more direct correlation with the front velocity.[50]

As shown in Figure 9, the transformation front velocities of MMT stable glasses are slightly faster than other stable glasses. The deposition rates for all the stable glasses in Figure 9 is 0.2 nm/s,[46,50,61,89] with the exception of toluene and ethylbenzene for which a 2 nm/s deposition rate was used.[86] If toluene and ethylbenzene stable glasses were deposited at 0.2 nm/s we would expect them to transform via fronts with slower velocities. Using the transformation front velocity as a metric, PVD glasses of MMT are the least stable of this group.

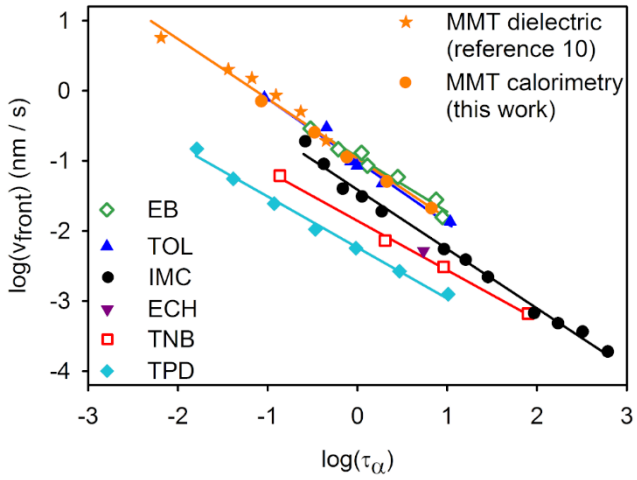

Figure 9: *Transformation front velocity as a function of τ_α at the annealing temperature for stable glass formers. MMT,[61] indomethacin (IMC),[50] α,α,β tris-naphylbenzene (TNB),[50] ethyl cyclohexane (ECH),[46] and N,N'-bis(3-methylphenyl)-N,N'-diphenylbenzidine (TPD)[89] stable glasses were deposited at about 0.85 T_g and 0.2 nm/s. Toluene (TOL) and ethylbenzene (EB)*

stable glasses were deposited at 0.9 T_g and 2 nm/s.[86] *We expect that TOL and EB would have lower front velocities if deposited at 0.85 T_g and 0.2 nm/s.*

2.6 Conclusions

We have used in situ AC nanocalorimetry to study vapor-deposited glasses of MMT. Via physical vapor deposition, MMT can form glasses with enhanced kinetic stability and up to 2.5 % lower heat capacity than liquid-cooled glasses. Stable glasses of MMT transform via propagating fronts and we performed the first quantitative analysis of the uniformity of these fronts. The front velocity varies by less than 4% over time which is consistent with previous qualitative statements that stable glasses transform via constant velocity fronts. We estimate that the spatial distribution of front velocities has a FWHM of approximately 25%. This estimate is consistent with our expectation for a stable glass that transforms via cooperatively rearranging regions of 5 molecular diameters. Our characterization of kinetic stability and measurement of front velocities extend previous measurements from dielectric spectroscopy experiments. The excellent agreement in front velocities supports the accuracy of thickness and temperature determination for each technique.

Our analysis of the quasi-isothermal annealing experiments demonstrates new methods to investigate the uniformity of the propagating fronts that transform stable glasses. A detailed investigation requires control over the number of fronts present during the stable glass transformation. We demonstrated the utility of creating bilayer stable glass films that transform via two fronts without any induction time. Future experiments with more precise control over

sample thickness and temperature could further quantify the spatial uniformity of the propagating fronts and potentially further enhance our knowledge of spatially heterogeneous dynamics in stable glasses.

2.7 Acknowledgments

We thank the U.S. National Science Foundation (No. CHE 1265737) and the German Science Foundation (No. DFG-SCHI 331 14-1) for support of this work.

Chapter 3

Vapor-deposited alcohol glasses reveal a wide range of kinetic stability

M. Tylinski[A], Y. Z. Chua[B], M. S. Beasley[A], C. Schick[B], and M. D. Ediger[A]

[A] Department of Chemistry, University of Wisconsin–Madison, Madison, Wisconsin 53706, USA

[B] Institute of Physics, University of Rostock, Albert-Einstein-Str. 23-24, 18051 Rostock, Germany and Competence Centre CALOR, Faculty of Interdisciplinary Research, University of Rostock, Albert-Einstein-Str. 25, 18051 Rostock, Germany

As published in The Journal of Chemical Physics, Volume 145, Article 174506, 2016

DOI: 10.1063/1.4966582

3.1 Abstract

In situ AC nanocalorimetry was used to characterize vapor-deposited glasses of six mono- and di-alcohol molecules. Benzyl alcohol glasses with high kinetic stability and decreased heat capacity were prepared. When annealed above the glass transition temperature T_g, transformation of these glasses into the supercooled liquid took $10^{3.4}$ times longer than the supercooled liquid relaxation time (τ_α). This kinetic stability is similar to other highly stable organic glasses prepared by vapor deposition and is the first clear demonstration of an alcohol forming a stable glass. Vapor deposited glasses of five other alcohols exhibited moderate or low kinetic stability with isothermal transformation times ranging from $10^{0.7}$ to $10^2\tau_\alpha$. This wide range of kinetic stabilities is useful for investigating the factors that control stable glass formation. Using our current results and literature data, we compare the kinetic stability of vapor deposited glasses prepared from 14 molecules and find a correlation with the value of τ_α at 1.25 T_g. We also observe that some vapor-deposited glasses exhibit decreased heat capacity without increased kinetic stability.

3.2 Introduction

Physical vapor deposition can be used to prepare glasses with high kinetic stability, known as stable glasses.[42,44–46,61,81,82,90,94] When heated, stable glasses retain their glassy structure until temperatures well above T_g.[42,44,81,82,90,94] Additionally, if a stable glass is annealed at a temperature T_{anneal} above T_g, the transformation into the supercooled liquid can take 10^5 times longer than the supercooled liquid structural relaxation time ($\tau_\alpha(T_{anneal})$).[42,45,46,61,81] For comparison, a liquid-cooled glass transforms in roughly 1 τ_α in such an annealing experiment.

The formation of stable glasses is thought to be enabled by enhanced surface mobility of molecules at temperatures below T_g.[43,75,81] During deposition at temperatures near ~0.8 T_g, molecules at the surface of a growing film have enough mobility to find low energy packing configurations. After being buried by further deposition, these configurations have high barriers to rearrangement, leading to the high kinetic stability observed in experiments. When compared to liquid-cooled glasses, stable glasses can also have lower enthalpy,[44,81,82,94] lower molar volume,[34,80,81,83,88] and lower heat capacity.[42,91] Since their discovery in 2007, stable glasses have been prepared from 28 organic molecules.[34,42,46,48,61,67,73,81–85,87,88,110] The properties of stable glasses have also been qualitatively replicated in simulations.[55,57,76,92,93,111]

Despite the many molecules that have been used to prepare stable glasses by vapor deposition, there have been a few cases in which stable glass formation has not occurred in the expected range of substrate temperatures. Some molecules crystallize too readily to prepare vapor-deposited glasses.[48] Other molecules, when vapor deposited using conditions expected to yield stable glasses, yield glasses with low kinetic stability.[79,112–114] For this paper, it is useful to define a "stable glass forming ability" which is analogous to glass forming ability. While glass forming ability might be assessed by determining whether or not crystallization occurs when cooling at a given rate, stable glass forming ability can be assessed by comparing the kinetic stability of vapor-deposited glasses prepared at a given deposition rate.

One proposed indicator of stable glass forming ability is supercooled liquid fragility. There are many ways to characterize how the temperature-dependent dynamics of a liquid deviate from Arrhenius behavior, but fragility is most often expressed by the fragility index *m*.

$$m = \left.\frac{d\log(\tau_\alpha)}{d\,T_g/T}\right|_{T_g} \quad (1)$$

Yu and Samwer deposited glasses of a metallic alloy with a low value of *m* and reported enhanced kinetic stability.[79] However the transformation temperature upon heating was only about 1.02 T_g in comparison to the value of 1.05 T_g that has often been observed for stable glasses of organic molecules.[42,46,48,54,85,86,96,110] Yu and Samwer reported a moderate correlation between the transformation temperature of the vapor-deposited glasses and the fragility index *m* of the corresponding supercooled liquid. Molecules with larger values of *m* generally produced glasses with higher transformation temperatures relative to T_g.[79] At about the same time, Ishii and co-workers found a correlation between *m* and the ability to form dense glasses via physical vapor deposition. In particular, two molecules with relatively low *m*, ethylcyclohexane (*m* = 57) and butyronitrile (*m* = 56) were reported not to form dense glasses.[80] Given the common correlation between kinetic stability and density in stable glasses, one might expect based upon this that low *m* molecules would not be able to form stable glasses.[103] However, it was later established that vapor-deposited glasses of methyl-*m*-toluate (*m* = 60) and ethylcyclohexane (*m* = 57) can exhibit high kinetic stability.[46,61,67] At present, glasses with high kinetic stability have been prepared from molecules with *m* ranging from very high (*m* = 146)[48] to moderately low (*m* = 57)[46,67]. Thus it seems unlikely that *m* is a good predictor of stable glass forming ability in this range. However, it has been argued that substances with very low values of *m* (approaching the strong liquid limit of *m* = 16) will not be able to form stable glasses.[115]

Molecules with extensive hydrogen bonding, particularly those with hydroxyl groups, may have difficulty forming stable glasses based upon the information presently available.

Wübbenhorst and coworkers have prepared vapor-deposited glasses of glycerol and two longer chain polyols. The deposition of these molecules yields glasses that, when heated, produce liquids with very interesting properties, including longer relaxation times and increased orientational order in comparison to the ordinary supercooled liquid.[112,113] However, the as-deposited glasses do not seem to exhibit substantial enhanced kinetic stability. Sepúlveda and coworkers have prepared vapor-deposited glasses of water using a wide range of substrate temperatures but did not report stable glass formation.[114] While Souda prepared n-propanol, ethanol and methanol glasses by vapor deposition, the substrate temperature was low enough that no conclusive statement can be made about stable glass formation.[116] Thus at present there is no clear example of an alcohol that can vapor-deposited into a glass with high kinetic stability. Recent experiments by Chen and co-workers provide a reason why it may be difficult to form stable glasses from alcohols.[18] They reported that the surface diffusion coefficients at T_g for three polyols (sorbitol, maltitol, and maltose) are at least four orders of magnitude smaller than for organic molecules with no hydrogen bonding. This suggests that the surface mobility needed during deposition to achieve efficient packing may not be available for such extensively hydrogen bonded systems.

In the current work, we survey the stable glass forming ability of alcohols by vapor-depositing glasses of six alcohols and characterizing them with AC nanocalorimetry. The molecules we have selected are shown in Figure 1 and include mono- and di-alcohols, aromatic and aliphatic molecules, and short and long alkyl chains. One of the molecules, benzyl alcohol, has the additional feature of being a structural analog of ethylbenzene, a well-studied stable glass forming molecule.[44,83,86,90] We use two experiments to test the kinetic stability of vapor-

deposited glasses. We measure the transformation temperature of the glass during a temperature ramping experiment and compare it to T_g. For stable glasses, this transformation temperature is often 5% higher than T_g.[42,46,48,54,85,86,96,110] In a second test, we perform isothermal annealing experiments at temperatures above T_g and use the reversing heat capacity to track the transformation of the as-deposited glass into the supercooled liquid.

We observe a wide range of stable glass forming ability in our survey of vapor-deposited alcohols. We prepared glasses with high kinetic stability from benzyl alcohol, which is the first clear demonstration of an alcohol forming a stable glass. Glasses of 2-ethyl-1-hexanol and ethanol exhibited at most moderate kinetic stability, and we were not able to prepare glasses with enhanced kinetic stability from ethylene glycol, n-propanol, or propylene glycol. We combine our measured kinetic stability results with data from 8 previously studied stable glass formers to investigate factors that may correlate with stable glass forming ability.[42,46,50,54,61,86,89] We find that stable glass forming ability correlates reasonably well with the supercooled liquid τ_α at 1.25 T_g; this value is a measure of liquid fragility and our consideration was inspired by the recent observation that a closely related quantity correlates with the surface diffusion coefficient at T_g.[18] Two more commonly used measures of fragility (*m* and $F_{1/2}$) do not correlate as well with stable glass forming ability. Vapor-deposited glasses of benzyl alcohol and 2-ethyl-1-hexanol were observed to have decreased heat capacities relative to the liquid-cooled glasses. At some deposition temperatures, vapor-deposited glasses of 2-ethyl-1-hexanol exhibit decreased heat capacity without having increased kinetic stability.

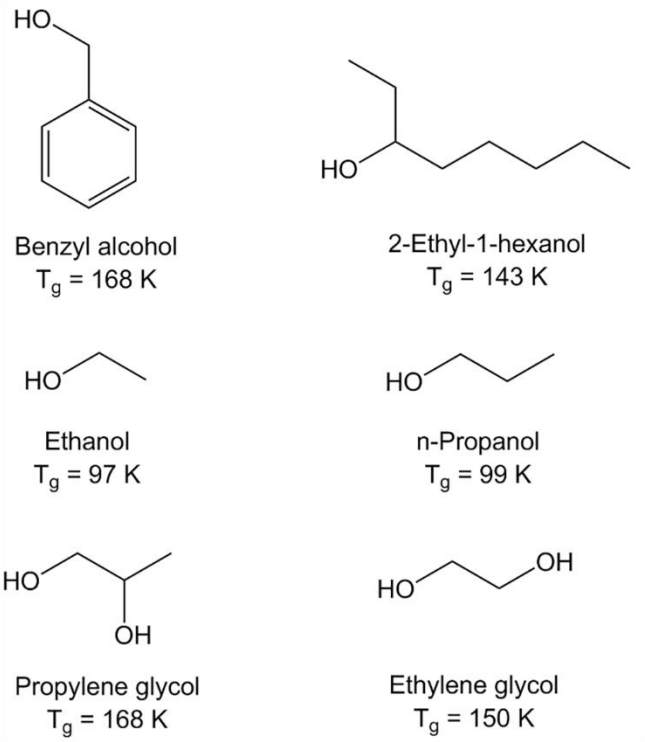

Figure 1: *Molecules tested in this study for ability to form stable glasses using physical vapor deposition.*

3.3 Experimental

3.3.1 Materials

Benzyl alcohol with 99.8% purity, 2-ethyl-1-hexanol with ≥ 99.6% purity, ethylene glycol with ≥ 99.8% purity, and propylene glycol with ≥99.5% purity were all purchased from Sigma Aldrich and used without further purification in experiments at the University of Wisconsin – Madison. Ethanol with 99.8% purity from Carl Roth and n-propanol with 99.5% purity from Sigma Aldrich. The molecules were used without further purification in experiments at the University of Rostock. The T_g values in Figure 1 for 2-ethyl-1-hexanol, ethanol, n-

propanol, propylene glycol and ethylene glycol correspond to τ_α = 100 seconds from dielectric spectroscopy data.[117–121] Dielectric experiments have not been reported for benzyl alcohol; the listed value was obtained from differential scanning calorimetry measurements at 5 K/min.[122,123]

3.3.2 Apparatus

The vacuum deposition chambers and AC nanocalorimetry instrumentation at the University of Wisconsin – Madison and at the University of Rostock have been described in detail previously.[54,71,86] The apparatuses are similar and we will give a general description that applies to both laboratories. Sample deposition and measurement took place inside an ultra-high vacuum chambers pumped by a turbo pump in series with a dry backing pump. The typical base pressure of both chambers is 10^{-9} mbar. Molecules are introduced into the chamber for deposition by a fine leak valve. The relative deposition rate is monitored by the ion gauge pressure. AC nanocalorimetry devices (chip calorimeters produced by Xensor Integration bv, The Netherlands) were held in copper housings attached to a cryostat. The copper housings contained a Resistive Thermometer Device and a cartridge heater to allow for temperature control. A thermal oscillation is created on the nanocalorimeter membrane by an AC voltage applied to the device heater by the internal oscillator of a Signal Recovery 7265 DSP (Digital Signal Processing) lock-in amplifier. We measure a differential thermopile signal between a nanocalorimeter containing a sample and an empty reference device. We subtract a background measurement of the two empty devices to account for the fact that both devices are not completely identical. The resulting differential signal is proportional to the reversing heat capacity of the films. No strain correction was applied in these experiments as the films are

sufficiently thin to make the correction negligible.[42,48] Except for one experiment in which a wide frequency range was utilized, all reversing heat capacity measurements reported here were measured at 20 Hz.

3.3.3 Experiments

The film thicknesses at the University of Wisconsin – Madison were estimated by comparing our deposition to previous tandem AC nanocalorimetry and ellipsometry measurements of methyl-*m*-toluate films.[54] At the University of Rostock, film thicknesses were estimated using previously-reported Finite Element Modeling calculations.[71] In each case, we deposited films that corresponded to particular heat capacity changes (rather than particular thicknesses) on the sensors. Since the deposited alcohols have somewhat different volumetric heat capacities, this results in (at most) a 26 % error in the reported thickness. The effect of this error on transformation times is much smaller than other uncertainties for the transformation times reported in Figures 6 and 8. Thus, we will only report approximate glass thicknesses and we did not adjust the transformation times for small differences in film thicknesses. Deposition rates calculated from the deposition time and thickness ranged from 0.1 to 0.3 nm/s. The films for temperature ramping experiments were approximately 250 nm thick. The films for quasi-isothermal annealing experiments were approximately 590 nm thick and were deposited on top of a 250 nm layer of liquid-cooled glass. The use of such a bilayer geometry ensures that there will be two growth fronts if the vapor-deposited glass transforms via front propagation.[54,58]

The temperature of the AC nanocalorimetry devices was calibrated by measuring the alpha relaxation of supercooled liquids and comparing to literature measurements as described

previously.[46,54,71] With this procedure, the absolute temperature is known to +/- 1 K. During temperature ramping experiments, a 5 K/min heating and cooling rate was used at the University of Wisconsin – Madison, while a 0.67 K/min heating rate was used at the University of Rostock. At most, the T_{onset}/T_g values for ethanol and n-propanol reported in Figure 5A are 0.013 lower than they would be if 5 K/min were used at Rostock. This effect is small enough that it does not affect our qualitative evaluation of stable glass forming ability. The quantitative evaluation of stable glass forming ability was done using quasi-isothermal annealing experiments, which are not affected by heating rate. (These annealing experiments are quasi-isothermal because of the ~ 0.3 K temperature oscillation of the AC calorimetry technique.) During the temperature jump prior to the quasi-isothermal annealing experiments, the temperature overshoot was 0.1 K or less, and subsequently the temperature was constant to +/- 0.1 K. The quasi-isothermal annealing temperatures utilized were 174 K for benzyl alcohol, 146 K for 2-ethyl-1-hexanol, 97 K for ethanol, 99 K for n-propanol, 151 K for ethylene glycol, and 167 K for propylene glycol.

3.3.4 Data Analysis

For comparisons shown below (Figures 7 and 8), we calculated isothermal annealing times for stable glass forming molecules from prior publications. Stable glasses transform via propagating fronts,[49,51,52,54,56–58] and the front velocity has been measured as a function of annealing temperature for many molecules.[42,46,50,54,61,86,89] All of this data was obtained using deposition rates near 0.2 nm/s and the substrate temperature that maximizes kinetic stability. We use this data to calculate the transformation times expected for 590 nm stable glass films with two transformation fronts (i.e., the time required for one front to propagate 295 nm), since we

used bilayer films in our current experiments. We calculate the transformation times (ratioed to τ_α) at an annealing temperature that correspond to τ_α = 50 seconds. Consistent with the calculation described above, for all but one of the known stable glassformers in Figures 7 and 8 a single transformation front has been shown to propagate at least 400 nm before the intervention of a bulk transformation mechanism. For stable glasses of N,N′-bis(3-methylphenyl)-N,N′-diphenylbenzidine (also known as TPD) experiments on thicker films have not been published, but we expect the transformation fronts of TPD will also propagate at least 295 nm during the transformation of thick films.

For comparisons shown below (Figure 8), we compiled supercool liquid dynamics data for the six alcohols studied here and for eight known stable glass formers. Most of this data is from dielectric spectroscopy and NMR experiments that directly report τ_α. In some cases, viscosity data was used to calculate $\tau_\alpha = \eta/G_\infty$ with G_∞ = 0.5 GPa for ethylcyclohexane,[124] G_∞ = 0.31 GPa for indomethacin, G_∞ = 0.159 GPa for TNB, and G_∞ = 81.1 MPa for ethylbenzene.[103] The values of G_∞ for indomethacin and TNB were chosen such that viscosity and dielectric measurements match in the temperature region where the measurements overlap. The G_∞ values for ethylcyclohexane and ethylbenzene have been used previously to calculate τ_α from viscosity data.[103,124] We used the Wirtz equation ($\tau = 4\pi\eta r^3 / 6kT$) to calculate τ_α from the benzyl alcohol viscosity data,[125,126] assuming a molecular radius of 0.31 nm.

We measured τ_α deep in the supercooled liquid of benzyl alcohol using AC nanocalorimetry measurements that spanned the frequency range of 4 Hz to 4 kHz.

We determined T_g, *m*, $T_{1/2}$, and also $\log(\tau_\alpha)$ at 1.25 T_g from the compiled data sets. We used a Stickel analysis to determine the characteristic temperature T_B for each system.[127,128] Then, we determined VTF fits (equation 2) to the data below T_B by first setting T_0 by linearizing $\log(\tau_\alpha)$ vs $1/(T-T_0)$.[129]

$$\log(\tau_\alpha) = A + \frac{B}{T - T_0} \quad (2)$$

The VTF parameters were then used to derive T_g (where τ_α = 100 s) and *m*, as described by Chen and Richert.[103] We also estimated *m* by two other methods, determining the slope of the lowest temperature data and performing a linear fit to the derivative of $\log(\tau_\alpha)$ vs T_g/T and extrapolating to T_g. The *m* values plotted in Figure 7A are averages of these 3 methods. We determined the values of $T_{1/2}$ and $\log(\tau_\alpha)$ at 1.25 T_g by interpolating the available data when possible, and extrapolating when necessary.

3.4 Results

3.4.1 Temperature ramping experiments

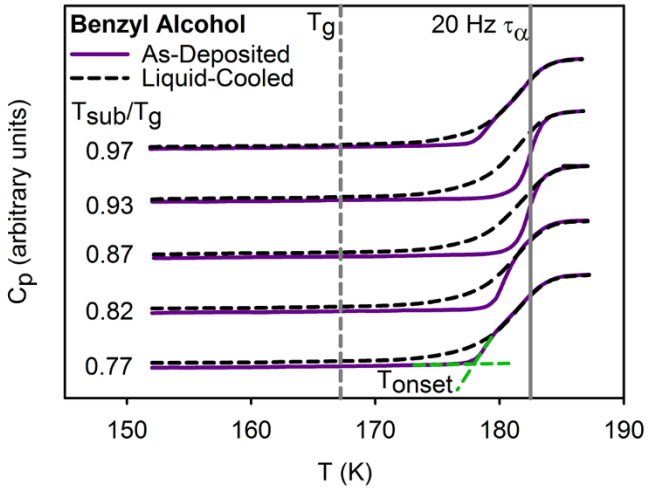

Figure 2: *Temperature ramping AC nanocalorimetry experiments of benzyl alcohol glasses. Solid purple curves are as-deposited glasses prepared by physical vapor deposition. Dashed black curves are glasses prepared by cooling the supercooled liquid. The green dashed tangent lines demonstrate the determination of T_{onset}. The as-deposited glasses exhibit significantly increased onset temperatures and decreased heat capacity, features that have been previously observed in stable glasses. The curves for different substrate temperatures have been vertically shifted. The noted value of T_g comes from 5 K/min DSC measurements.*[122,123] *The 20 Hz τ_α value comes from the minimum in the phase data from AC nanocalorimetry measurements.*

As shown in Figure 2, temperature ramping AC nanocalorimetry experiments demonstrate that benzyl alcohol can from stable glasses via vapor deposition. The as-deposited glasses maintain their glassy heat capacity until temperatures as high as 13 K above T_g (1.08 T_g) before transforming into the supercooled liquid. This significantly increased onset temperature is an indication of the enhanced kinetic stability that defines a stable glass.[42,44,81,82,90,94] The benzyl

alcohol stable glasses also have lower reversing heat capacities than the liquid-cooled glass. Reduced heat capacity is a feature that has been observed previously in many other stable glasses.[42,45,46,48,54,86,91,110]

The AC calorimetry measurements are made by applying an oscillating heat input to the sample at a frequency of 20 Hz, and measuring the amplitude of the 20 Hz temperature oscillation; the amplitude is proportional to the reversing heat capacity. The liquid-cooled glass (dashed black lines) shows an increase in the reversing heat capacity value at the temperature when the structural relaxation occurs at 20 Hz. At lower temperatures, the structural relaxation process is too slow to adsorb energy from the 20 Hz heating, and the reversing heat capacity is low. As the temperature increases, a growing fraction of molecules undergo structural relaxation at a frequency of 20 Hz and the reversing heat capacity increases. Eventually the value of the reversing heat capacity levels off at a temperature where the structural relaxation of all molecules is faster than 20 Hz. The transformation of the vapor-deposited glass begins at the onset temperature (T_{onset}) where the reversing heat capacity deviates from the nearly flat response of the glass. The tangent lines drawn for the 0.77 T_{sub}/T_g glass provide an example of how T_{onset} is determined. We will compare the features of the temperature ramping experiments for all six alcohols in Figure 5.

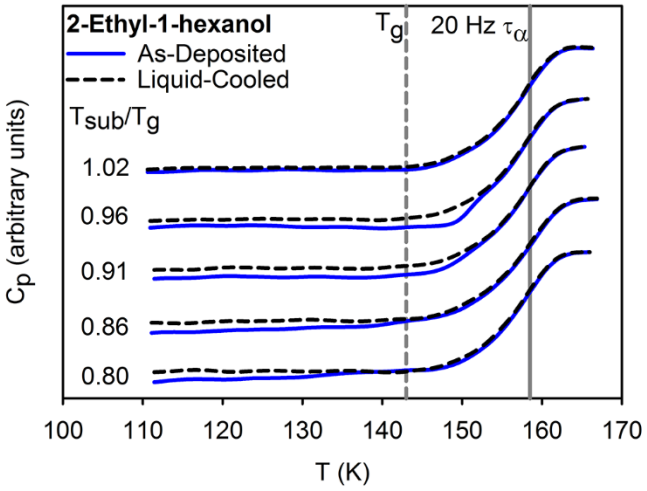

Figure 3: *Temperature ramping AC nanocalorimetry experiments of 2-ethyl-1-hexanol glasses. Solid blue curves are as-deposited glasses prepared by physical vapor deposition. Dashed black curves are liquid-cooled glasses. 2-Ethyl-1-hexanol glasses deposited at 0.96 T_g and 0.91 T_g have moderately enhanced kinetic stability but glasses prepared with lower substrate temperatures do not. The curves for different substrate temperatures have been vertically shifted. The noted value of T_g is the temperature when τ_α = 100 s.*[117]

Vapor-deposited glasses of 2-ethyl-1-hexanol exhibit modestly enhanced kinetic stability when deposited near T_g. These temperature ramping experiments are shown in Figure 3. Glasses deposited at 0.96 T_g and 0.91 T_g have onset temperatures that are, at most, 5 K higher than T_g. This is a smaller increase (up to 1.036 T_g) compared to the 1.08 T_g value observed for the most stable benzyl alcohol glasses. All the vapor-deposited glasses of 2-ethyl-1-hexanol exhibit decreased reversing heat capacities compared to the liquid-cooled glass. The heat capacity of vapor-deposited glasses with T_{sub}/T_g = 0.87 and 0.80 goes through a small step before T_g which

is a feature of an unstable glass. The combination of low stability and a lower reversing heat capacity is surprising and discussed below.

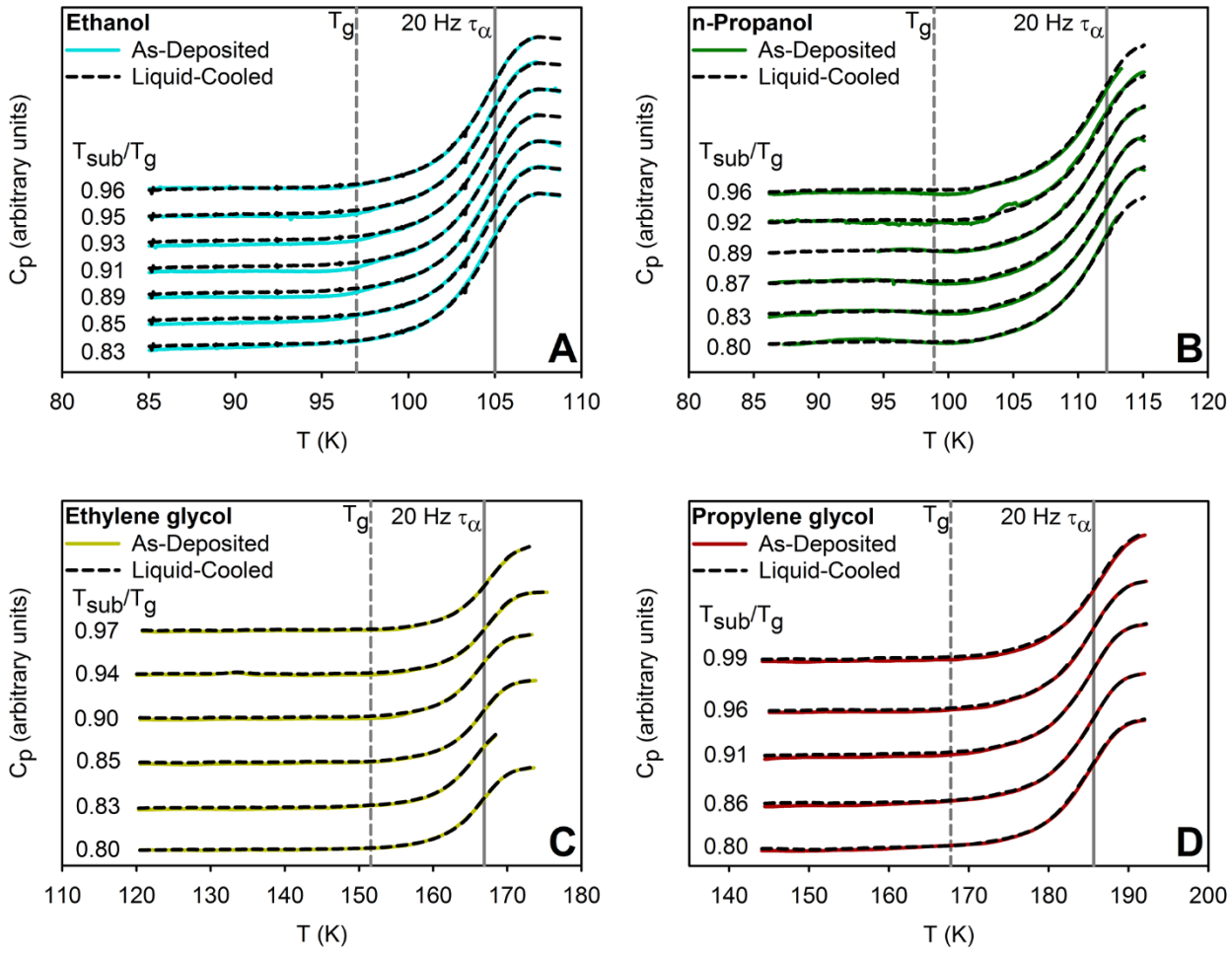

Figure 4: *Temperature ramping AC nanocalorimetry experiments of ethanol (**A**) n-propanol (**B**) ethylene glycol (**C**) and propylene glycol (**D**) glasses. The solid colored lines are as-deposited (AD) glasses while the dashed black curves are liquid-cooled glasses. None of the vapor-deposited glasses show enhanced kinetic stability. The curves for different substrate temperatures have been vertically shifted. The noted value of T_g is the temperature when τ_α = 100 s.*[118–121]

As shown in Figure 4, the vapor-deposited glasses of ethanol, n-propanol, ethylene glycol, and propylene glycol exhibit little to no enhanced kinetic stability. The vapor-deposited glasses of ethanol, ethylene glycol, and propylene glycol have reversing heat capacities that are slightly lower than the liquid-cooled glass, but the magnitude of the decrease is much less than for benzyl alcohol and 2-ethyl-1-hexanol. The reversing heat capacities of the as-deposited n-propanol glasses are very similar to that of the liquid-cooled glass, and instrumental noise does not allow us to quantify any slight differences.

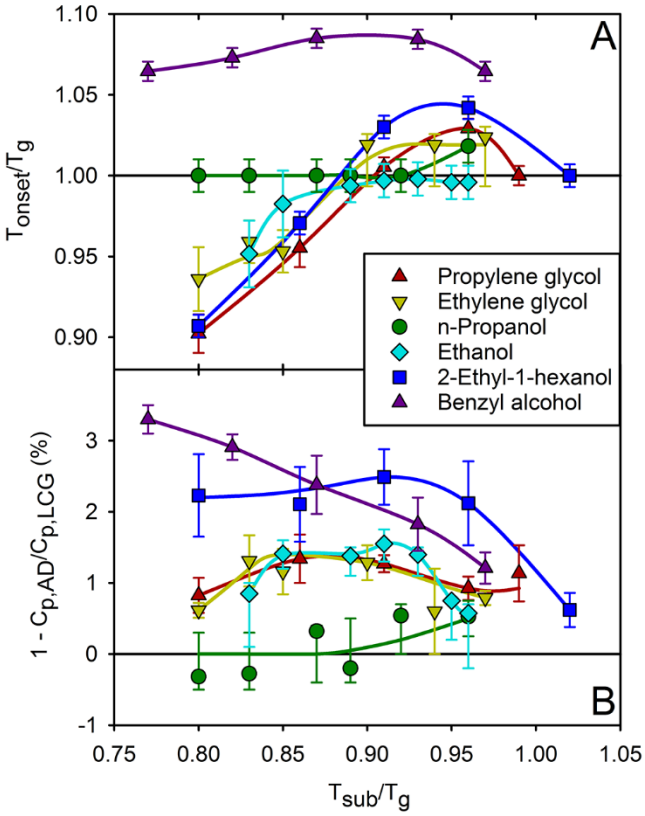

Figure 5: *Comparison of the properties of vapor-deposited glasses of six alcohols.* ***A)*** T_{onset}/T_g *vs normalized substrate temperature during deposition* (T_{sub}/T_g). *Error bars represent the uncertainty in the observed* T_{onset} *and in the absolute temperature.* ***B)*** *Reversing heat capacity decrease of vapor-deposited glasses compared to liquid-cooled glasses as a function of substrate temperature during deposition. The heat capacity decrease is determined in the glassy region before any onset temperature.*

The onset temperatures of the as-deposited glasses of these six alcohols are compared in Figure 5A as a function of the substrate temperature during deposition. Glasses that have a T_{onset}/T_g value greater than 1 maintain their glassy properties to temperatures higher than T_g and

can be said to have enhanced kinetic stability.[42,44,81,82,90,94] Vapor-deposited glasses of benzyl alcohol have a maximum T_{onset}/T_g of 1.08 and exhibit increased onset temperatures from T_{sub}/T_g = 0.97 to below T_{sub}/T_g = 0.77. This behavior is typical of previously studied stable glasses. 2-Ethyl-1-hexanol, propylene glycol, ethylene glycol, and n-propanol have elevated onset temperatures when deposited just below T_g, but these onset temperatures are relatively low. When 2-ethyl-1-hexanol, propylene glycol, ethylene glycol, and ethanol are deposited at temperatures below 0.90 T_g, they make unstable glasses as evidenced by changes in their glassy heat capacity at temperatures below T_g. In contrast, for known stable glass forming molecules, the phenomenon of preparing an unstable glass does not occur unless the glass is deposited at temperatures below 0.70 T_g.[42,46,86] The vapor-deposited glasses of n-propanol had reversing heat capacity traces that were very similar to the liquid-cooled glass. Because of this small difference and instrument noise, we were unable to observe any unstable glass behavior if it exists for this molecule.

Figure 5B shows the decrease in the reversing heat capacity for vapor-deposited glasses of the six alcohols, relative to the liquid-cooled glasses. Decreased heat capacity is a property that has been observed in many stable glasses.[42,45,46,48,54,86,91,110] Vapor-deposited glasses of benzyl alcohol have heat capacities that are 1% to 3% lower than a liquid-cooled glass depending on substrate temperature; this range and temperature dependence is similar to what has been seen in known stable glasses. Figure 5 also illustrates the interesting result of unstable glasses with decreased reversing heat capacity. 2-Ethyl-1-hexanol glasses deposited below 0.90 T_g provide the best examples of this phenomenon.

3.4.2 Quasi isothermal annealing experiments

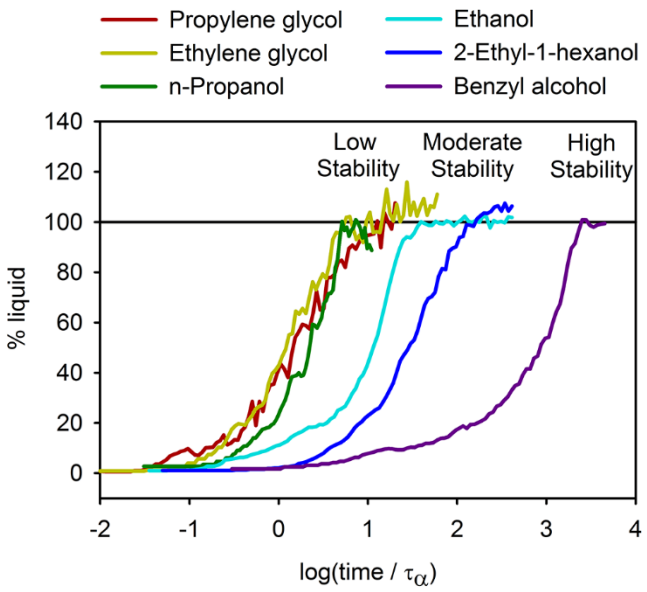

Figure 6: *Isothermal transformation kinetics of vapor-deposited glasses of six alcohols. For each alcohol, vapor-deposited glasses were prepared at the substrate temperature that yielded the highest* T_{onset} *and then heated to* $T_{anneal} \geq T_g$*. The vertical axis represents the change in the reversing heat capacity signal from the initial glassy value to the super-cooled liquid value. The annealing time is normalized by* τ_α *of the supercooled liquid at the annealing temperature. Data has been smoothed for clarity.*

We performed quasi-isothermal annealing experiments to quantify the kinetic stability of the vapor-deposited alcohols, with the results shown in Figure 6. During annealing, the reversing heat capacity of the sample increases as it transforms from glass to supercooled liquid. The "% liquid" value is obtained by normalizing the heat capacity increase with respect to the value of the supercooled liquid. Thus during the annealing, the % liquid increases as the sample

transforms and levels off once the transformation is complete. We have also normalized the time axis by dividing by τ_α of the supercooled liquid at the annealing temperature.

The six alcohols shown in Figure 6 exhibit a wide range of isothermal transformation times. The transformation times of the propylene glycol, ethylene glycol and n-propanol glasses are less than 10 τ_α and we characterize these glasses as having low kinetic stability. For comparison, a liquid-cooled glass should transform in about 1 τ_α under the conditions of these experiments. The vapor-deposited glasses of ethanol and 2-ethyl-1-hexanol have transformation times between 10 and 1000 τ_α, and exhibit moderate kinetic stability. The vapor-deposited glass of benzyl alcohol has a transformation time greater than 1000 τ_α. Known stable glasses have transformation times that range from $\log(t_{transformation}/\tau_\alpha) = 3$ to $\log(t_{transformation}/\tau_\alpha) = 5$,[42,46,50,54,61,86,89] and we designate the benzyl alcohol data as showing high kinetic stability. The precise transformation time cutoffs for low, moderate, and high kinetic stability are arbitrary, but these classifications will facilitate further discussion.

3.5 Discussion

3.5.1 The role of the hydroxyl group in stable glass formation

We have prepared stable glasses of benzyl alcohol and this is the first clear example of an alcohol that can form a stable glass. As discussed in the introduction, previous studies of vapor deposition of alcohols were inconclusive.[18,112–114,116] The high onset temperatures and long transformation times for vapor-deposited glasses of benzyl alcohol (Figures 2 and 6) unambiguously show the high kinetic stability that defines a stable glass. The proposed mechanism of stable glass formation is that molecules have enhanced surface mobility during

deposition and thus are able to reach packing arrangements that have high barriers to relaxation once the molecule is buried by further deposition.[43,75,81] Enhanced surface mobility has been observed in many experiments[16,17,75,81,130] and simulations,[35,37,131,132] and has been described by theory.[39,41] Because it can form a stable glass, we expect that benzyl alcohol has significantly enhanced surface mobility.

In contrast, 2-ethyl-1-hexanol, ethanol, n-propanol, ethylene glycol, and propylene glycol do not form stable glasses and we speculate that this occurs because their surface mobility is too low. During vapor deposition, these molecules apparently sample configurations only slowly and do not find low energy configurations with high barriers to rearrangement. If this view is correct, then we expect that highly stable glasses of molecules like 2-ethyl-1-hexanol could be prepared if we use extremely slow deposition rates; we plan to test this prediction in further experiments. The temperature dependence of the onset temperature for the five alcohols that do not form stable glasses is consistent with limited surface mobility during deposition. For these five molecules, the optimal deposition temperature is around 0.95 T_g as seen in Figure 5A for 2-ethyl-1-hexanol, ethanol, n-propanol, ethylene glycol, and propylene glycol. This is much higher than the optimum substrate temperature of ~0.85 T_g that is typically observed in stable glass forming molecules.[34,42,87,110,133] The optimal substrate temperature is the result of the competition between the temperature dependence of the surface mobility and the energy levels of available configurations, where a low energy level often results in a high barrier to rearrangement.[43,81] At higher deposition temperatures, molecules have sufficient surface mobility to sample configurations, but the available configurations have lower barriers to rearrangement. At lower

deposition temperatures there are configurations with much higher barriers, but molecules do not have enough mobility to reach these configurations during the time that they remain near the surface. If a glass has limited surface mobility, we would expect the optimal deposition temperature to be higher than for stable glass formers.

Our hypothesis of limited surface mobility for the five alcohols that do not form stable glasses is related to a recent study of the effect of hydrogen bonding on diffusion at the surface of glasses. Stable glass forming molecules with no hydrogen bonding have surface diffusion coefficients that can exceed the bulk diffusion coefficient as much as 8 orders of magnitude at T_g.[17,75,130] For a molecule that is only subject to van-der-Waals forces, it is natural to imagine that the reduction of neighbors at the surface significantly reduces the barriers to motion. Chen and coworkers discovered that the surface diffusion of polyols at T_g is at least 4 orders of magnitude slower than for similarly sized non-hydrogen-bonding molecules.[17,18,134] They hypothesize that polyol molecules restructure at the surface such that they maintain a high number of hydrogen bonds despite losing some neighbors. Because of these strong intermolecular interactions, the barriers to motion at the surface would still be relatively high.[18] Based on the work of Chen and coworkers, one would predict that molecules with extensive hydrogen bonding would not have the surface mobility required to form highly stable glasses. (In this paragraph, we have assumed that high rates of surface diffusion are associated with high rates of configurational sampling and this assumption may need to be carefully examined.)

In light of the work of Chen and coworkers, it is natural to ask whether the five alcohols that fail to form stable glasses exhibit more extensive hydrogen bonding than benzyl alcohol? The literature indicates that this is likely to be the case. The two diol liquids (propylene glycol

and ethylene glycol) are understood to have hydrogen bonding clusters or hydrogen bonded networks.[135–140] Extensive intermolecular hydrogen bonding is observed in simulations of these liquids[135,138,139] and presumably has a major influence on the liquid dynamics.[136,137,140] n-Propanol, and 2-ethyl-1-hexanol exhibit Debye peaks in the dielectric spectra of the supercooled liquids.[117,119] This strong peak that occurs at frequencies below the α process for mono alcohols is understood to report the dynamics of supramolecular structures held together by intermolecular hydrogen bonding.[141] Various experiments support the picture of hydrogen bonded structures in n-propanol[142] and 2-ethyl-1-hexanol,[143,144] while simulations of liquid n-propanol also predict hydrogen bonded clusters.[145] It is not yet clear if supercooled ethanol exhibits a Debye peak,[118] but experimental and computational work agree that the structure of liquid ethanol is dominated by hydrogen bonded clusters.[142,145,146] There is not yet a consensus on the structure of liquid benzyl alcohol. Some authors have presented evidence of extended structures,[147,148] but others have claimed that benzyl alcohol only forms dimers[149] or that the interaction between aromatic groups is responsible for any clusters since only a small fraction of the OH groups participate in intermolecular hydrogen bonding.[150] While there is not a clear answer from the literature, if one considers the steric size of the phenyl group, it is plausible that benzyl alcohol contains smaller hydrogen bonded clusters or fewer clusters compared to the five alcohols that fail to form stable glasses. Based on the experiments in this study, we hypothesize that benzyl alcohol glasses exhibit significantly enhanced surface mobility while the five other alcohols do not. The above literature concerning intermolecular hydrogen bonding for the six molecules in this work and the recent report from Chen and co-workers support our hypothesis.

3.5.2 Vapor-deposited glass kinetic stability and supercooled liquid dynamics

As discussed in the introduction, there have been several attempts to connect stable glass forming ability with supercooled liquid fragility.[79,80,103,115] Our data on vapor-deposited alcohol glasses considerably expands the range of systems that can be evaluated and so we further consider this possible connection. We have compiled transformation times from annealing experiments for the vapor-deposited alcohols studied here and for 8 previously studied stable glass forming molecules. We expand the earlier discussion of the role of fragility by considering additional measures of fragility beyond "*m*".

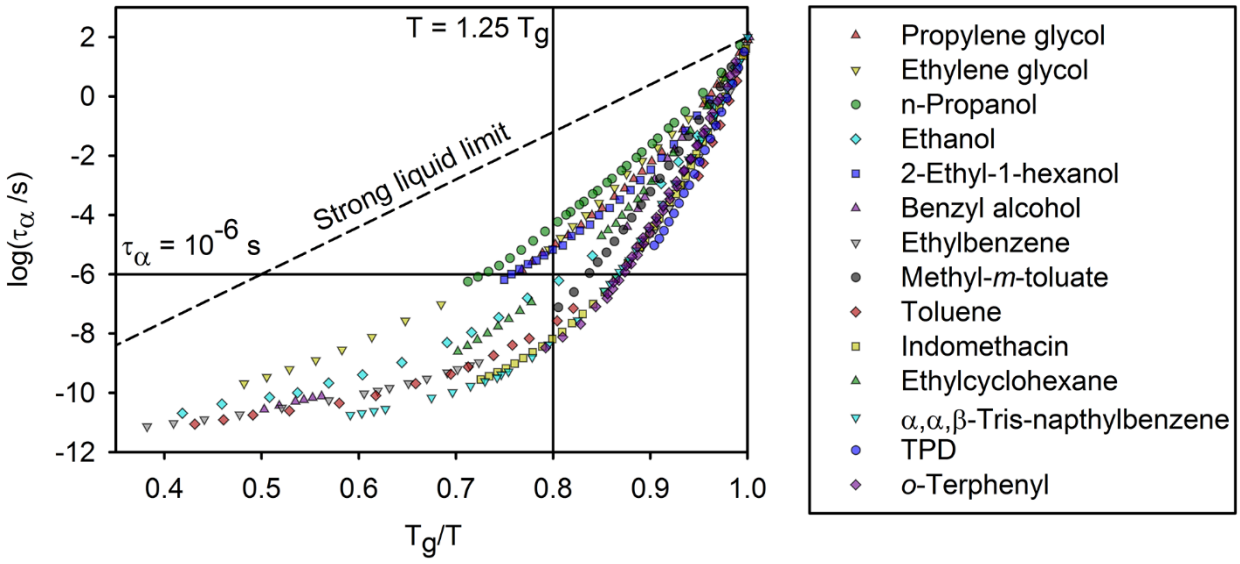

Figure 7. *Supercooled liquid dynamic data for 14 glass-forming liquids, for comparison with kinetic stability of vapor-deposited glasses. The fragility index m can be evaluated by taking the slope at $T_g/T = 1$. The $F_{1/2}$ measure of fragility is related to the value of T_g/T when $\tau_\alpha = 10^{-6}$ seconds (horizontal solid line). Smaller values of log(τ_α) at 1.25 T_g are further from the strong liquid limit and thus represent greater fragility; this value of log(τ_α) can be identified from the*

vertical solid line. Data sources given in text. TPD is the acronym used for N,N′-bis(3-methylphenyl)-N,N′-diphenylbenzidine.

Figure 7 presents log(τ_α) as a function of scaled inverse temperature for the 14 liquids for which we have kinetic stability data for the vapor-deposited glasses. The values of τ_α come from dielectric spectroscopy, NMR, and viscosity literature.[89,101,103,117–121,124,151–164] Our procedure for calculating τ_α from viscosity data can be found in the experimental section. In the case of benzyl alcohol, AC calorimetry measurements were used to determine τ_α for values between 10^{-5} seconds and 10^{-1} seconds.

We utilized three measures of supercooled liquid fragility for the comparison with vapor-deposited glass stability. The "*m*" fragility parameter, defined by equation 1, is equal to the slope of the data at T_g/T is approached. We also utilized the $F_{1/2}$ measure of fragility proposed by Angell and co-workers.[165]

$$F_{1/2} = 2 * \frac{T_g}{T_{1/2}} - 1 \quad (3)$$

$$where\ \tau_\alpha = 100\ seconds\ at\ T_g, and\ \tau_\alpha = 10^{-6}\ seconds\ at\ T_{1/2}$$

$T_{1/2}$ can be identified in Figure 7 from the solid horizontal line. Similar to *m*, larger values of $F_{1/2}$ indicate greater deviation from the strong liquid limit. As a third measure of fragility, we consider log(τ_α) at 1.25 T_g The value of log(τ_α) at 1.25 T_g is a measure of fragility in that smaller values represent a greater deviation from the Arrhenius behavior of strong liquids, and thus greater fragility. Our choice of the log(τ_α) at 1.25 T_g is inspired by the recent paper from Chen

and coworkers.[18] They have found that the surface diffusion constant at T_g of glass formers correlates well with log(η) at 1.25 T_g. For consistency with the other two fragility measures, we elected to use τ_α rather than η, but since these quantities are nearly proportional to each other in supercooled liquids, we do not think that this would have a significant impact on our conclusions.

In Figure 8, the transformation times for vapor-deposited glasses are plotted versus the three measures of supercooled liquid fragility. Transformation times for the six alcohols come from Figure 6 while published data is used for the other molecules. In Figure 8A we observe a poor correlation between stable glass forming ability and *m* (equation 1). In particular, note that *m* values near 55 are associated with a range of transformation times that covers more than 3 orders of magnitude. Given the lack of correlation in previously published comparisons utilizing the *m* fragility parameter, this result was expected.[46,61,67,79] In Figure 8B we plot the normalized transformation times as a function of the $F_{1/2}$ measure of fragility. We consider that this correlation is modestly improved in comparison to the *m* fragility parameter. Finally in Figure 8C we observe that log(τ_α) at 1.25 T_g correlates reasonably well with stable glass forming ability. The different measures of fragility compared in Figure 8 emphasize deviations from strong liquid behavior in different temperature regimes. One might expect that *m* would best correlate with stable glass forming ability because it is evaluated closest to the temperature range where vapor deposition is performed. In contrast, Figure 8 shows that the measures of fragility that are sensitive to higher temperature dynamics provide a better correlation.

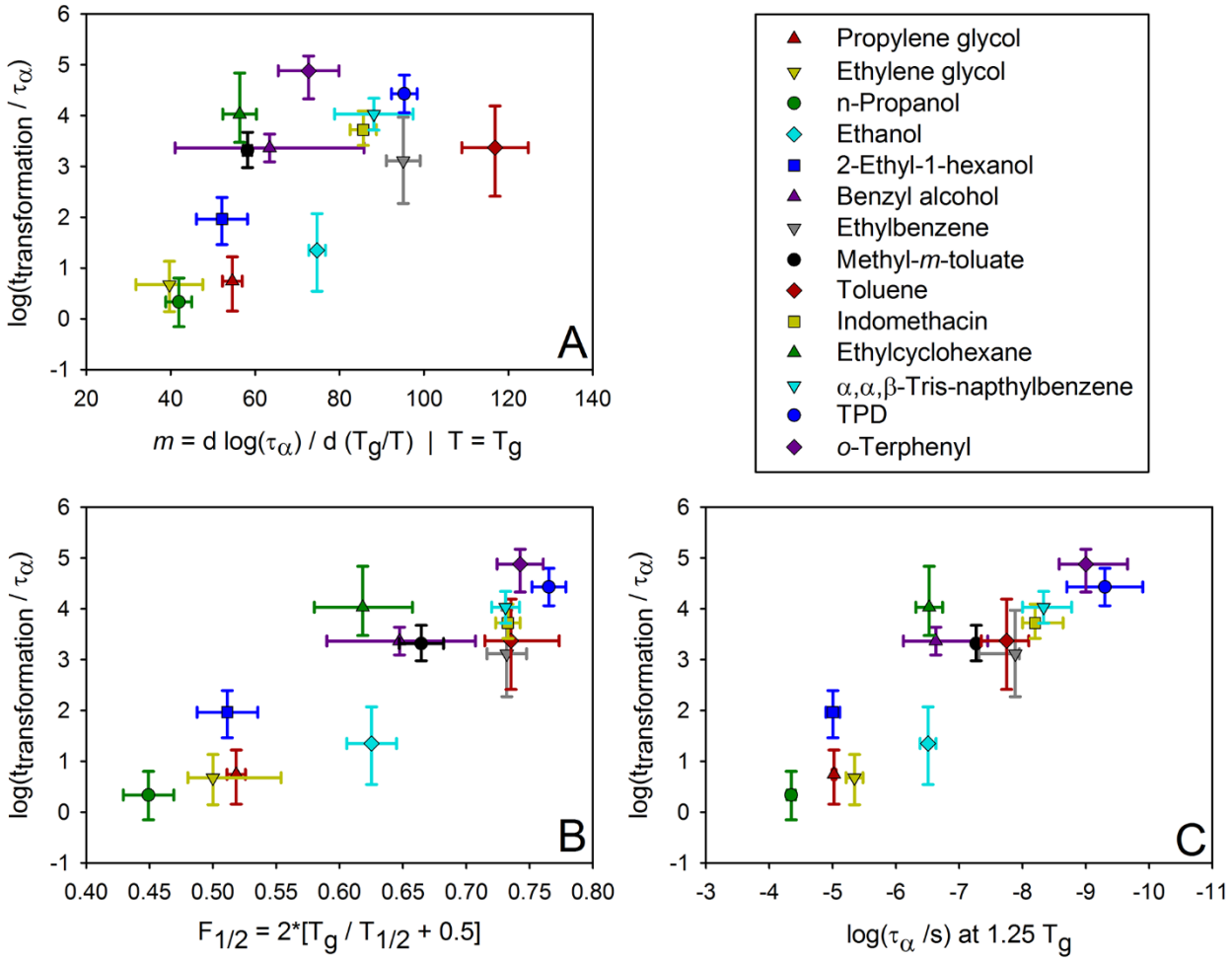

Figure 8: *Transformation times of 590 nm vapor-deposited glasses for 14 liquids, as a function of three different measures of supercooled liquid fragility. Data for the six alcohols are from this work. For the previously published data on eight other liquids, we use transformation front velocities for stable glasses deposited at ~0.2 nm/s and optimized* $T_{substrate}$ [42,46,50,54,61,86,89] *to*

calculate the transformation time for 590 nm films. In panels B and C we observe a moderate correlation between transformation times and fragility, as discussed in the text.

Beyond the empirical correlations shown in Figure 8, we briefly describe two reasons why one might expect stable glass forming ability to correlate with some measure of fragility. We understand stable glass forming ability for a particular molecular system to be influenced by both the surface mobility at substrate temperatures below T_g and by the height of barriers for equilibrium configurations at these temperatures. As mentioned above, Chen and coworkers recently showed that fragility (measured by $\log(\eta)$ at 1.25 T_g) correlates with enhancement of surface diffusion. They argue that the loss of neighbors at the surface can be thought of as an "excitation" similar to a temperature increase.[18] In this view, since bulk dynamics of low fragility molecules are less sensitive to temperature, these molecules should have less mobility at the surface. It is unknown if surface diffusion is precisely the relevant measure of the surface mobility for stable glass formation, but the argument by Chen and coworkers could also be extended to surface structural relaxation. A second reason why fragility might influence stable glass forming ability arises from the expected connection between fragility and barrier heights at low temperatures. For an equilibrium liquid at the strong limit of fragility, the barrier heights in the potential energy landscape do not increase at lower temperatures[20] (consistent with the Arrhenius temperature dependence for structural relaxation). Therefore, the ability to sample more configurations during vapor-deposition would produce a glass with the same-sized barriers as a liquid-cooled glass, and thus the vapor-deposited glass would not demonstrate any enhanced

kinetic stability. In contrast, for a fragile equilibrium supercooled liquid, the barrier heights at equilibrium increase with decreasing temperature (as indicated by the non-Arrhenius temperature dependence for structural relaxation), with a greater rate of increase for more fragile systems. This reasoning leads to the expectation that more fragile systems potentially have more kinetic stability to gain through vapor deposition. While there is some debate as to whether fragile liquids continue to have non-Arrhenius dynamics in equilibrium near T_g,[66,166,167] configurations with higher barriers must be accessible via vapor deposition for otherwise glasses with high kinetic stability could not be obtained. At present, we view any relationship between fragility and stable glass forming ability shown in Figure 8 as an empirical observation that has a plausible rationalization. If the correlation shown in Figure 8C holds for future studies of vapor-deposited glasses, it will be desirable to sort out the role of the two contributions to stable glass forming ability that are described above.

3.5.3 Unstable glasses with decreased heat capacity

Vapor-deposited glasses of 2-ethyl-1-hexanol prepared at substrate temperatures below 0.90 T_g have the intriguing combination of an onset temperature below T_g, and reduced heat capacity. This combination has been observed previously for toluene and ethylbenzene glasses deposited near 0.60 T_g.[86] We will briefly explain why we find this combination surprising and how it might be interpreted. The heat capacity of glasses is attributed to vibrational modes, vibrational anharmonicities, and secondary relaxations.[106] A decrease in the glassy heat capacity could be explained by a shift in vibrational frequencies to higher frequencies, more harmonic vibrations, or by suppression of secondary relaxations. We can easily imagine that a liquid

equilibrated at a lower temperature or a better packed glass would have all of these properties, and in addition have higher barriers to relaxation and thus increased kinetic stability. Thus we would expect that low molar volume, low heat capacity, suppressed beta relaxation, and increased kinetic stability would all be correlated in vapor-deposited glasses. These correlations hold for almost all the published literature for vapor-deposited glasses. For example, stable glasses have been found to have lower molar volumes than liquid-cooled glasses.[34,80,81,83,88] The heat capacity decrease and the onset temperature increase have similar relationships with substrate temperature for vapor-deposited glasses of many molecules.[42,45,46,48,54,86,91,110] Also, some previous investigations of unstable glasses produced at very low substrate temperatures have shown higher heat capacities (before going through an irreversible relaxation upon heating towards T_g).[42,168,169] In contrast to these correlations which we regard as easy to explain, some vapor-deposited glasses of 2-ethyl-1-hexanol, toluene, and ethylbenzene have the seemingly contradictory combination of low kinetic stability (as indicated by rearrangements below T_g) and decreased heat capacity. This indicates that there must be regions of the potential energy landscape with low barriers that nevertheless are better packed in some respect. There is further evidence for such regions in a recent publication by Yu and coworkers.[107] They found that the secondary relaxation in toluene vapor-deposited glasses is suppressed compared to the liquid-cooled glass. While such a suppression would be expected (and is observed) for highly stable glasses, secondary relaxation was suppressed even for glasses deposited at very low substrate temperatures ($T_{sub}/T_g = 0.2$) that were likely unstable. Experiments combining calorimetry, dielectric spectroscopy, and vibrational spectroscopy on vapor-deposited glasses of a single

system would further our understanding of the diversity of the states found in the potential energy landscape.

3.6 Conclusions

We have prepared glasses of six mono- and di-alcohols via physical vapor deposition to investigate how the presence of -OH groups might prevent stable glass formation. We investigated the properties of these glasses using AC nanocalorimetry. Quasi-isothermal annealing experiments were used to quantify the kinetic stability of the glasses. Benzyl alcohol forms a stable glass when deposited onto substrates near 0.85 T_g, with transformation times that exceed 10^3 τ_α; this is the first clear demonstration of an alcohol forming a highly stable glass via vapor deposition. Propylene glycol, ethylene glycol, and propanol form low stability glasses, showing transformation times that barely exceed those expected for a liquid-cooled glass. Ethanol and 2-ethyl-1-hexanol form moderate stability glasses. We speculate the benzyl alcohol has higher surface mobility than the other alcohols and that this is the primary reason for its high stable glass forming ability.

Collectively, this series of vapor-deposited alcohol glasses shows a range of kinetic stabilities that has not previously been observed. Using these six alcohols and eight previously studied molecules, we have found a reasonably good correlation between kinetic stability and a recently-proposed measure of fragility: $\log(\tau_\alpha)$ at 1.25 T_g. This correlation is better than the correlation between kinetic stability and other measures of fragility ($F_{1/2}$ and m). We discussed why liquids with higher fragility might be expected to have higher stable glass forming ability, either through enhanced surface mobility or because configurations with higher energy barriers

are present deeper in the potential energy landscape. We also used AC nanocalorimetry to compare the reversing heat capacity of the vapor-deposited glasses to liquid-cooled glasses. Consistent with previous work, glasses with high kinetic stability show decreased heat capacity. In a few cases, decreased heat capacity was also observed in glasses with low kinetic stability.

3.7 Acknowledgements

We thank the U.S. National Science Foundation (CHE-1265737 and CHE-1564663) for support of this work. We thank Lian Yu and Ranko Richert for helpful discussions.

Chapter 4

Surface mobility limits stable glass formation for 2-ethyl-1-hexanol

M. Tylinski[A], M. S. Beasley[A], Y. Z. Chua[B], C. Schick[B], M. D. Ediger[A]

[A] Department of Chemistry, University of Wisconsin–Madison, Madison, Wisconsin 53706, USA

[B] Institute of Physics, University of Rostock, Albert-Einstein-Str. 23-24, 18051 Rostock, Germany and Competence Centre CALOR, Faculty of Interdisciplinary Research, University of Rostock, Albert-Einstein-Str. 25, 18051 Rostock, Germany

Submitted to The Journal of Chemical Physics, Volume 145, Article 174506, 2016

DOI: 10.1063/1.4966582

4.1 Abstract

Previous work has shown that vapor-deposition can prepare organic glasses with extremely high kinetic stabilities and other properties that would be expected from liquid-cooled glasses only after aging for thousands of years or more. However, recent reports have shown that some molecules form vapor-deposited glasses with only limited kinetic stability when prepared using conditions expected to yield a stable glass. In this work, we vapor deposit glasses of 2-ethyl-1-hexanol over a wide range of deposition rates and test several hypotheses for why this molecule does not form highly stable glasses under normal deposition conditions. The kinetic stability of 2-ethyl-1-hexanol glasses is found to be highly dependent on deposition rate. For deposition at $T_{substrate} = 0.90\ T_g$, the kinetic stability increases by 3 orders of magnitude (as measured by isothermal transformation times) when the deposition rate is decreased from 0.2 nm/s to 0.005 nm/s. We also find that, for the same preparation time, a vapor-deposited glass has much more kinetic stability than an aged liquid-cooled glass. Our results support the hypothesis that the formation of highly stable 2-ethyl-1-hexanol glasses is inhibited by limited surface mobility. We compare our deposition rate experiments to similar ones performed with ethylcyclohexane (which forms glasses of high kinetic stability); we estimate that the surface mobility of 2-ethyl-1-hexanol is more than 4 orders of magnitude less than that of ethylcyclohexane at $0.85\ T_g$.

4.2 Introduction

There has been considerable effort in the last twenty years to understand mobility at the free surface of organic glasses, both polymeric and non-polymeric.[9,170] For polymers, high mobility at the free surface is often invoked to explain the decrease in the glass transition

temperature (T_g) observed for thin ($\sim$10 nm) films of many different polymers.[171–176] High surface mobility has also been implicated in the unusual embedding behavior exhibited by nanoparticles at the surface of polymer films.[177] For low molecular weight glassformers, enhanced surface mobility has been linked to enhanced surface crystallization rates that may limit the utility of amorphous pharmaceuticals.[17,75,134,178] Enhanced surface mobility is also thought to play a key role in the preparation of vapor-deposited molecular glasses with high kinetic stability, known as stable glasses.[81,179] The properties of stable glasses resemble those expected for liquid-cooled glasses that have been aged for thousands of years or more.[43] Vapor-deposited glasses are also used in organic electronics and their distinctive features, in comparison to liquid-cooled glasses, are important for the function of these devices.[32,34] Our understanding of the phenomenon of enhanced surface mobility in both polymeric and non-polymeric glassformers has been aided by simulations[35–37,180–185] and by theoretical studies.[39,41,62,186]

Stable glasses are characterized by their high kinetic stability in comparison to liquid-cooled glasses.[43,97] The kinetic stability of a glass can be quantified by the temperature at which it begins to transform into the supercooled liquid upon heating. For stable glasses, the transformation temperature can be up to 8% higher than the conventional T_g.[42] In addition, the isothermal transformation of stable glass into the supercooled liquid can take up to 10^5 times longer than the supercooled liquid structural relaxation time (τ_α).[5] Qualitatively, these indications of high kinetic stability are consistent with results expected for highly aged liquid-cooled glasses. The low molar

volumes[80,88,96] and low enthalpies[43,67,187] exhibited by stable glasses also resemble properties expected for liquid-cooled glasses after extremely long aging times. Experiments,[43,46,81] simulations,[76,111] and theory[39] suggest that stable glasses are the result of high surface mobility that allows molecules to sample low energy configurations during deposition even though the temperature is below T_g. After continued deposition, surface molecules become part of the bulk. The low energy configurations found during deposition have very high barriers to rearrangement, giving rise to the kinetic stability of stable glasses. Configurations with similarly high barriers are inaccessible to liquid-cooled glasses on laboratory time scales because bulk mobility is extremely slow below T_g.

Although stable glasses have been prepared from more than 30 organic molecules, our recent report[5] found several molecules that failed to form stable glasses under similar deposition conditions. There are three likely hypotheses for why some molecules do not form highly stable glasses. First, it could be that amorphous packing arrangements with higher barriers to relaxation do not exist for these systems. In such a scenario, the configurations that would be found during deposition, even with a highly mobile surface, would have relaxation barriers similar to a liquid-cooled glass. Some work in the literature supports the view that the equilibrium temperature dependence of τ_α becomes Arrhenius below T_g;[188–191] for liquids with this behavior, the barriers to relaxation would grow slowly or not at all as the temperature decreases. Second, for some molecules, the lowest energy configurations at the surface might not, upon further deposition, lead to bulk configurations with high barriers. It has been found that many vapor-deposited glasses have anisotropic packing and/or anisotropic molecular orientation,[32,34] suggesting that the

preferred surface configurations are different from the bulk.[70] While anisotropic glasses can have high kinetic stabilities,[34] it might not be universally true that preferred surface configurations result in high barriers in the bulk. Third, it may be that molecules that do not form highly stable glasses have limited surface mobility, and thus deposition at the standard rate (~ 0.2 nm/s) does not allow surface molecules enough time to find the low energy configurations. All the molecules that did not form stable glasses in our previous work participate in intermolecular hydrogen bonding. Chen and coworkers have suggested that hydrogen bonding networks can inhibit surface mobility,[18] and without sufficient surface mobility, stable glass formation would not be expected.

In the present work, we characterize the kinetic stability of 2-ethyl-1-hexanol glasses prepared by vapor deposition using a wide range of deposition rates, an approach that has previously been used successfully to understand stable glass formation for other organic molecules.[43,46,86,94,187] For comparison, we also performed experiments on an aged liquid-cooled glass. We characterized the kinetic stability of the glasses using AC nanocalorimetry experiments. The onset temperature for transformation into the supercooled liquid was measured during temperature ramping experiments and we also determined the glass to liquid transformation time during isothermal annealing experiments. These experiments allow us to test the three hypotheses described above and to deduce why 2-ethyl-1-hexanol does not form a highly stable glass when using standard deposition conditions. In our previous publication, we found that glasses of 2-ethyl-1-hexanol had a transformation temperature of 1.04 T_g and an isothermal transformation time of 10^2 τ_α.[5] For other organic molecules, the same deposition rate

can produce glasses that have transformation temperatures up to 1.08 T_g and isothermal transformation times up to 10^5 τ_α.[5,42]

We find that the kinetic stability of vapor-deposited glasses of 2-ethyl-1-hexanol increases when deposition rate is decreased below 0.2 nm/s and approaches values typical of highly stable glasses. We also observe that a vapor-deposited glass prepared at 0.95 T_g has greater kinetic stability than a liquid-cooled glass that has been aged at 0.95 T_g for a time equal to the deposition time. These findings are consistent with the hypothesis that the formation of stable glasses of 2-ethyl-1-hexanol is inhibited by limited surface mobility. We estimate the surface mobility of 2-ethyl-1-hexanol by comparing our deposition rate results to those for ethylcyclohexane, which forms a highly stable glass when deposited at 0.2 nm/s.[46] We find that the surface mobility of 2-ethyl-1-hexanol is more than 4 orders of magnitude less than that of ethylcyclohexane at 0.85 T_g.

4.3 Experimental

4.3.1 Material

2-ethyl-1-hexanol with a purity ≥ 99.6% was purchased from Sigma Aldrich and used without further purification. Throughout this paper, we make comparisons to the structural relaxation times (τ_α) for 2-ethyl-1-hexanol and to various data for ethylcyclohexane. The τ_α data for 2-ethyl-1-hexanol and ethylcyclohexane supercooled liquids were obtained from literature sources.[124,155,192,193] We have previously applied a VTF fit to the low temperature regime of the τ_α data and obtained T_g (τ_α = 100 s) values of 143.8 K and 100.9 K for 2-ethyl-1-hexanol and ethylcyclohexane respectively.[5]

4.3.2 Apparatus

Glasses of 2-ethyl-1-hexanol were prepared by vapor-deposition onto an AC nanocalorimetry device housed inside an ultra-high vacuum chamber. AC nanocalorimetry experiments were then performed *in-situ*. The AC nanocalorimetry technique and our apparatus have been described in detail previously[54,71] Molecules for deposition are introduced into the vacuum chamber via a fine leak valve. The deposition is monitored by the ion gauge pressure and AC nanocalorimetry signal. The film thickness and deposition rate are calculated from the AC nanocalorimetry signal and a conversion factor determined from previously published *in-situ* ellipsometry experiments.[54] The base pressure in the chamber is typically below 10^{-7} Pa and ensures that there is no significant deposition of any contaminants during our experiments. By measuring the signal change on a calorimeter held at a typical deposition temperature, we estimate that films prepared using the lowest deposition rate are at least 99% 2-ethyl-1-hexanol. The AC nanocalorimeters are held in a copper housing that is attached to a liquid nitrogen reservoir. A heater and RTD attached to the copper housing allow for temperature control. The temperature of the sample is tentatively determined by measuring a resistor that is part of the AC nanocalorimeter active area. We have calibrated this resistor by measuring τ_α of various supercooled liquids and our uncertainty in absolute temperature is +/- 1 K.[54] A more precise estimate of the temperature of each experiment is determined by measuring the 20 Hz τ_α process of 2-ethyl-1-hexanol supercooled liquid after transformation of the glass and comparing to the literature value.[192] The temperature determined in this manner agreed with the previously described method within +/- 0.4 K.

For the nanocalorimetry experiment, a heater on the device membrane is driven by a 10 Hz AC current. The current produces heat at 20 Hz that results in a temperature oscillation of about 0.3 K at the sample. The temperature oscillation is detected by thermocouples patterned onto the device and the amplitude and phase of the voltage oscillation is measured by a lock-in amplifier. We perform a differential measurement between a device that has a sample on it and an empty device. We also perform a background subtraction to account for small differences between the devices. The resulting signal is proportional to the reversing heat capacity of the sample.[71]

4.3.3 Experiments

We performed temperature ramping and quasi-isothermal annealing experiments to characterize the kinetic stability of the vapor-deposited glasses. During temperature ramping experiments, we measure the reversing heat capacity while heating our samples at 5 K/min from 111 K (0.77 T_g) to 164 K (1.14 T_g). The temperature where the vapor-deposited glass begins to transform into the supercooled liquid (T_{onset}) is one measure of kinetic stability. The reversing heat capacity values of the vapor-deposited glasses are compared to a liquid-cooled glass prepared by cooling the sample from the supercooled liquid at 5 K/min. For quasi-isothermal annealing experiments, the glass is heated at 8 K/min to an annealing temperature near T_g. The annealing temperatures ranged from 146.5 K (T_g + 2.7 K) to 141.2 K (T_g – 2.6 K). The annealing temperatures were chosen to ensure that the transformation of glasses with low kinetic stability was slow enough for us to resolve and that the transformation of glasses with higher kinetic stability was completed before our liquid nitrogen supply was depleted. The transformation time

for each experiment is normalized by τ_α for the equilibrium supercooled liquid at the annealing temperature. It is known that for some stable glasses the velocity of the transformation front is not quite proportional to τ_α;[50,52,54] if this applies to the transformation of 2-ethyl-1-hexanol glasses, the effect would be small compared to our error bars and so we have not attempted to correct the data. During isothermal annealing, we measured the reversing heat capacity to track the transformation of the glass into the supercooled liquid and to determine the transformation time, a second measure of kinetic stability. Films for temperature ramping experiments were approximately 120 nm thick. To prepare samples for quasi-isothermal annealing experiments, we deposited an approximately 250 nm thick film on top of a 120 nm layer of liquid-cooled glass. This bilayer sample geometry ensures that if the glass transforms via a front mechanism, there will be two fronts and both will start without any induction time.[54] The 0.90 T_g glass deposited at 0.004 nm/s was only 170 nm thick (rather than 250 nm) due to the time limit associated with our liquid nitrogen supply. This thickness difference will shorten the transformation time by a factor of 1.5 or less, which is small compared to the changes observed in Figures 4 and 6. The positive error bar for this data point in Figures 4 and 6 accounts for this uncertainty.

4.4 Results

4.4.1 Temperature ramping experiments

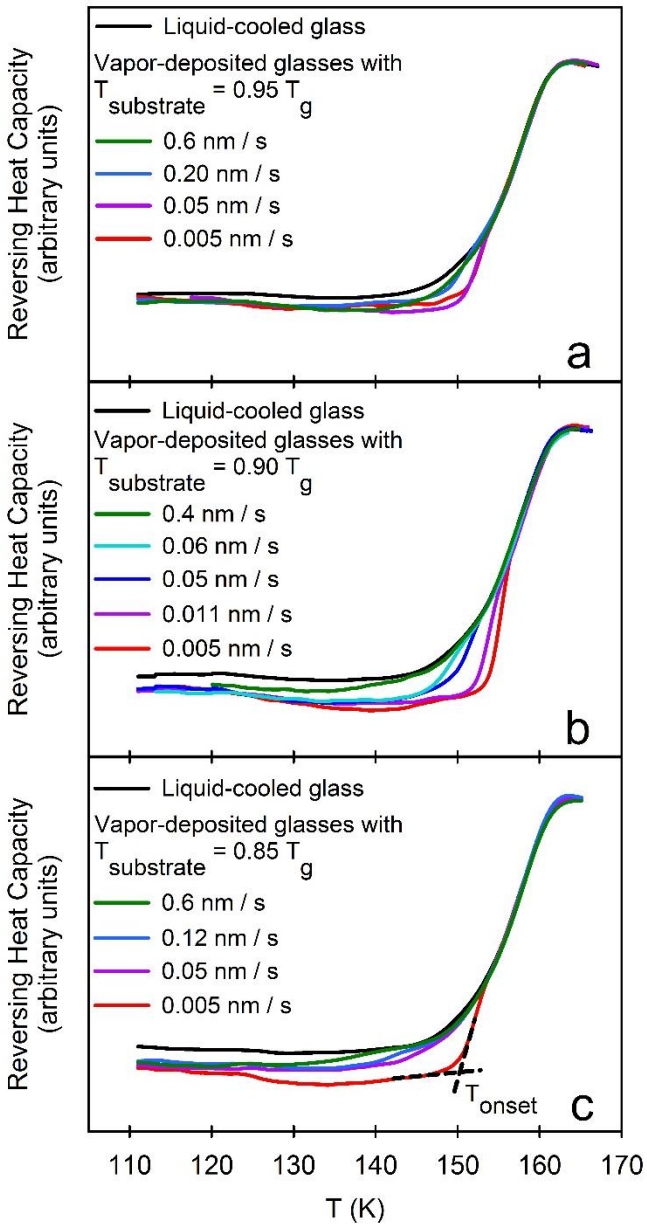

Figure 1: *Reversing heat capacity data from 20 Hz AC nanocalorimetry experiments on 2-ethyl-1-hexanol glasses, obtained during heating at 5 K/min. Panel* ***a****: Glasses deposited at* $T_{substrate}$ =

*0.95 T_g. Panel **b**: Glasses deposited at $T_{substrate}$ = 0.90 T_g. Panel **c**: Glasses deposited at $T_{substrate}$ = 0.85 T_g. The black dashed lines in panel c demonstrate how the onset temperature (T_{onset}) for the transformation of the as-deposited glass into the supercooled liquid is defined. For these experiments, the glasses are about 120 nm thick.*

Figure 1 shows the results of temperature ramping experiments on vapor-deposited glasses of 2-ethyl-1-hexanol that were used to determine the onset temperate (T_{onset}) for the transformation from as-deposited glass to supercooled liquid. The large step in the reversing heat capacity between 150 and 160 K occurs when the alpha relaxation process becomes fast enough to contribute to the 20 Hz reversing heat capacity. We determine the temperature at which the vapor-deposited glass begins to transform (T_{onset}) as indicated in Figure 1c. The T_{onset} values are a measure of kinetic stability of the vapor-deposited glasses. Values greater than T_g indicate that a vapor-deposited glass has greater kinetic stability than the liquid-cooled glass. The reversing heat capacity of the vapor-deposited glasses is lower than that of the liquid-cooled glass, as has been observed for many vapor-deposited organic glasses.[42]

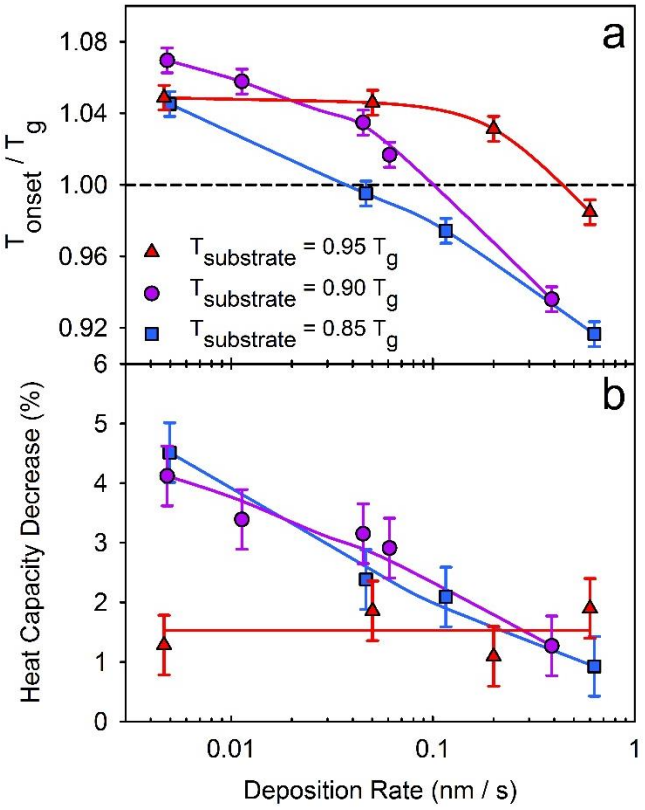

Figure 2: *Characteristics of vapor-deposited glasses of 2-ethyl-1-hexanol, as a function of deposition rate, from the temperature ramping experiments shown in Figure 1. Panel* ***a****: Onset temperature relative to* T_g*. Panel* ***b****: Heat capacity decrease of vapor-deposited glass compared to the liquid-cooled glass. The heat capacity decrease is determined at 0.95* T_g *(136.6 K). Lines are guides to the eye.*

Figure 2 summarizes how the deposition rate influences the T_{onset}/T_g values (panel a) and the heat capacity decrease relative to the liquid-cooled glass (panel b) for vapor-deposited glasses of 2-ethyl-1-hexanol. The T_{onset}/T_g values increase most significantly with decreasing deposition rate for the $T_{substrate}$ = 0.90 and 0.85 T_g glasses. For the $T_{substrate}$ = 0.95 T_g glasses, the

T_{onset}/T_g values increase and then reach a plateau for lower deposition rates. For the two lower substrate temperatures, the heat capacity of the as-deposited glass decreases significantly with lower deposition rates while the heat capacity for the $T_{substrate} = 0.95\ T_g$ glasses does not exhibit a trend with deposition rate. The error bars for the heat capacity values are large because we have used quite thin films for these experiments (120 nm). The thin films allow us to prepare samples with very low deposition rates while keeping the deposition time reasonable.

Figure 2 shows that the substrate temperature that yields the glass with the highest value of T_{onset}/T_g changes as the deposition rate decreases. At rates near 0.2 nm/s the 0.95 T_g glasses have the highest T_{onset}, which is consistent with our earlier work.[5] However, at lower deposition rates, the $T_{substrate} = 0.95\ T_g$ glasses reach a plateau in T_{onset}/T_g and the $T_{substrate} = 0.90\ T_g$ glasses have higher values of T_{onset}/T_g. At high deposition rates, the $T_{substrate} = 0.85\ T_g$ glasses have very low values of T_{onset}/T_g, but at the lowest deposition rate the value increases to match that of the $T_{substrate} = 0.95\ T_g$ glass. The trend suggests that, at even lower deposition rates, the T_{onset}/T_g values for the glasses deposited at 0.85 T_g would surpass those of glasses deposited at 0.95 T_g. As we will discuss below, all these results are consistent with the explanation that stable glass formation of 2-ethyl-1-hexanol deposited at 0.2 nm/s is inhibited by limited surface mobility.

4.4.2 Quasi-isothermal transformation of vapor-deposited glasses

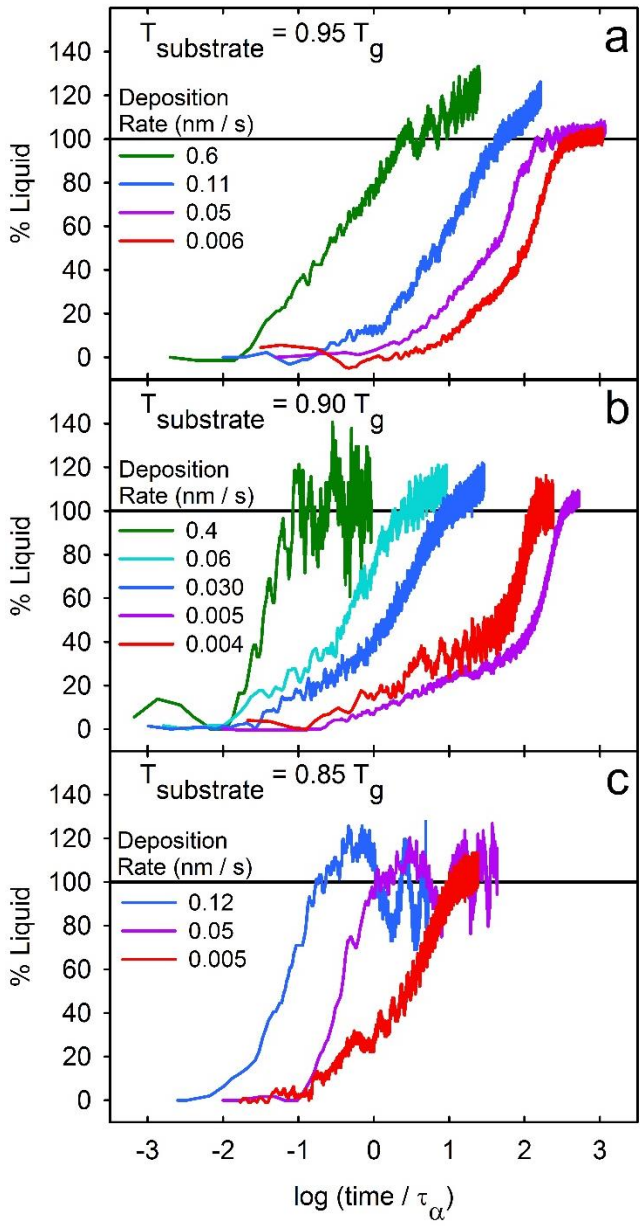

Figure 3: *Quasi-isothermal annealing experiments at $T_{anneal} \sim T_g$ for vapor-deposited glasses of 2-ethyl-1-hexanol prepared at different deposition rates. The "% Liquid" axis is determined from the reversing heat capacity increase from the as-deposited glass value to the supercooled*

*liquid value. For the x-axis, the annealing time is normalized by the structural relaxation time of the supercooled liquid (τ_α) at the annealing temperature. Panels **a**, **b**, and **c** plot the transformation times for glasses deposited at $T_{substrate}$ = 0.95 T_g, 0.90 T_g, and 0.85 T_g respectively. With one exception (see experimental section), the vapor-deposited glasses are 250 nm thick.*

We performed quasi-isothermal annealing experiments to measure how long it takes vapor-deposited glasses of 2-ethyl-1-hexanol to transform into the supercooled liquid when held near T_g. These transformation times are a second (and more precise) measure of kinetic stability. We measure the reversing heat capacity during the annealing experiment to track the transformation. The heat capacity increases from the as-deposited glass value until plateauing at the value of the supercooled liquid. In Figure 3 we have normalized this heat capacity increase and plot it as "% Liquid" to indicate what fraction of the sample is responding with the heat capacity of the supercooled liquid. We also have normalized the annealing time on the x-axis to account for annealing experiments performed at slightly different temperatures and to give a reference to the transformation times. We divide the annealing time by the structural relaxation time (τ_α) of the supercooled liquid at the annealing temperature. We expect that a liquid-cooled glass would transform in approximately 1 τ_α and thus transformation times greater than τ_α indicate that the vapor-deposited glass has greater kinetic stability than a liquid-cooled glass. The increase above the 100% level seen for some samples is due to instrument drift and has been previously observed in quasi-isothermal experiments.[42,46] It may be due to very slow deposition

of molecules that are present in the chamber after the leak valve is closed at the end of the deposition. We present figures with linear time axes in the Supplemental Material that provide a clearer view of the end of the transformation and the determination of the transformation times (Figures S1, S2, and S3).

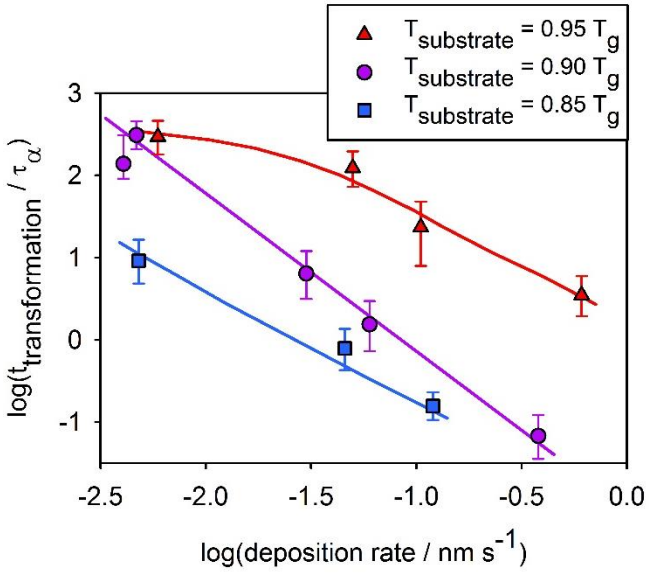

Figure 4: *Transformation times for vapor-deposited 2-ethyl-1-hexanol glasses during quasi-isothermal annealing experiments at $T_{anneal} \sim T_g$ as a function of deposition rate, as obtained from data in Figure 3. The lines are guides to the eye.*

We show the transformation times from the quasi-isothermal annealing experiments as a function of deposition rate in Figure 4. The transformation times of the vapor-deposited glasses generally increase with decreasing deposition rate. The $T_{substrate}$ = 0.95 T_g glasses seem to approach a plateau in transformation time for low deposition rates; this is similar to the plateau in the T_{onset}/T_g values shown for these glasses in Figure 2. For glasses deposited at 0.90 T_g, the

transformation times increase by about 3 orders of magnitude as the deposition rate is decreased below the rate of 0.2 nm/s that has typically been used in our previous efforts to prepare stable glasses. At the lowest deposition rates the transformation times for 0.90 T_g glasses meet the values for the 0.95 T_g glasses and approach $\log(t_{transformation}/\tau_\alpha) = 3$. In our previous work we compiled isothermal transformation times for known stable glasses and found that they were all greater than 10^3 τ_α.[5] That comparison utilized 590 nm thick films. Thin films of highly stable glasses are known to transform via a front mechanism. If we assume that the transformation time of the most stable glasses of 2-ethyl-1-hexanol scale with thickness, the longest transformation time in Figure 4 is equivalent to $10^{2.9}$ τ_α for a 590 nm thick film, and very close to values associated with highly stable glasses.

4.4.3 Aging experiments on a liquid-cooled glass

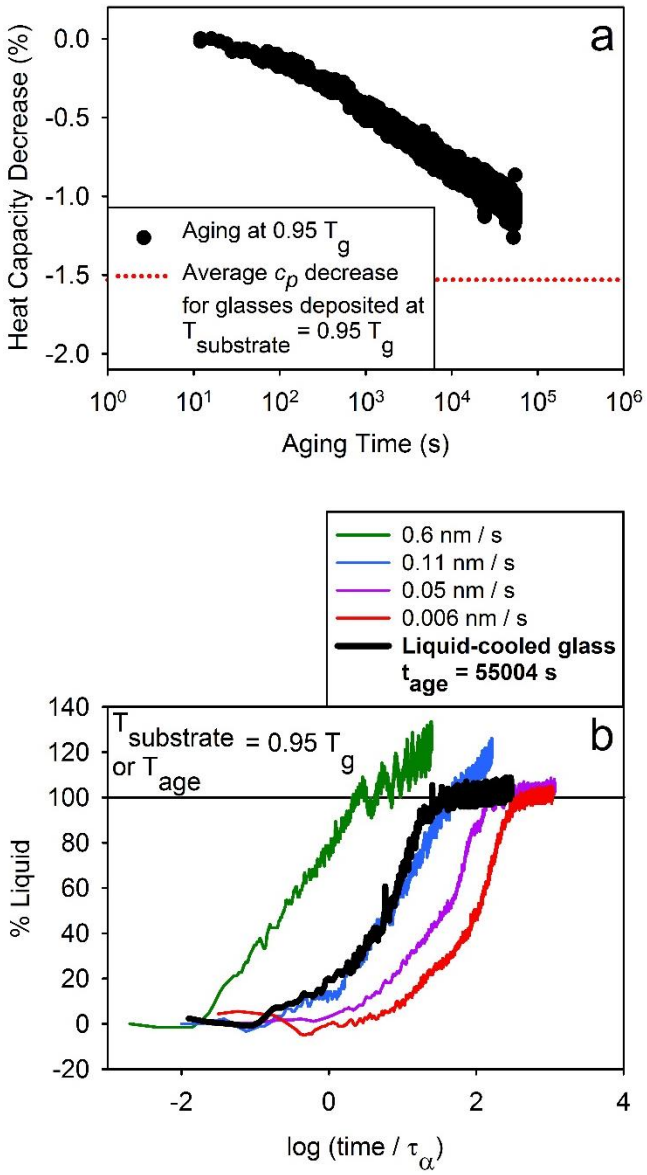

Figure 5: *Aging experiments on a liquid-cooled glass of 2-ethyl-1-hexanol. Panel* ***a****: Heat capacity decrease during aging at 0.95 T_g. The total aging time is equal to the time required for the longest deposition utilized to prepare the samples in Figure 3. For comparison, the red dashed line shows the average heat capacity decrease for glasses vapor-deposited at $T_{substrate}$ =*

*0.95 T_g. Panel **b**: Quasi-isothermal annealing transformation of the aged glass from panel a, in comparison to glasses vapor-deposited at $T_{substrate}$ = 0.95 T_g. The aged glass was about 370 nm thick.*

We aged a liquid-cooled glass to provide a comparison for the kinetic stability and heat capacity decrease of the vapor-deposited glasses. We prepared a glass by cooling the supercooled liquid at 5 K/min and aged it at 0.95 T_g for 55,000 seconds. We chose this time to be equal to the longest time used for vapor deposition of the samples presented in this work. The decrease in reversing heat capacity during aging is shown in Figure 5a. The data in Figure 5a shows that this aging time was not sufficient to reach equilibrium (based upon the continuing decrease of the heat capacity). The heat capacity also did not reach the value of the heat capacity observed for the glasses vapor-deposited at $T_{substrate}$ = 0.95 T_g (red dotted line).

We performed a quasi-isothermal annealing experiment on the aged glass and the results are overlaid in Figure 5b with those from the glasses vapor-deposited at $T_{substrate}$ = 0.95 T_g. The aged glass has a transformation time that is much less than the vapor-deposited sample prepared at 0.006 nm/s, despite similar preparation times. The aged glass transformation time is approximately the same as for the vapor-deposited glass prepared at 0.11 nm/s, whose preparation took only 2,300 seconds (24 times less than the aging time). These comparisons show that the kinetic stabilities of the vapor-deposited 2-ethyl-1-hexanol glasses are not simply a result of aging during the deposition process,

and suggest that the kinetic stability of these vapor-deposited glass is controlled by surface mobility. We expand upon this argument in the discussion section.

4.5 Discussion

The goal of this work is to investigate three hypotheses that offer an explanation for why 2-ethyl-1-hexanol does not form a highly stable glass when prepared at the conventional deposition rate of 0.2 nm/s. The first hypothesis is that 2-ethyl-1-hexanol does not possess amorphous configurations with barriers appreciably higher than those associated with the liquid cooled glass. In Figure 2a and Figure 4 we see that the kinetic stability of the vapor-deposited glasses increases greatly with decreasing deposition rate. For glasses prepared at $T_{substrate}$ = 0.90 T_g and the lowest deposition rate, T_{onset} reaches 1.07 T_g and $\log(t_{transformation}/\tau_\alpha)$ reaches $10^{2.5}$. These values of kinetic stability indicate that the configurations of these glasses have much higher barriers to relaxation than configurations typical of a liquid-cooled glass where $T_{onset} = T_g$ and $\log(t_{transformation}/\tau_\alpha) \sim 10^0$. The T_{onset} and $\log(t_{transformation}/\tau_\alpha)$ for 0.90 T_g glasses are approaching values typical of highly stable glasses and the trend of the data suggest the kinetic stability is likely to increase further with lower deposition rates. Therefore, we reject the hypothesis that 2-ethyl-1-hexanol does not have amorphous configurations with high barriers.

The second hypothesis is that glasses of 2-ethyl-1-hexanol deposited at 0.2 nm/s have limited kinetic stability because the configurations preferred at the surface, upon further deposition, do not result in bulk packing with high kinetic stability. From this perspective, one would interpret the experimental observation that kinetic stability increases with decreasing deposition rate (Figure 4) as the result of physical aging that occurs during the deposition, since

longer depositions are required at lower deposition rates. We performed the comparison between vapor-deposited glasses and an aged glass in Figure 5b to test this hypothesis. The transformation time of the liquid-cooled glass that aged for ~ 55,000 s was at least an order of magnitude less than for a vapor-deposited glass that took ~ 43,000 s to prepare (deposition rate = 0.006 nm/s). In addition, the glass vapor-deposited at 0.11 nm/s showed the same transformation time as the aged glass despite a preparation time that is shorter by a factor of 24. These observations in combination with the reasonably high kinetic stability achieved at the lowest deposition rates allow us to reject the second hypothesis.

The third hypothesis, that stable glass formation in 2-ethyl-1-hexanol is inhibited by limited surface mobility, is consistent with our experimental results as we discuss below. For the rest of the discussion we will interpret our results from this viewpoint. We will use our data to estimate the surface mobility of 2-ethyl-1-hexanol and make comparisons to molecules that form highly stable glasses using typical deposition rates.

4.5.1 Kinetic stability as a function of deposition rate

We observe that kinetic stability of the vapor-deposited 2-ethyl-1-hexanol glasses increases with decreasing deposition rate and that very low rates are needed to prepare glasses with high kinetic stability. We quantify kinetic stability using the onset temperature during temperature ramping experiments (Figure 2a) and transformation time during quasi-isothermal annealing experiments (Figure 4). Many stable glasses display maximal onset temperatures of 1.05 – 1.08 T_g, and isothermal transformation times greater than 10^3 τ_α.[5,42] By using deposition rates 2 orders of magnitude lower than a typical rate of 0.2 nm/s, we prepared 2-ethyl-1-hexanol

glasses with T_{onset} = 1.07 T_g and $t_{transformation} = 10^{2.5} \tau_\alpha$. The trend of the data suggests that for $T_{substrate}$ = 0.90 T_g and 0.85 T_g, glasses prepared at lower deposition rates may have even greater kinetic stability.

The results of Figure 2a and Figure 4 shed light on the properties of amorphous configurations available at temperatures below T_g. The kinetic stability of the glasses deposited at 0.95 T_g demonstrate that there are configurations at this temperature with higher barriers than those occupied at equilibrium at T_g. At high deposition rates, the 0.95 T_g glasses have greater kinetic stability than 0.90 T_g glasses, but the situation is reversed at the lowest rates. We interpret this to indicate that configurations with higher barriers are available at 0.90 T_g; however, since surface mobility decreases with decreasing temperature, surface molecules at 0.90 T_g require more time to sample configurations that lead to high kinetic stability. It may be the case that there are configurations with even higher barriers at 0.85 T_g, but the surface mobility for 2-ethyl-1-hexanol at this temperature appears to be so slow that our lowest deposition rates do not allow nearly enough time for molecules to sample such configurations. In contrast, for molecules that more readily form stable glasses, surface mobility is fast enough that glasses with the highest kinetic stability are usually produced at $T_{substrate} \sim 0.85\ T_g$ using a rate of 0.2 nm/s.[42]

4.5.2 Surface vs. bulk relaxation times

The kinetic stability of glasses prepared at $T_{substrate}$ = 0.95 T_g appears to plateau at our lowest deposition rates, allowing us to estimate the time needed for surface relaxation at this temperature. The plateau indicates that the mobility of 2-ethyl-1-hexanol molecules is high enough that the surface has apparently equilibrated during deposition at the lowest rates. We can

estimate a surface relaxation time in the following manner. At a deposition rate of ~ 0.03 nm/s, the onset temperature and transformation times of glasses deposited at 0.95 T_g reaches or approaches a plateau. For this calculation, similar to previous work,[17,43,46] we estimate that the mobile layer is one monolayer thick (~ 0.6 nm for 2-ethyl-1-hexanol). At 0.03 nm/s, it takes 20 seconds to deposit one monolayer and we use this as an estimate of the surface relaxation time. This surface relaxation time is about 4 orders of magnitude faster than the equilibrium value of τ_α for the bulk liquid, obtained by extrapolation. For ethylcyclohexane, a molecule that forms a highly stable glass when prepared at 0.2 nm/s, the surface relaxation time has been estimated to be 6-7 orders of magnitude faster than τ_α at 0.95 T_g using a similar analysis.[46] These comparisons support the hypothesis that 2-ethyl-1-hexanol has enhanced mobility at the surface in comparison to the bulk, but that this enhancement is not sufficient to enable the formation of highly stable glasses at 0.2 nm/s. (Experiments and simulations indicate that, depending on temperature, the mobile layer may be as thick as two or three monolayers,[16,35,81] rather than the single monolayer assumed above. These various possibilities have only a small effect on the order of magnitude comparisons that we make here.)

We can use the data in Figure 5b to develop a second comparison between the surface and bulk relaxation processes. The aged glass and the glass deposited at 0.11 nm/s have approximately the same transformation time. During the deposition of the 0.11 nm/s glass, each molecule had about 5.5 seconds as part of the mobile surface layer. Allowing each molecule 5.5 seconds as part of the surface layer results in the same kinetic stability as aging the liquid-cooled glass for 55,000 seconds. Thus, we estimate that the surface relaxation process is 4 orders of

magnitude faster than the bulk process for 2-ethyl-1-hexanol at 0.95 T_g. It is reassuring that this estimate of the surface relaxation time is in good agreement with the completely independent estimate of the previous paragraph. From a similar analysis, Kearns and coworkers compared the fictive temperatures of indomethacin glasses that were aged or vapor-deposited at 0.94 T_g.[43] They estimated that the surface relaxation process for indomethacin was 7 orders of magnitude faster than the bulk aging process. From this comparison, we deduce that indomethacin has much faster surface relaxation than does 2-ethyl-1-hexanol at similar temperatures below T_g. This is consistent with the observation that indomethacin forms highly stable glasses when deposited at 0.2 nm/s, while 2-ethyl-1-hexanol does not. Yu and coworkers have used a surface grating decay method to measure surface diffusion on indomethacin glasses.[130] The surface diffusion coefficient at 0.95 T_g is about 7 orders of magnitude faster than bulk diffusion. We do not know if surface diffusion is the most relevant measure of surface mobility for stable glass formation, but the grating decay experiments provide a comparison between bulk and surface dynamics that is consistent with estimates obtained from vapor deposition experiments.

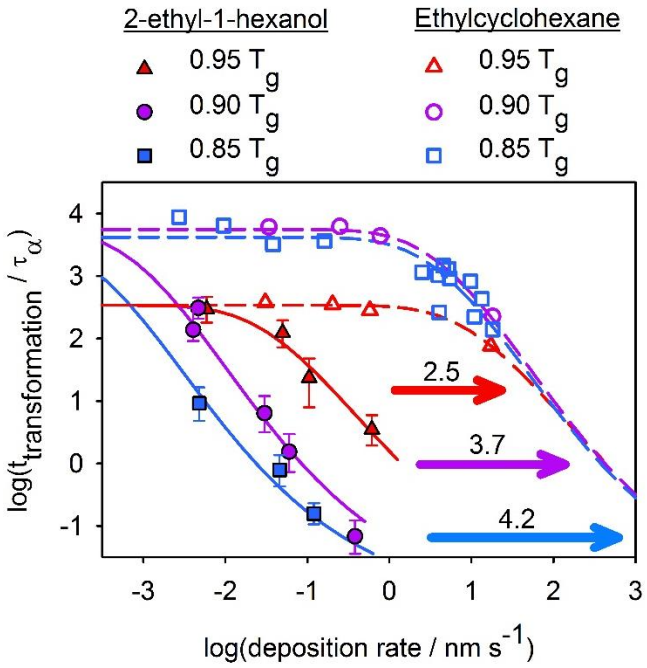

Figure 6: *Comparison of quasi-isothermal transformation times for vapor-deposited glasses of 2-ethyl-1-hexanol and ethylcyclohexane. The data for 2-ethyl-1-hexanol are the same as in Figure 4. The transformation times for ethylcyclohexane are slightly adjusted from the transformation times reported by Chua and coworkers,*[46] *as described in the text. The lines are stretched exponential fits to the data at each substrate temperature. Solid and dashed lines of the same color have the same plateau values at large and small deposition rates and are horizontally shifted by the number of decades above each colored arrow; this number is an estimate of the difference (in orders of magnitude) in surface relaxation times for the two molecules.*

4.5.3 Estimation of surface relaxation times via comparison with ethylcyclohexane

We estimate surface relaxation times for 2-ethyl-1-hexanol by comparing our deposition rate dependent transformation times to those of ethylcyclohexane glasses[46] as shown in Figure 6. The ethylcyclohexane experiments were performed on slightly thicker films (390 nm); assuming that these films transformed via a single propagation front, we have multiplied the transformation times from reference[46] by 0.32 to account for this difference. Chua and coworkers fit their transformation times to a Kohlrausch-Williams-Watts (KWW) function that plateaus at low deposition rates. A characteristic time (τ_{KWW}) for each $T_{substrate}$ is a parameter obtained from the fit. We fit the data for both molecules together in order to obtain τ_{KWW} for these two systems. At each substrate temperature we apply the following fit to the transformation time data:

$$\log\left(t_{transformation}/\tau_{\alpha}\right) = A\left(1 - exp\left[-\left(t_{surface}/\tau_{KWW}\right)^{\beta}\right]\right) + B \qquad (1)$$

The sum A+B gives the value of $\log(t_{transformation}/\tau_{\alpha})$ in the limit of large $t_{surface}$ or low deposition rate. The amount of time on the surface is given by: $t_{surface}$ = 0.6 nm / deposition rate (nm/s). Following Chua and coworkers, the value of β was fixed to 0.35. We assume the values of A and B at a given $T_{substrate}$ are the same for both molecules (see following paragraph). After preliminary fits in which B was allowed to vary with $T_{substrate}$, we decided to set B = -2.3 for all $T_{substrate}$ for simplicity; the effect of this on the $\tau_{surface}$ values in Figure 7 is within the error bars. To fit the 2-ethyl-1-hexanol and ethylcyclohexane data together, we shifted the 2-ethyl-1-hexanol $t_{surface}$ values for a given $T_{substrate}$ by a common factor, choosing the factor of maximize the quality of the fit to the combined data sets. The colored arrows in Figure 6 represent the size of the shift (in orders of magnitude) obtained from the fitting procedure and also give the number

of orders of magnitude difference between τ_{KWW} for 2-ethyl-1-hexanol and ethylcyclohexane. As done by Chua and coworkers, we calculate the surface relaxation time as $\tau_{surface} = 10\ \tau_{KWW}$; this time represents the minimum time on the surface needed to sample configurations that correspond to the highest observed kinetic stability. The $\tau_{surface}$ values are plotted in Figure 7 along with τ_α data for both molecules. The $\tau_{surface}$ values for ethylcyclohexane at $T_{substrate} < 0.85\ T_g$ were obtained in a similar manner, but there was no 2-ethyl-1-hexanol data included for these substrate temperatures. The $\tau_{surface}$ values for ethylcyclohexane obtained here are in good agreement with those obtained in reference [46].

We have assumed in our fitting that the low deposition rate limit of $\log(t_{transformation}/\tau_\alpha)$ is the same for 2-ethyl-1-hexanol and ethylcyclohexane for a given value of $T_{substrate}/T_g$. We see in Figure 6 that for $T_{substrate} = 0.95\ T_g$, the data suggest that this is indeed the case. We also expect the molecules to have similar $\log(t_{transformation}/\tau_\alpha)$ plateaus based on their similar supercooled liquid dynamics. Both the $\log(t_{transformation}/\tau_\alpha)$ plateau value and τ_α are controlled by the barrier heights for the lowest energy configurations at a given temperature. In Figure 7 we see that the VTF predictions of τ_α below T_g for 2-ethyl-1-hexanol and ethylcyclohexane are very similar. This implies that when normalized by T_g, the extrapolated barrier heights for these two liquids are the same at low temperatures. Thus, at a given $T_{substrate}/T_g$ and in the limit of low deposition rate, the low energy amorphous configurations for the two molecules should have similarly sized barriers relative to T_g and we expect the transformation times of the two glasses to be similar.

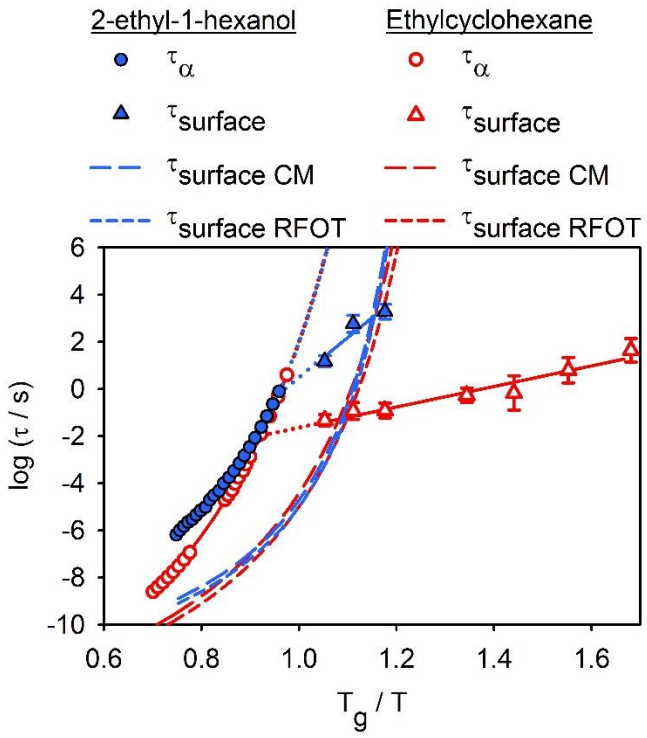

Figure 7: *Relaxation times τ_α and $\tau_{surface}$ for 2-ethyl-1-hexanol and ethylcyclohexane. The $\tau_{surface}$ values are obtained by fitting the data shown in Figure 6 and data from reference* [46] *using the procedure described in the text. The τ_α values for 2-ethyl-1-hexanol are from dielectric spectroscopy measurements in reference* [192]*. The τ_α values for ethylcyclohexane are from dielectric spectroscopy measurements in references* [124] *and* [193]*, and the calculation of τ_α in reference* [124] *using viscosity measurements in reference* [155]*. Predictions of $\tau_{surface}$ from the Random First Order Transition (RFOT) theory*[21] *and the Coupling Model*[23] *(CM) are plotted as dashed lines. VTF fits are plotted with the τ_α data. Arrhenius fits to the $\tau_{surface}$ data are shown. Dotted lines are used to indicate extrapolation of a fitting function beyond the range of experimental data.*

Figure 7 shows that the enhancement of surface mobility is less significant for 2-ethyl-1-hexanol than for ethylcyclohexane. At 0.95 T_g ($T/T_g = 1.05$), $\tau_{surface}$ is about 4 orders of magnitude smaller than the extrapolated τ_α, consistent with the other comparisons made earlier in the discussion section. As expected from Figure 6, we observe that $\tau_{surface}$ is longer for 2-ethyl-1-hexanol than for ethylcyclohexane and has a stronger temperature dependence. Work by Chen and coworkers[18] suggests that the ability to form intermolecular hydrogen bonds may limit the surface mobility and this would be consistent with the slower surface relaxation of 2-ethyl-1-hexanol.

In Figure 7, we also plot predictions of $\tau_{surface}$ from the Random First Order Transition (RFOT) theory[21] and the Coupling Model (CM).[23] For the RFOT calculation, we use $\tau_{surface} = (\tau_0\ \tau_\alpha)^{0.5}$ and a τ_0 value of 1 ps. The CM predicts $\tau_{surface} = (t_c)^{1-\beta}(\tau_\alpha)^\beta$ where $t_c = 2$ ps and β is the stretching exponent from a KWW fit to the alpha relaxation; we used β values of 0.51 for 2-ethyl-1-hexanol and 0.53 for ethylcyclohexane as obtained from dielectric spectroscopy experiments.[143,193] The predictions of the RFOT and CM approaches are quite similar and both predict a very different temperature dependence than what is obtained experimentally. Also, these calculations do not capture the significant difference between $\tau_{surface}$ for 2-ethyl-1-hexanol and ethylcyclohexane. We emphasize that the $\tau_{surface}$ value shown in Figure 7 are not direct measurements of this quantity but rather an inference based upon the stability of vapor-deposited glasses. It is possible that more direct measurements of surface relaxation for these compounds, such as the surface diffusion coefficients obtained from the grating decay method, would show

behavior more similar to the predictions of references [39] and [62]. There has also been interest in assessing whether the beta relaxation is closely related to the surface relaxation time;[62] we make that comparison for these two molecules in Figure S4 of the Supplemental Material. For ethylcyclohexane, there is a significant difference between $\tau_{surface}$ and the Johari Goldstein beta relaxation time.

The apparent intersection of $\tau_{surface}$ and τ_α at temperatures near 1.1 T_g is an interesting phenomenon that presents a challenge to our understanding of enhanced surface mobility. Similar behavior has been previously observed for polymers and recently for low molecular weight glassformers.[46,170,173,177,194–197] From our perspective, this intersection (by extrapolation) at temperatures $\leq$ 1.1 T_g (or $\tau_\alpha \geq 10^{-2}$ s) is surprising based upon the following understanding of supercooled liquid behavior. The τ_α values of fragile supercooled liquids becomes very large with decreasing temperature because the alpha relaxation requires the cooperative motion of multiple molecules.[198] The number of cooperating molecules increases with decreasing temperature,[199] and thus τ_α exhibits a super-Arrhenius temperature dependence. Molecules at the surface are expected to relax faster than those in the bulk because they have fewer neighbors to inhibit their motion.[39,41] Supercooled liquids commonly show evidence of cooperative dynamics well above 1.1 T_g (or for $\tau_\alpha < 10^{-2}$ s).[8,199,200] Thus, we would expect $\tau_{surface}$ to be faster than τ_α at temperatures higher than the intersection suggested by the data. Theoretical treatments of surface mobility also do not predict an intersection of $\tau_{surface}$ and τ_α at any temperature.[39,41,62] The predictions of RFOT and CM theories in Figure 7 illustrate this behavior. Until recently, the evidence for the intersection of surface and bulk relaxation processes has largely come from

experiments with polymers.[170,173,177,194,196,197] Studies of surface and bulk diffusion coefficients of low molecular weight glassformers do not show any indication of such an intersection .[17,75,130,134] It has been suggested that the intersection of the surface and bulk relaxation processes might be due to chain connectivity effects in polymers.[41,173] However, it appears that the intersection of surface and bulk processes also occurs for small molecules based on the $\tau_{surface}$ data in Figure 7 for 2-ethyl-1-hexanol and ethylcylohexane,[46] and based on thin film experiments with N,N′-Bis(3-methylphenyl)-N,N′-diphenylbenzidine (TPD).[195] While we do not have a way to reconcile all these results, it seems important to more fully understand what is being measured by the various experiments. It would be useful to perform surface diffusion measurements and deposition rate dependent vapor deposition on the same low molecular weight glassformer. Such experiments would be expected to contribute, although indirectly, to our understanding of dynamics in thin polymer films.

4.6 Conclusion

We prepared vapor-deposited glasses of 2-ethyl-1-hexanol using a wide range of deposition rates and assessed the kinetic stability of the glasses using AC nanocalorimetry. At deposition rates typically used to prepare highly stable glasses (0.2 nm/s), 2-ethyl-1-hexanol forms glasses with moderate kinetic stability. We observed that the kinetic stability increases significantly when the deposition rate is decreased, consistent with the hypothesis that the surface mobility for this molecule is limited in comparison to those that form highly stable glasses when deposited at 0.2 nm/s. We performed experiments with an aged glass to confirm

that the increase in kinetic stability is indeed a result of surface relaxation and is not due to bulk aging during the long deposition period. We used our results to estimate that the surface relaxation process in 2-ethly-1-hexanol is faster than bulk relaxation, but is slower than the surface relaxation of molecules like ethylcylohexane and indomethacin that readily form highly stable glasses at conventional deposition rates. We estimated $\tau_{surface}$ values for 2-ethyl-1-hexanol and compared these to results for ethylcyclohexane and to theoretical predictions. $\tau_{surface}$ values for both 2-ethyl-1-hexanol and ethylcyclohexane show an apparent intersection with τ_{α} near 1.1 T_g that is not predicted by the RFOT or Coupling Model. This feature, which is similar to reports for polymeric glassformers, deserves further investigation.

4.7 Acknowledgements

We thank the U.S. National Science Foundation (CHE-1265737 and CHE-1564663) for support of this work.

4.8 Supplemental Material

4.8.1 Quasi-isothermal annealing experiments

In Figures S1 – S3 we replot of the quasi-isothermal annealing experiments shown in Figure 3 with linear time axes in order to clarify the transformation times for these experiments. We have added dashed lines to demonstrate the determination of the transformation time.

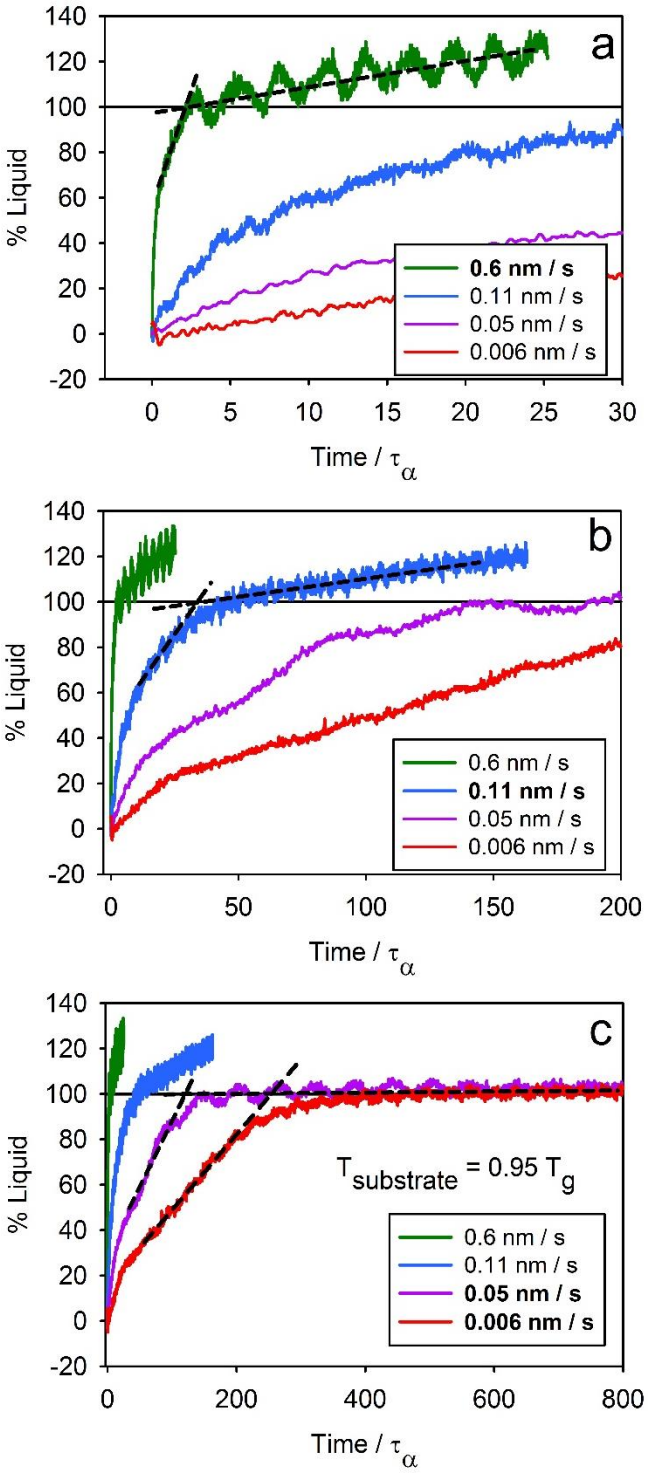

Figure S1: *Quasi-isothermal transformations of $T_{substrate}$ = 0.95 T_g glasses with linear time axes.*

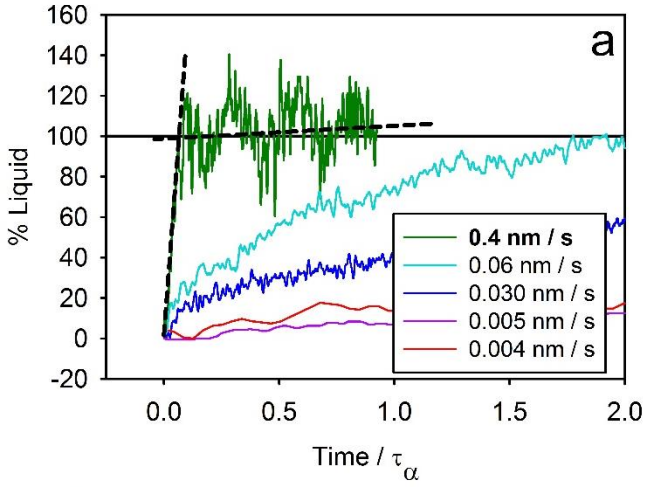
a
% Liquid
Time / τα
0.4 nm / s
0.06 nm / s
0.030 nm / s
0.005 nm / s
0.004 nm / s

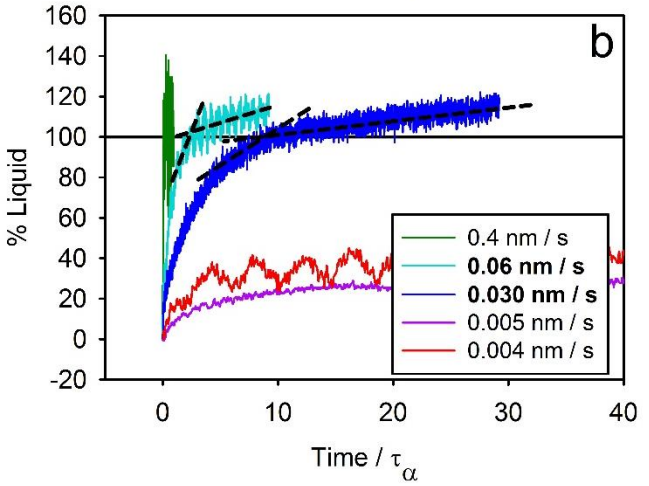
b
% Liquid
Time / τα
0.4 nm / s
0.06 nm / s
0.030 nm / s
0.005 nm / s
0.004 nm / s

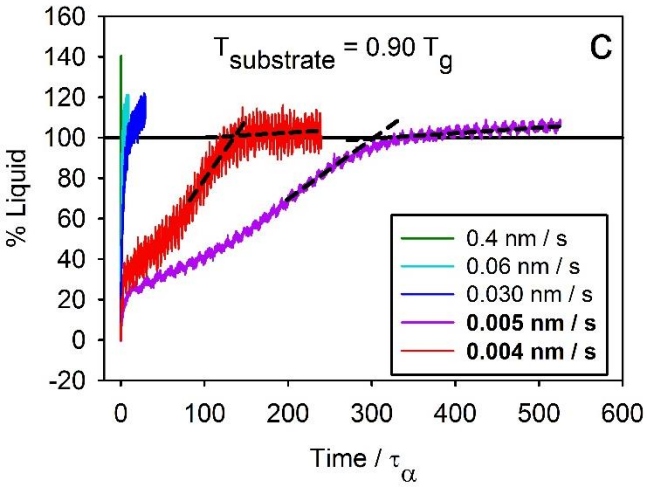
c
Tsubstrate = 0.90 Tg
% Liquid
Time / τα
0.4 nm / s
0.06 nm / s
0.030 nm / s
0.005 nm / s
0.004 nm / s

Figure S2: *Quasi-isothermal transformations of $T_{substrate}$ = 0.90 T_g glasses with linear time axes. The film deposited at 0.004 nm/s was 170 nm thick, compared to 250 nm for the other samples. If the transformation time scales with thickness, the 0.004 nm/s film would have a similar transformation time compared to the 0.005 nm/s sample when adjusted for thickness.*

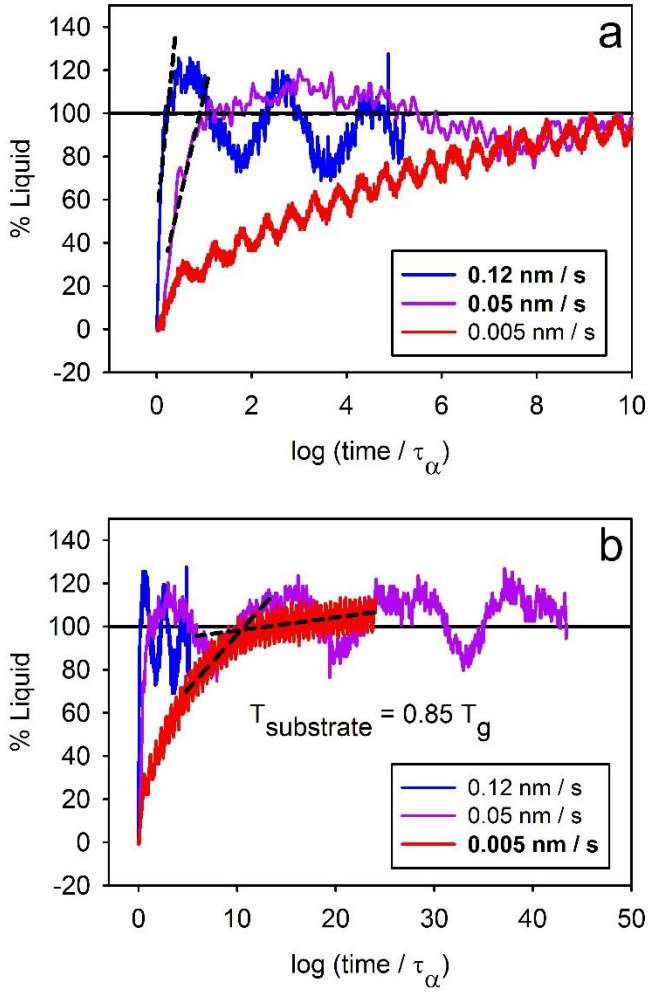

Figure S3: *Quasi-isothermal transformations of $T_{substrate}$ = 0.85 T_g glasses with linear time axes.*

4.8.2 Comparison of $\tau_{surface}$, τ_{α}, and τ_{β} relaxation times

In Figure S4 we plot the $\tau_{surface}$ and τ_{α} values for 2-ethyl-1-hexanol and ethylcyclohexane (as in Figure 7) with the addition of experimentally determined and τ_{β} values. We have included the comparison between $\tau_{surface}$ and τ_{β} because it has been suggested that the beta relaxation process and the surface relaxation process are related and thus might be expected to have similar relaxation times.[46,62] The Coupling Model in particular predicts that the Johari Goldstein beta relaxation time will be approximately the same as the surface relaxation time ($\tau_{\beta\ JG} \approx \tau_{surface}$).[62] For 2-ethyl-1-hexanol the observed τ_{β} values do not agree with the $\tau_{surface}$ values and for ethylcyclohexane the calculated $\tau_{\beta\ JG}$ values do not agree with the $\tau_{surface}$ values.

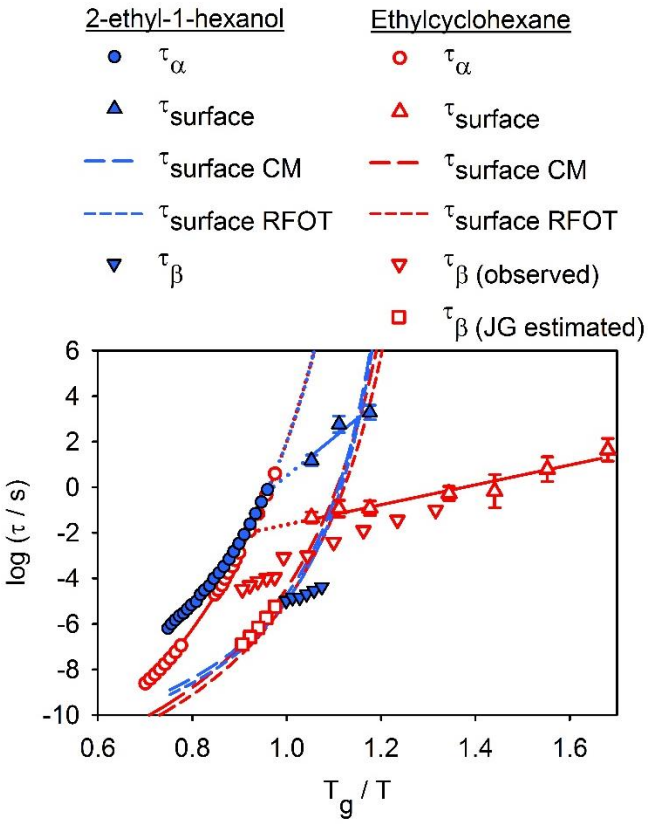

Figure S4: *Relaxation plot showing τ_α, $\tau_{surface}$, and τ_β values for 2-ethyl-1-hexanol and ethylcyclohexane. The τ_α and τ_β values for 2-ethyl-1-hexanol are from dielectric spectroscopy measurements in reference* [192]*.The $\tau_{surface}$ values for 2-ethyl-1-hexanol are obtained by the comparison with ethylcyclohexane data shown in Figure 6. The τ_α values for ethylcyclohexane are from dielectric spectroscopy measurements in references* [124] *and* [193]*, and the calculation of τ_α in reference* [124] *using viscosity measurements in reference* [155]*. The $\tau_{\beta\,(observed)}$ values for ethylcyclohexane are from dielectric spectroscopy measurements in references* [124] *and* [193]*. The authors of those papers have argued that the observed beta relaxation is not the Johari-Goldstein (JG) beta relaxation. The $\tau_{\beta\,(JG\ estimated)}$ values for ethylcyclohexane were calculated by*

the authors in reference [124] *based on the Coupling Model. The ethylcyclohexane* $\tau_{surface}$ *values were obtained by the fitting procedure described in the main text using slightly modified data from Chua and coworkers and are in good agreement with the* $\tau_{surface}$ values obtained in that work.[46] *Predictions of* $\tau_{surface}$ *from the Random First Order Transition (RFOT) theory and Coupling Model (CM) are plotted as lines.*[39,62]

Chapter 5

Future Directions

5.1 Introduction

In this final chapter I will propose several future experiments inspired by the work in this thesis or related to this thesis. There are two major questions I that am intrigued by. First, it appears that intermolecular hydrogen bonding can inhibit surface mobility. Can we predict how hydrogen bonding influences surface mobility? Second, the kinetic stability of vapor-deposited glasses is a result of amorphous configurations below T_g that have higher barriers than configurations at T_g. How far does the trend of increasing barriers with decreasing temperature go? Can this provide an estimation of supercooled liquid behavior below T_g? I also suggest an experiment for Christoph Schick's group at the University of Rostock.

5.2 Intermolecular Hydrogen Bonding and Surface Mobility

Recent work has demonstrated that hydrogen bonding can influence surface mobility, but more work is needed to characterize and predict the role of hydrogen bonding. Chen and coworkers have demonstrated that intermolecular hydrogen bonding can inhibit surface diffusion in polyols.[18] In the work of Chapter 3 my colleagues and I observed that several alcohol molecules that participate in intermolecular bonding do not form highly stable glasses when deposited at the typical rate of 0.2 nm/s.[5] It was hypothesized that those alcohol molecules have limited surface mobility that inhibits the formation of stable glasses. In the work of Chapter 4 I performed experiments that supported this hypothesis for 2-ethyl-1-hexanol.[23] At 0.85 T_g, I estimated that the surface mobility of 2-ethyl-1-hexanol is at least 4 orders of magnitude less

than for ethylcyclohexane; a molecule that does form stable glasses at typical deposition rates. The limited surface mobility is likely due the intermolecular hydrogen bonding present in 2-ethyl-1-hexanol. In chapter 3, benzyl alcohol was able to prepare a stable glass when deposited at the typical rate of 0.2 nm/s,[5] suggesting that this alcohol molecule does have high surface mobility. We could explain this apparent difference between benzyl alcohol and 2-ethyl-1-hexanol surface mobilites with the hypothesis that steric hindrance limits hydrogen bonding in benzyl alcohol. There is limited evidence that the formation of intermolecular hydrogen bonds is limited in benzyl alcohol liquid.[150] More data is needed to develop an understanding of how the strength or prevalence of intermolecular hydrogen bonds influences surface mobility. Lavanture and coworkers have also studied the role of hydrogen bonding in the properties of vapor-deposited glasses.[201] They found that the kinetic stability of vapor deposited triazine glasses was the lowest for glasses of the molecule that participated in more intermolecular hydrogen bonds. However, they did not attempt to determine or rank the surface mobilities of the triazine molecules. I believe the field needs a study to compare the surface mobility of glasses with a quantification that describes the intermolecular hydrogen bonding.

Deposition rate studies like those pioneered by Chua and coworkers[46] and used in Chapter 4[23] could help quantify the effect of hydrogen bonding on surface mobility if the correct molecules are used for the study. Measuring kinetic stability as a function of deposition rate has proven to be an effective method of estimating surface mobility. I propose performing this technique with a series of glassformers with varying amounts of intermolecular hydrogen bonding. The systematic change in intermolecular bonding can be achieved by systematically

varying the steric hindrance to intermolecular hydrogen bonding and by diluting the hydrogen bonding by mixing an alcohol with a molecule that does not participate in hydrogen bonding.

5.2.1 Reducing hydrogen bonding via steric hindrance in phenyl propanols

The amount of intermolecular hydrogen bonding can be varied by depositing molecules with changing steric hindrance to hydrogen bonding. The series of 1-phenyl-1-propanol, 1-phenyl-2-propanol, and 3-phenyl-1-propanol is a good candidate for using steric hindrance to change hydrogen bonding. Johari and coworkers have studied all three of these supercooled liquids via dielectric spectroscopy.[202–204] As the phenyl group is moved closer to the hydroxyl group, the spectra shows evidence of decreasing hydrogen bonding in the liquid. The presence of a Debye relaxation peak at frequencies lower than the structural relaxation (alpha) peak in mono alcohols has been attributed to the formation of hydrogen bonded chains.[205] As the steric hindrance to forming hydrogen bonds in these phenyl propanols is increases, the Debye peak decreases in strength and appears to be eliminated for 1-phenyl-1-propanol. The trend is consistent with a reduction in the length of hydrogen bonded chains as steric hindrance increases. The permittivity of the three isomers also decreases with increasing steric hindrance. The dipole moments are these three isomers are similar. The permittivity of the three molecules is then expected to be similar, unless there is variation in the formation of intermolecular structures with aligned dipole moments, like hydrogen bonded chains. Thus, the decrease in permittivity as the phenyl group is moved closer to the hydroxyl group is interpreted as a decrease in the number and/or length of hydrogen bonded chains. Johari and coworkers have calculated the Kirkwood correlation factor (g) for these liquids which is used to quantify the contribution to the total

permittivity from structures with correlated dipoles. The correlation factor decreases with increasing steric hindrance suggesting that hydrogen bonded chains become shorter. The value of the correlation factor for 1-phenyl-1-propanol ($g \approx 1$) suggests that this molecule does not form any hydrogen bonded chains. I expect that the surface mobility of these molecules would increase as the Kirkwood correlation factor decreases.

I think the proposed experiments of evaluating the surface mobility of three phenyl propanol isomers has a high likelihood of success. The procedure for using deposition rate dependent kinetic stability to estimate surface mobility has been established by Chua and coworkers and I have used this procedure to produce the results in Chapter 4. The proposed molecules of 1-phenyl-1-propanol, 1-phenyl-2-propanol, and 3-phenyl-1-propanol have glass transition temperatures (~ 190 K) in the operating range of the *in-situ* chamber and the dielectric properties of the supercooled liquids have already been studied.[202–204] The Kirkwood correlation factors determined from dielectric spectroscopy strictly give information about the potential formation of structures with aligned dipoles. The reduced values of *g* do not necessarily prove a reduction of the number or strength of intermolecular hydrogen bonds because it is possible to form a mixture of structures with aligned and anti-aligned dipoles that ultimately cancel each other out.[202] There is a slight reduction in the boiling points as the phenyl group is moved closer to the OH ($T_{B\ 3\text{-phenyl-1-propanol}}$ = 509 K,[206] $T_{B\ 1\text{-phenyl-2-propanol}}$ = 493 K,[207] $T_{B\ 1\text{-phenyl-1-propanol}}$ = 492 K[206]) which is consistent with the interpretation of a reduction in hydrogen bonding with increasing steric hindrance. Additional methods of quantifying intermolecular hydrogen bonding such as modeling liquid phase IR spectra[201,208] and determining the hydrogen bonding contribution to vaporization enthalpies would be helpful in this study.[209,210] The evaluation of the

strength of hydrogen bonding or number of hydrogen bonds per molecule by these techniques should avoid the ambiguity associated the Kirkwood correlation factor. I expect that both the strength and number of hydrogen bonds will be inversely related to the surface mobility. It appears that experiments may be needed to acquire the liquid IR spectra and the vaporization enthalpies for all of these molecules.

5.2.2 Diluting hydrogen bonding by mixing 2-ethyl-1-hexanol with 2-ethyl-1-hexyl bromide

Hydrogen bonding in vapor-deposited glasses could also be varied by depositing mixtures of 2-ethyl-1-hexanol and 2-ethyl-1-hexyl bromide. These two molecules are miscible and their supercooled liquid mixtures have been studied by Preuß and coworkers.[211] As the concentration of 2-ethyl-1-hexanol decreases, the low frequency Debye relaxation peak in the dielectric spectra decreases in strength, indicating a decrease in the number and/or length of hydrogen bonded chains that are responsible for the Debye peak in mono alcohols. Infrared spectroscopy measurements suggest that that chains get shorter as the concentration of 2-ethyl-1-hexanol decreases to about 60 % while the number of chains appears to be constant. At lower concentrations, the number of hydrogen bonded structures may decrease as well. Modeling of the infrared spectra may be able to quantify the fraction of 2-ethyl-1-hexanol molecules participating in hydrogen bonding.[208] A relative measure of hydrogen bonding in these mixtures can be estimated in a number of ways (Debye peak intensity, IR spectra, modeling) and all could be compared to determinations of surface mobility from deposition rate dependent experiments. If we crudely treat the hydrogen bonded chains as polymers, we might predict that the surface mobility would increase most significantly when the chain length decreases. Experiments by

Lian Yu's research group has demonstrated that for aromatic hydrocarbons surface diffusion is inversely related to molecular weight.[17,134,212] The trend is likely related to the estimations that mobility decays quickly as a function of depth in the film. Long chains near the surface are likely to have part of the molecule several layers below the surface where mobility is very low. I would predict then that the surface mobility of the mixtures will increase quickly as the 2-ethyl-1-hexanol chains become shorter (from 100 % 2-ethyl-1-hexanol to 60 %) and then the surface mobility will be relatively constant for lower concentrations of the alcohol (below 50 %).

The proposed project of performing deposition rate dependent experiments of these mixtures has many features that will promote successful experiments. The two molecules are both well studied glassformers with glass transition temperatures in the operating range of the *in-situ* chamber (144 K for the alcohol, 131 K for the bromide). Furthermore, I have already characterized the surface mobility of pure 2-ethyl-1-hexanol in Chapter 4.[23] The current apparatus has been used to successfully deposited and characterize binary mixed glasses.[48] The composition of the mixed glasses can be estimated from the ion gauge pressure after opening each leak valve to introduce each component. I anticipate that the nanocalorimeters would be the best devices for performing kinetic stability experiments because they are sensitive to thinner films and allow for lower deposition rates for a given deposition time compared to the dielectric spectroscopy device. However, dielectric spectroscopy measurements of supercooled liquid films after transformation of the as deposited glasses would allow for an internal comparison of hydrogen bonding between samples by measuring the height of the Debye peak (either in absolute units following an adjustment for the film thickness, or relative to the height of the alpha peak). The Debye peak height measured *in-situ* as a function of estimated composition

during deposition could be compared to the Preuß work to calibrate the compositions of the deposited films.

5.3 Increasing barriers with decreasing temperature

Stable glasses allow experiments to probe the evolution of the PEL for temperatures below T_g. The kinetic stability of vapor-deposited glasses is a result of amorphous configurations at temperatures below T_g that have higher barriers to relaxation compared to configurations available at T_g.[43,81] It is not surprising that there are metabasins available at temperatures below T_g that have higher barriers than the metabasins available at T_g. Many glass-formers have fragile τ_α vs temperature behavior in the supercooled liquid which is consistent with increasing barriers for decreasing temperature above T_g.[2] Thus, the increasing barrier height for decreasing temperatures below T_g could be expected based on supercooled liquid behavior. There are two major questions about barriers below T_g that can be studied with vapor-deposited glasses. How far below T_g do barriers continue to decrease with decreasing temperature? How much do barriers increase with decreasing temperature below T_g?

The questions of how far and how steeply barriers continue to increase below T_g is related to the debates over what the behavior of τ_α is for a supercooled liquid below T_g. This is hard to measure because of the extreme times needed to equilibrate at low temperatures. The τ_α vs T data for fragile supercooled liquids are often fit to the empirical Vogel Tamman Fulcher (VTF) equation,[129] which has a form that predicts τ_α becomes infinite at a $T_0 > 0$ K. Since an infinite τ_α at T > 0 K is rather surprising, (it suggests the scenario of a configuration with infinitely high barriers) this divergence draws a lot of attention. Some researchers have found a

correlation between T_0 and the Kauzmann temperature T_K,[213] and argue that this link between the Kauzmann entropy crisis and diverging τ_α for many supercooled liquids means the extrapolation of the VTF equation is meaningful. However, it should be noted that the equality between T_0 and T_K does not appear to be universal.[214] Others have demonstrated that the τ_α vs T data for supercooled liquids can be fit just as well by equations that do not diverge at T > 0 K just as well as by the VTF equation.[63] Thus it is argued that the diverging τ_α from the VTF equation is not meaningful. Finally, there is the possibility that the supercooled liquid behavior of fragile systems becomes Arrhenius below T_g,[188,190] switching from increasing barriers with decreasing temperature to a constant barrier at all lower temperatures. There is some experimental evidence that is used to support this idea.[189,191] I think it's also worthy of noting that the switch from fragile to Arrhenius behavior has also been seen above T_g for simulations of silica when the sample finds the bottom of the amorphous part of the potential energy landscape (see Chapter 1).[20]

Previous experiments with stable glasses have already provided results related to the above questions. Dawson and coworkers measured isothermal transformation times of stable glasses of *tris*-napthyl benzene isomers.[97] They transformed the glasses at several annealing temperatures which provided information about the temperature dependence of the transformation times. They extrapolated the transformation time vs temperature behavior down to the deposition temperature. The transformation time for a small temperature change near $T_{substrate}$ would be equivalent to τ_α at that temperature if the sample was an equilibrated supercooled liquid. The authors only prepared samples at a single deposition rate, so it is

unknown if they reached the slow deposition rate limit. For the sake of demonstrating what we can learn from such data, I'll assume their films were equilibrated supercooled liquids. They found that the estimates of τ_α at 0.85 T_g varied from 10^2 years for the α,α,β isomer to 10^7 years for the α,β,β isomer. This is an interesting observation because the supercooled liquid of the α,α,β isomer appears to be slightly more fragile than α,β,β. Thus the I would predict that there are metabasins with higher barriers available α,α,β isomer at 0.85 T_g and this stable glass should have the longer transformation time. The data shows the opposite behavior. If the glasses were equilibrated supercooled liquids, the result would demonstrate that the τ_α vs T behavior above T_g does not follow the same trend that is seen above T_g. Similar experiments using multiple deposition rates and multiple substrate temperatures could provide estimates of τ_α below T_g and test various extrapolations of τ_α data.

The experiments done by Chua and coworkers revealed data related to the question of how far below T_g do barriers continue to increase with decreasing temperature.[46] They determined the kinetic stability of ethylcyclohexane stable glasses in the limit of low deposition rates at many substrate temperatures. This plateau value of the kinetic stability showed a maximum near 0.90 T_g. That maximum could be interpreted as the result of a change in the temperature dependence of barriers in the PEL. I think it would be interesting to do similar experiments with other molecules. If there are fragile to strong transitions where the amorphous energy landscape reaches a bottom and helps avert the entropy crisis and prevent τ_α form diverging, we would expect to see such transitions relatively close to T_g for very fragile liquids

because T_0 and T_K are close to T_g for fragile liquids. For ethylcyclohexane, T_0 and T_K are around 0.7 T_g.

5.3.1 Investigating barrier height below T_g using stable glasses

I'm proposing measurements of the kinetic stability in the limit of low deposition rate as a function of substrate temperature for multiple glassformers. The first goal of the project would be to see if there is a maximum in the limiting kinetic stability for other molecules besides ethylcyclohexane. If the extrapolations associated with T_0 and T_K are meaningful, we would expect to see plateaus in the kinetic stability vs $T_{substrate}$ data before T_0 or T_K. The second goal would be to use isothermal transformation experiments done a different temperatures to estimate $t_{transformation}$ for temperatures below T_g. If the vapor-deposited glass is the supercooled liquid, $t_{transformation}$ for $T \approx T_g$, the transformation time is about equal to τ_α. We could test if τ_α is larger at a given $T_{substrate}/T_g$ for a highly fragile glass-former compared to a less fragile glass former. In the work in Chapter 4, I explored alternate quantifications of fragility and we could evaluate which fragility measure does the best job of predicting τ_α below T_g. It would also be interesting to test the results against various equations that fit τ_α vs T data above T_g and differ in their predictions below T_g.

The glassformers *cis/trans* decalin (50:50 ratio), methyl-*m*-toluate, and *o*-terphenyl would all be interesting systems for this project. *Cis/trans* decalin has an extremely high *m* fragility index (147) and the T_0 value from a VTF fit of the τ_α data is only 12 K below T_g (T_0 = 0.91 T_g).[215] If there is a change in the evolution of amorphous configurations near T_0, vapor-deposited glasses may be sensitive to it because surface mobility at temperatures near T_0 will still be high

enough for rapid sampling of configurations during deposition. Also, τ_α vs T fitting equations with different predictions below T_g should become very different rather quickly because one of the equations a divergence only slightly below T_g. Methyl-*m*-toluate is a relatively low fragility molecule while still appearing to have high enough surface mobility to prepare stable glasses with high deposition rate.[54,61] This low fragility system would be a nice comparison to the high fragility *cis-trans* decalin. *o*-Terphenyl has a very high fragility when measured by $\log(\tau_\alpha)$ at 1.25 T_g but a moderate fragility when measured by *m* (see Chapter 3).[5] The inclusion of this system would be useful in evaluating how various measures of fragility correlate with changes to the limiting kinetic stability temperature dependence. It also could help evaluate how measures of fragility correlate with the limiting value of kinetic stability for a given $T_{substrate}$ across multiple glassformers. These vapor-deposited glasses have been studied before with the *in-situ* chamber,[42,48,54] but those studies were performed with a single deposition rate. *o*-Terphenyl has a T_g near the upper limit for the operating temperature of the *in-situ* chamber and has a low vapor pressure. As such, there are some technical challenges to doing experiments with this molecule and it may be desirable to find another molecule with similar temperature dependence of τ_α but a lower T_g.

5.4 Further investigation of n-propanol kinetic stability at the University of Rostock

R Souda has investigated n-propanol glass deposited near 0.2 T_g and his results indicate an onset temperature for the transformation from vapor-deposited glass to supercooled liquid is 1.13 T_g.[116] Souda interprets his data as demonstrating high kinetic stability for this glass. The result is quite surprising from the perspective of the Ediger and Schick groups. In Chapter 3, the

experiments done by Yeong Zen Chua at the University of Rostock indicated that vapor-deposited glasses of n-propanol prepared at 0.2 nm/s have minimal kinetic stability when deposited at $T_{substrate} = 0.96\ T_g$, and no measurable kinetic stability when prepared at $0.80\ T_g \leq T_{substrate} \leq 0.92\ T_g$.[5] Additionally, we have found that for many stable glass formers that deposition at $T_{substrate} < 0.6\ T_g$ using deposition rates near 0.2 nm/s produces unstable glasses.[42] These glasses go through irreversible changes below T_g when being heated. The resulting glasses do not have any kinetic stability. The production of unstable glasses at low substrate temperatures is explained as the result of surface mobility decreasing with temperature until it is too slow with respect to the deposition rate to allow sampling of configurations corresponding to increased kinetic stability. Given the behavior or vapor-deposited *n*-propanol glasses in Chapter 3, and the phenomenon of unstable glasses for low $T_{substrate}$, it is surprising that the n-propanol glass produced by Souda at $T_{substrate} = 0.2\ T_g$ showed evidence of kinetic stability. If n-propanol glasses deposited at $T_{substrate} = 0.2\ T_g$ at the University of Rostock show signs of kinetic stability then it would challenge our expectation that surface mobility at such low temperatures would not be enough to be able to produce a stable glass. This would also cause us to reconsider our hypothesis that n-propanol glasses in Chapter 4 did have high kinetic stability because of limited surface mobility.

References

1. M. D. Ediger, C. A. Angell and S. R. Nagel, Supercooled Liquids and Glasses, *J. Phys. Chem.* **100** 13200–13212. (1996).; DOI:10.1021/JP953538D

2. P. G. Debenedetti and F. H. Stillinger, Supercooled liquids and the glass transition., *Nature* **410** 259–67. (2001).; DOI:10.1038/35065704

3. M. D. Ediger and P. Harrowell, Perspective: Supercooled liquids and glasses., *J. Chem. Phys.* **137** 80901. (2012).; DOI:10.1063/1.4747326

4. C. P. Royall and S. R. Williams, The role of local structure in dynamical arrest, *Phys. Rep.* **560** 1–75. (2015).; DOI:10.1016/j.physrep.2014.11.004

5. M. Tylinski, Y. Z. Chua, M. S. Beasley, C. Schick and M. D. Ediger, Vapor-deposited alcohol glasses reveal a wide range of kinetic stability, *J. Chem. Phys.* **145** 174506. (2016).; DOI:10.1063/1.4966582

6. L.-M. Wang, Y. Tian, R. Liu and R. Richert, Calorimetric versus kinetic glass transitions in viscous monohydroxy alcohols., *J. Chem. Phys.* **128** 84503. (2008).; DOI:10.1063/1.2840357

7. L. C. E. Struik, Physical aging in plastics and other glassy materials, *Polym. Eng. Sci.* **17** 165–173. (1977).; DOI:10.1002/pen.760170305

8. R. Richert, Supercooled Liquid Dynamics: Advances and Challenges, *Struct. Glas. Supercooled Liq.* 1–30. (2012), Hoboken, NJ, USA: John Wiley & Sons, Inc.; DOI:10.1002/9781118202470.ch1

9. L. Yu, Surface mobility of molecular glasses and its importance in physical stability, *Adv. Drug Deliv. Rev.* **100** 3–9. (2016).; DOI:10.1016/j.addr.2016.01.005

10. M. D. Ediger and J. A. Forrest, Dynamics near Free Surfaces and the Glass Transition in Thin Polymer Films: A View to the Future, *Macromolecules* **47** 471–478. (2014).; DOI:10.1021/ma4017696

11. C. . Angell, Relaxation in liquids, polymers and plastic crystals — strong/fragile patterns and problems, *J. Non. Cryst. Solids* **131** 13–31. (1991).; DOI:10.1016/0022-3093(91)90266-9

12. M. D. Ediger, Spatially Heterogenous Dynamics in Supercooled Liquids, *Annu. Rev. Phys. Chem.* **51** 99–128. (2000).; DOI:10.1146/annurev.physchem.51.1.99

13. K. Paeng, H. Park, D. T. Hoang and L. J. Kaufman, Ideal probe single-molecule experiments reveal the intrinsic dynamic heterogeneity of a supercooled liquid., *Proc. Natl. Acad. Sci. U. S. A.* **112** 4952–7. (2015).; DOI:10.1073/pnas.1424636112

14. M. T. Cicerone, F. R. Blackburn and M. D. Ediger, How do molecules move near Tg? Molecular rotation of six probes in o-terphenyl across 14 decades in time, *J. Chem. Phys.* **102** 471. (1995).; DOI:10.1063/1.469425

15. U. Tracht, M. Wilhelm, A. Heuer, H. Feng, K. Schmidt-Rohr and H. W. Spiess, Length Scale of Dynamic Heterogeneities at the Glass Transition Determined by Multidimensional Nuclear Magnetic Resonance, *Phys. Rev. Lett.* **81** 2727–2730. (1998).; DOI:10.1103/PhysRevLett.81.2727

16. R. C. Bell, H. Wang, M. J. Iedema and J. P. Cowin, Nanometer-Resolved Interfacial Fluidity, *J. Am. Chem. Soc.* **125** 5176–5185. (2003).; DOI:10.1021/ja0291437

17. W. Zhang, C. Brian and L. Yu, Fast Surface Diffusion of Amorphous ortho-Terphenyl and its Competition with Viscous Flow in Surface Evolution, *J. Phys. Chem. B* **119** 5071–5078. (2015).; DOI:10.1021/jp5127464

18. Y. Chen, W. Zhang and L. Yu, Hydrogen Bonding Slows Down Surface Diffusion of Molecular Glasses, *J. Phys. Chem. B* **120** 8007–8015. (2016).; DOI:10.1021/acs.jpcb.6b05658

19. B. Doliwa and A. Heuer, What Does the Potential Energy Landscape Tell Us about the Dynamics of Supercooled Liquids and Glasses?, *Phys. Rev. Lett.* **91** 235501. (2003).; DOI:10.1103/PhysRevLett.91.235501

20. A. Saksaengwijit, J. Reinisch and A. Heuer, Origin of the Fragile-to-Strong Crossover in Liquid Silica as Expressed by its Potential-Energy Landscape, *Phys. Rev. Lett.* **93** 235701. (2004).; DOI:10.1103/PhysRevLett.93.235701

21. W. Kauzmann, The Nature of the Glassy State and the Behavior of Liquids at Low Temperatures., *Chem. Rev.* **43** 219–256. (1948).; DOI:10.1021/cr60135a002

22. L. Berthier and G. Biroli, Theoretical perspective on the glass transition and amorphous materials, *Rev. Mod. Phys.* **83** 587–645. (2011).; DOI:10.1103/RevModPhys.83.587

23. M. Tylinski, M. S. Beasley, Y. Z. Chua, C. Schick and M. D. Ediger, Surface mobility limits stable glass formation for 2-ethyl-1-hexanol, *J. Chem. Phys.* (2016).

24. A. K. Varshneya, Chemical Strengthening of Glass: Lessons Learned and Yet To Be Learned, *Int. J. Appl. Glas. Sci.* **1** 131–142. (2010).; DOI:10.1111/j.2041-1294.2010.00010.x

25. Gorilla Glass Cover Glass | Corning Gorilla Glass, . (n.d.).; Retrieved from http://www.corning.com/gorillaglass/worldwide/en.html

26. J. M. Caruthers and G. A. Medvedev, Thermo-mechanical Signatures of Polymeric Glasses, In C. B. Roth (Ed.), *Polym. Glas.* (2016), Boca Raton, Florida: CRC Press - In press.; Retrieved from https://www.crcpress.com/Polymer-Glasses/Roth/p/book/9781498711876

27. B. C. Hancock and G. Zografi, Characteristics and Significance of the Amorphous State in Pharmaceutical Systems, *J. Pharm. Sci.* **86** 1–12. (1997).; DOI:10.1021/js9601896

28. L. Yu, Amorphous pharmaceutical solids: preparation, characterization and stabilization, *Adv. Drug Deliv. Rev.* **48** 27–42. (2001).; DOI:10.1016/S0169-409X(01)00098-9

29. W. A. Gambling, The rise and rise of optical fibers, *IEEE J. Sel. Top. Quantum Electron.* **6** 1084–1093. (2000).; DOI:10.1109/2944.902157

30. M. Chen, A brief overview of bulk metallic glasses, *NPG Asia Mater.* **3** 82–90. (2011).; DOI:10.1038/asiamat.2011.30

31. Is metallic glass poised to come of age?, *Nat. Mater.* **14** 553–555. (2015).; DOI:10.1038/nmat4297

32. D. Yokoyama, Molecular orientation in small-molecule organic light-emitting diodes, *J. Mater. Chem.* **21** 19187. (2011).; DOI:10.1039/c1jm13417e

33. W. Ping, D. Paraska, R. Baker, P. Harrowell and C. A. Angell, Molecular Engineering of the Glass Transition: Glass-Forming Ability across a Homologous Series of Cyclic Stilbenes, *J. Phys. Chem. B* **115** 4696–4702. (2011).; DOI:10.1021/jp110975y

34. S. S. Dalal, D. M. Walters, I. Lyubimov, J. J. de Pablo and M. D. Ediger, Tunable molecular orientation and elevated thermal stability of vapor-deposited organic semiconductors, *Proc. Natl. Acad. Sci.* **112** 4227–4232. (2015).; DOI:10.1073/pnas.1421042112

35. R. Malshe, M. D. Ediger, L. Yu and J. J. de Pablo, Evolution of glassy gratings with variable aspect ratios under surface diffusion., *J. Chem. Phys.* **134** 194704. (2011).; DOI:10.1063/1.3573903

36. J. H. Mangalara, M. D. Marvin and D. S. Simmons, Three-Layer Model for the Emergence of Ultrastable Glasses from the Surfaces of Supercooled Liquids, *J. Phys. Chem. B* **120** 4861–4865. (2016).; DOI:10.1021/acs.jpcb.6b04736

37. Z. Shi, P. G. Debenedetti and F. H. Stillinger, Properties of model atomic free-standing thin films, *J. Chem. Phys.* **134** 114524. (2011).; DOI:10.1063/1.3565480

38. V. Lubchenko and P. G. Wolynes, Theory of Structural Glasses and Supercooled Liquids, *Annu. Rev. Phys. Chem.* **58** 235–266. (2007).; DOI:10.1146/annurev.physchem.58.032806.104653

39. J. D. Stevenson and P. G. Wolynes, On the surface of glasses., *J. Chem. Phys.* **129** 234514. (2008).; DOI:10.1063/1.3041651

40. S. Mirigian and K. S. Schweizer, Unified Theory of Activated Relaxation in Liquids over 14 Decades in Time, *J. Phys. Chem. Lett.* **4** 3648–3653. (2013).; DOI:10.1021/jz4018943

41. S. Mirigian and K. S. Schweizer, Theory of activated glassy relaxation, mobility gradients, surface diffusion, and vitrification in free standing thin films, *J. Chem. Phys.* **143** 244705. (2015).; DOI:10.1063/1.4937953

42. K. R. Whitaker, M. Tylinski, M. Ahrenberg, C. Schick and M. D. Ediger, Kinetic stability and heat capacity of vapor-deposited glasses of o-terphenyl, *J. Chem. Phys.* **143** 84511. (2015).; DOI:10.1063/1.4929511

43. K. L. Kearns, S. F. Swallen, M. D. Ediger, T. Wu, Y. Sun and L. Yu, Hiking down the energy landscape: progress toward the Kauzmann temperature via vapor deposition, *J. Phys. Chem. B* **112** 4934–4942. (2008).; DOI:10.1021/jp7113384

44. S. L. L. M. Ramos, M. Oguni, K. Ishii and H. Nakayama, Character of devitrification, viewed from enthalpic paths, of the vapor-deposited ethylbenzene glasses, *J. Phys. Chem. B* **115** 14327–32. (2011).; DOI:10.1021/jp203612s

45. K. R. Whitaker, M. Ahrenberg, C. Schick and M. D. Ediger, Vapor-deposited α,α,β-tris-naphthylbenzene glasses with low heat capacity and high kinetic stability., *J. Chem. Phys.* **137** 154502. (2012).; DOI:10.1063/1.4758807

46. Y. Z. Chua, M. Ahrenberg, M. Tylinski, M. D. Ediger and C. Schick, How much time is

needed to form a kinetically stable glass? AC calorimetric study of vapor-deposited glasses of ethylcyclohexane, *J. Chem. Phys.* **142** 54506. (2015).; DOI:10.1063/1.4906806

47. M. S. Beasley, Y. Z. Chua, M. Tylinski, C. Schick and M. D. Ediger, unpublished work for 1 pentene, triethyl phosphate, tripropyl phosphate and tributyl phosphate. (2016).

48. K. R. Whitaker, D. J. Scifo, M. D. Ediger, M. Ahrenberg and C. Schick, Highly stable glasses of cis-decalin and cis/trans-decalin mixtures, *J. Phys. Chem. B* **117** 12724–33. (2013).; DOI:10.1021/jp400960g

49. S. F. Swallen, K. Traynor, R. J. McMahon, M. D. Ediger and T. E. Mates, Stable Glass Transformation to Supercooled Liquid via Surface-Initiated Growth Front, *Phys. Rev. Lett.* **102** 65503. (2009).; DOI:10.1103/PhysRevLett.102.065503

50. A. Sepúlveda, S. F. Swallen, L. A. Kopff, R. J. McMahon and M. D. Ediger, Stable glasses of indomethacin and α,α,β-tris-naphthylbenzene transform into ordinary supercooled liquids, *J. Chem. Phys.* **137** 204508. (2012).; DOI:10.1063/1.4768168

51. S. S. Dalal and M. D. Ediger, Influence of substrate temperature on the transformation front velocities that determine thermal stability of vapor-deposited glasses, *J. Phys. Chem. B* **119** 3875–82. (2015).; DOI:10.1021/jp512905a

52. C. Rodríguez-Tinoco, M. Gonzalez-Silveira, J. Ràfols-Ribé, A. F. Lopeandía, M. T. Clavaguera-Mora and J. Rodríguez-Viejo, Evaluation of growth front velocity in ultrastable glasses of indomethacin over a wide temperature interval, *J. Phys. Chem. B* **118** 10795–10801. (2014).; DOI:10.1021/jp506782d

53. Z. Chen, A. Sepúlveda, M. D. Ediger and R. Richert, Dynamics of glass-forming liquids. XVI. Observation of ultrastable glass transformation via dielectric spectroscopy., *J. Chem. Phys.* **138** 12A519. (2013).; DOI:10.1063/1.4771695

54. M. Tylinski, A. Sepúlveda, D. M. Walters, Y. Z. Chua, C. Schick and M. D. Ediger, Vapor-deposited glasses of methyl-m-toluate: How uniform is stable glass transformation?, *J. Chem. Phys.* **143** 244509. (2015).; DOI:10.1063/1.4938420

55. S. Léonard and P. Harrowell, Macroscopic facilitation of glassy relaxation kinetics: ultrastable glass films with frontlike thermal response, *J. Chem. Phys.* **133** 244502. (2010).; DOI:10.1063/1.3511721

56. P. G. Wolynes, Spatiotemporal structures in aging and rejuvenating glasses, *Proc. Natl. Acad. Sci. U. S. A.* **106** 1353–8. (2009).; DOI:10.1073/pnas.0812418106

57. I. Lyubimov, M. D. Ediger and J. J. de Pablo, Model vapor-deposited glasses: growth front and composition effects, *J. Chem. Phys.* **139** 144505. (2013).; DOI:10.1063/1.4823769

58. A. Sepúlveda, S. F. Swallen and M. D. Ediger, Manipulating the properties of stable organic glasses using kinetic facilitation, *J. Chem. Phys.* **138** 12A517. (2013).; DOI:10.1063/1.4772594

59. I. Douglass and P. Harrowell, Can a stable glass be superheated? Modelling the kinetic stability of coated glassy films, *J. Chem. Phys.* **138** 12A516. (2013).; DOI:10.1063/1.4772480

60. K. L. Kearns, M. D. Ediger, H. Huth and C. Schick, One Micrometer Length Scale Controls Kinetic Stability of Low-Energy Glasses, *J. Phys. Chem. Lett.* **1** 388–392. (2010).; DOI:10.1021/jz9002179

61. A. Sepúlveda, M. Tylinski, A. Guiseppi-Elie, R. Richert and M. D. Ediger, Role of Fragility in the Formation of Highly Stable Organic Glasses, *Phys. Rev. Lett.* **113** 45901. (2014).; DOI:10.1103/PhysRevLett.113.045901

62. S. Capaccioli, K. L. Ngai, M. Paluch and D. Prevosto, Mechanism of fast surface self-diffusion of an organic glass, *Phys. Rev. E* **86** 51503. (2012).; DOI:10.1103/PhysRevE.86.051503

63. T. Hecksher, A. I. Nielsen, N. B. Olsen and J. C. Dyre, Little evidence for dynamic divergences in ultraviscous molecular liquids, *Nat. Phys.* **4** 737–741. (2008).; DOI:10.1038/nphys1033

64. H. Wagner and R. Richert, Dielectric relaxation of the electric field in poly(vinyl acetate): a time domain study in the range 10-3–106 s, *Polymer (Guildf).* **38** 255–261. (1997).; DOI:10.1016/S0032-3861(96)00524-1

65. J. Zhao and G. B. McKenna, Temperature divergence of the dynamics of a poly(vinyl acetate) glass: Dielectric vs. mechanical behaviors, *J. Chem. Phys.* **136** 154901. (2012).; DOI:10.1063/1.3701736

66. R. Richert, Comment on “Temperature divergence of the dynamics of a poly(vinyl acetate) glass: Dielectric vs. mechanical behaviors” [J. Chem. Phys. 136, 154901 (2012)],

J. Chem. Phys. **139** 137101. (2013).; DOI:10.1063/1.4823797

67. S. L. L. M. Ramos, A. K. Chigira and M. Oguni, Devitrification properties of vapor-deposited ethylcyclohexane glasses and interpretation of the molecular mechanism for formation of vapor-deposited glasses, *J. Phys. Chem. B* **119** 4076–4083. (2015).; DOI:10.1021/jp5109174

68. I. Saika-Voivod, F. Sciortino and P. H. Poole, Free energy and configurational entropy of liquid silica: Fragile-to-strong crossover and polyamorphism, *Phys. Rev. E* **69** 41503. (2004).; DOI:10.1103/PhysRevE.69.041503

69. D. V Matyushov and C. A. Angell, Gaussian excitations model for glass-former dynamics and thermodynamics., *J. Chem. Phys.* **126** 94501. (2007).; DOI:10.1063/1.2538712

70. I. Lyubimov, L. Antony, D. M. Walters, D. Rodney, M. D. Ediger and J. J. de Pablo, Orientational anisotropy in simulated vapor-deposited molecular glasses, *J. Chem. Phys.* **143** 94502. (2015).; DOI:10.1063/1.4928523

71. M. Ahrenberg, E. Shoifet, K. R. Whitaker, H. Huth, M. D. Ediger and C. Schick, Differential alternating current chip calorimeter for in situ investigation of vapor-deposited thin films, *Rev. Sci. Instrum.* **83** 33902. (2012).; DOI:10.1063/1.3692742

72. Xensor Integration - Calorimeter Chips, . (n.d.).; Retrieved from http://xensor.nl/index.php/products/calorimeter-chips

73. L. Zhu and L. Yu, Generality of forming stable organic glasses by vapor deposition, *Chem. Phys. Lett.* **499** 62–65. (2010).; DOI:10.1016/j.cplett.2010.09.010

74. L. Zhu, C. W. Brian, S. F. Swallen, P. T. Straus, M. D. Ediger and L. Yu, Surface Self-Diffusion of an Organic Glass, *Phys. Rev. Lett.* **106** 256103. (2011).; DOI:10.1103/PhysRevLett.106.256103

75. C. W. Brian and L. Yu, Surface self-diffusion of organic glasses, *J. Phys. Chem. A* **117** 13303–13309. (2013).; DOI:10.1021/jp404944s

76. S. Singh and J. J. de Pablo, A molecular view of vapor deposited glasses, *J. Chem. Phys.* **134** 194903. (2011).; DOI:10.1063/1.3586805

77. A. Wisitsorasak and P. G. Wolynes, Fluctuating mobility generation and transport in glasses, *Phys. Rev. E* **88** 22308. (2013).; DOI:10.1103/PhysRevE.88.022308

78. X. Xia and P. G. Wolynes, Fragilities of liquids predicted from the random first order transition theory of glasses, *Proc. Natl. Acad. Sci.* **97** 2990–2994. (2000).; DOI:10.1073/pnas.97.7.2990

79. H.-B. Yu, Y. Luo and K. Samwer, Ultrastable metallic glass., *Adv. Mater.* **25** 5904–8. (2013).; DOI:10.1002/adma.201302700

80. H. Nakayama, K. Omori, K. Ino-u-e and K. Ishii, Molar volumes of ethylcyclohexane and butyronitrile glasses resulting from vapor deposition: dependence on deposition temperature and comparison to alkylbenzenes., *J. Phys. Chem. B* **117** 10311–9. (2013).; DOI:10.1021/jp404256r

81. S. F. Swallen, K. L. Kearns, M. K. Mapes, Y. S. Kim, R. J. McMahon, M. D. Ediger, T. Wu, L. Yu and S. Satija, Organic glasses with exceptional thermodynamic and kinetic

stability, *Science* **315** 353–356. (2007).; DOI:10.1126/science.1135795

82. E. León-Gutierrez, G. Garcia, M. T. Clavaguera-Mora and J. Rodríguez-Viejo, Glass transition in vapor deposited thin films of toluene, *Thermochim. Acta* **492** 51–54. (2009).; DOI:10.1016/j.tca.2009.05.016

83. K. Ishii, H. Nakayama, S. Hirabayashi and R. Moriyama, Anomalously high-density glass of ethylbenzene prepared by vapor deposition at temperatures close to the glass-transition temperature, *Chem. Phys. Lett.* **459** 109–112. (2008).; DOI:10.1016/j.cplett.2008.05.050

84. K. Ishii, H. Nakayama, R. Moriyama and Y. Yokoyama, Behavior of Glass and Supercooled Liquid Alkylbenzenes Vapor-Deposited on Cold Substrates: Toward the Understanding of the Curious Light Scattering Observed in Some Supercooled Liquid States, *Bull. Chem. Soc. Jpn.* **82** 1240–1247. (2009).; DOI:10.1246/bcsj.82.1240

85. K. Dawson, L. Zhu, L. A. Kopff, R. J. McMahon, L. Yu and M. D. Ediger, Highly Stable Vapor-Deposited Glasses of Four Tris-naphthylbenzene Isomers, *J. Phys. Chem. Lett.* **2** 2683–2687. (2011).; DOI:10.1021/jz201174m

86. M. Ahrenberg, Y. Z. Chua, K. R. Whitaker, H. Huth, M. D. Ediger and C. Schick, In situ investigation of vapor-deposited glasses of toluene and ethylbenzene via alternating current chip-nanocalorimetry, *J. Chem. Phys.* **138** 24501. (2013).; DOI:10.1063/1.4773354

87. C. Rodríguez-Tinoco, M. Gonzalez-Silveira, J. Ràfols-Ribé, G. Garcia and J. Rodríguez-Viejo, Highly stable glasses of celecoxib: Influence on thermo-kinetic properties,

microstructure and response towards crystal growth, *J. Non. Cryst. Solids* **407** 256–261. (2014).; DOI:10.1016/j.jnoncrysol.2014.07.031

88. T. Liu, K. Cheng, E. Salami-Ranjbaran, F. Gao, C. Li, X. Tong, Y.-C. Lin, Y. Zhang, W. Zhang, L. Klinge, P. J. Walsh and Z. Fakhraai, The effect of chemical structure on the stability of physical vapor deposited glasses of 1,3,5-triarylbenzene, *J. Chem. Phys.* **143** 84506. (2015).; DOI:10.1063/1.4928521

89. D. M. Walters, R. Richert and M. D. Ediger, Thermal stability of vapor-deposited stable glasses of an organic semiconductor, *J. Chem. Phys.* **142** 134504. (2015).; DOI:10.1063/1.4916649

90. R. S. Smith, R. A. May and B. D. Kay, Probing Toluene and Ethylbenzene Stable Glass Formation Using Inert Gas Permeation, *J. Phys. Chem. Lett.* 3639–3644. (2015).; DOI:10.1021/acs.jpclett.5b01611

91. K. L. Kearns, K. R. Whitaker, M. D. Ediger, H. Huth and C. Schick, Observation of low heat capacities for vapor-deposited glasses of indomethacin as determined by AC nanocalorimetry, *J. Chem. Phys.* **133** 14702. (2010).; DOI:10.1063/1.3442416

92. R. L. Jack, L. O. Hedges, J. P. Garrahan and D. Chandler, Preparation and Relaxation of Very Stable Glassy States of a Simulated Liquid, *Phys. Rev. Lett.* **107** 275702. (2011).; DOI:10.1103/PhysRevLett.107.275702

93. G. M. Hocky, L. Berthier and D. R. Reichman, Equilibrium ultrastable glasses produced by random pinning, *J. Chem. Phys.* **141** 224503. (2014).; DOI:10.1063/1.4903200

94. D. Bhattacharya and V. Sadtchenko, Enthalpy and high temperature relaxation kinetics of stable vapor-deposited glasses of toluene, *J. Chem. Phys.* **141** 94502. (2014).; DOI:10.1063/1.4893716

95. H. Staley, E. Flenner and G. Szamel, Cooling-rate dependence of kinetic and mechanical stabilities of simulated glasses, *J. Chem. Phys.* **142** 244508. (2015).; DOI:10.1063/1.4922937

96. S. S. Dalal, Z. Fakhraai and M. D. Ediger, High-throughput ellipsometric characterization of vapor-deposited indomethacin glasses, *J. Phys. Chem. B* **117** 15415–25. (2013).; DOI:10.1021/jp405005n

97. K. Dawson, L. A. Kopff, L. Zhu, R. J. McMahon, L. Yu, R. Richert and M. D. Ediger, Molecular packing in highly stable glasses of vapor-deposited tris-naphthylbenzene isomers, *J. Chem. Phys.* **136** 94505. (2012).; DOI:10.1063/1.3686801

98. D. S. Ivanov and L. V. Zhigilei, Kinetic Limit of Heterogeneous Melting in Metals, *Phys. Rev. Lett.* **98** 195701. (2007).; DOI:10.1103/PhysRevLett.98.195701

99. R. Richert, Heterogeneous dynamics in liquids: fluctuations in space and time, *J. Phys. Condens. Matter* **14** R703–R738. (2002).; DOI:10.1088/0953-8984/14/23/201

100. A. I. Nielsen, T. Christensen, B. Jakobsen, K. Niss, N. B. Olsen, R. Richert and J. C. Dyre, Prevalence of approximate square root(t) relaxation for the dielectric alpha process in viscous organic liquids, *J. Chem. Phys.* **130** 154508. (2009).; DOI:10.1063/1.3098911

101. Z. Chen, Y. Zhao and L.-M. Wang, Enthalpy and dielectric relaxations in supercooled

methyl m-toluate, *J. Chem. Phys.* **130** 204515. (2009).; DOI:10.1063/1.3142142

102. N. O. Birge, Specific-heat spectroscopy of glycerol and propylene glycol near the glass transition, *Phys. Rev. B* **34** 1631–1642. (1986).; DOI:10.1103/PhysRevB.34.1631

103. Z. Chen and R. Richert, Dynamics of glass-forming liquids. XV. Dynamical features of molecular liquids that form ultra-stable glasses by vapor deposition, *J. Chem. Phys.* **135** 124515. (2011).; DOI:10.1063/1.3643332

104. S. S. Dalal and M. D. Ediger, Molecular Orientation in Stable Glasses of Indomethacin, *J. Phys. Chem. Lett.* **3** 1229–1233. (2012).; DOI:10.1021/jz3003266

105. S. S. Dalal, A. Sepúlveda, G. K. Pribil, Z. Fakhraai and M. D. Ediger, Density and birefringence of a highly stable α,α,β-trisnaphthylbenzene glass, *J. Chem. Phys.* **136** 204501. (2012).; DOI:10.1063/1.4719532

106. M. Goldstein, Viscous liquids and the glass transition. V. Sources of the excess specific heat of the liquid, *J. Chem. Phys.* **64** 4767. (1976).; DOI:10.1063/1.432063

107. H. B. Yu, M. Tylinski, A. Guiseppi-Elie, M. D. Ediger and R. Richert, Suppression of β relaxation in vapor -deposited ultrastable glasses, *Phys. Rev. Lett.* (2015).

108. A. Sepúlveda, E. Leon-Gutierrez, M. Gonzalez-Silveira, C. Rodríguez-Tinoco, M. T. Clavaguera-Mora and J. Rodríguez-Viejo, Accelerated Aging in Ultrathin Films of a Molecular Glass Former, *Phys. Rev. Lett.* **107** 25901. (2011).; DOI:10.1103/PhysRevLett.107.025901

109. V. Lubchenko and P. G. Wolynes, Theory of aging in structural glasses, *J. Chem. Phys.* **121** 2852–65. (2004).; DOI:10.1063/1.1771633

110. Y. Z. Chua, M. Tylinski, S. Tatsumi, M. D. Ediger and C. Schick, Glass transition and stable glass formation of tetrachloromethane, *J. Chem. Phys.* **144** 244503. (2016).; DOI:10.1063/1.4954665

111. J. Helfferich, I. Lyubimov, D. Reid and J. J. de Pablo, Inherent structure energy is a good indicator of molecular mobility in glasses, *Soft Matter* **12** 5898–5904. (2016).; DOI:10.1039/C6SM00810K

112. S. Capponi, S. Napolitano and M. Wübbenhorst, Supercooled liquids with enhanced orientational order., *Nat. Commun.* **3** 1233. (2012).; DOI:10.1038/ncomms2228

113. A. Kasina, T. Putzeys and M. Wübbenhorst, Dielectric and specific heat relaxations in vapor deposited glycerol, *J. Chem. Phys.* **143** 244504. (2015).; DOI:10.1063/1.4937795

114. A. Sepúlveda, E. Leon-Gutierrez, M. Gonzalez-Silveira, C. Rodríguez-Tinoco, M. T. Clavaguera-Mora and J. Rodríguez-Viejo, Glass transition in ultrathin films of amorphous solid water., *J. Chem. Phys.* **137** 244506. (2012).; DOI:10.1063/1.4771964

115. C. A. Angell, On the uncertain distinction between fast landscape exploration and second amorphous phase (ideal glass) interpretations of the ultrastable glass phenomenon, *J. Non. Cryst. Solids* **407** 246–255. (2014).; DOI:10.1016/j.jnoncrysol.2014.08.044

116. R. Souda, Structural Relaxation of Vapor-Deposited Water, Methanol, Ethanol, and 1-Propanol Films Studied Using Low-Energy Ion Scattering, *J. Phys. Chem. B* **114** 11127–

11132. (2010).; DOI:10.1021/jp104523h

117. H. Huth, L.-M. Wang, C. Schick and R. Richert, Comparing calorimetric and dielectric polarization modes in viscous 2-ethyl-1-hexanol., *J. Chem. Phys.* **126** 104503. (2007).; DOI:10.1063/1.2539105

118. R. Brand, P. Lunkenheimer, U. Schneider and A. Loidl, Excess wing in the dielectric loss of glass-forming ethanol: A relaxation process, *Phys. Rev. B* **62** 8878–8883. (2000).; DOI:10.1103/PhysRevB.62.8878

119. C. Hansen, F. Stickel, T. Berger, R. Richert and E. W. Fischer, Dynamics of glass-forming liquids. III. Comparing the dielectric α- and β-relaxation of 1-propanol and o-terphenyl, *J. Chem. Phys.* **107** 1086. (1997).; DOI:10.1063/1.474456

120. C. León, K. L. Ngai and C. M. Roland, Relationship between the primary and secondary dielectric relaxation processes in propylene glycol and its oligomers, *J. Chem. Phys.* **110** 11585. (1999).; DOI:10.1063/1.478006

121. A. Huwe, F. Kremer, P. Behrens and W. Schwieger, Molecular Dynamics in Confining Space: From the Single Molecule to the Liquid State, *Phys. Rev. Lett.* **82** 2338–2341. (1999).; DOI:10.1103/PhysRevLett.82.2338

122. C. L. Jackson and G. B. McKenna, The glass transition of organic liquids confined to small pores, *J. Non. Cryst. Solids* **131**–**133** 221–224. (1991).; DOI:10.1016/0022-3093(91)90305-P

123. C. L. Jackson and G. B. McKenna, Vitrification and Crystallization of Organic Liquids

Confined to Nanoscale Pores, *Chem. Mater.* **8** 2128–2137. (1996).; DOI:10.1021/cm9601188

124. A. Mandanici, W. Huang, M. Cutroni and R. Richert, Dynamics of glass-forming liquids. XII. Dielectric study of primary and secondary relaxations in ethylcyclohexane., *J. Chem. Phys.* **128** 124505. (2008).; DOI:10.1063/1.2844797

125. A. Gierer and K. Wirtz, Molekulare Theorie der Mikroreibung, *Zeitschrift für Naturforsch. A* **8** 532–538. (1953).; DOI:10.1515/zna-1953-0903

126. E. Hill, Nora, Theoretical Treatment of Permitivity and Loss, *Dielectr. Prop. Mol. Behav.* 1–106. (1969), London: Van Nostrand Reinhold Companty Ltd.

127. F. Stickel, E. W. Fischer and R. Richert, Dynamics of glass-forming liquids. I. Temperature-derivative analysis of dielectric relaxation data, *J. Chem. Phys.* **102** 6251. (1995).; DOI:10.1063/1.469071

128. F. Stickel, E. W. Fischer and R. Richert, Dynamics of glass-forming liquids. II. Detailed comparison of dielectric relaxation, dc-conductivity, and viscosity data, *J. Chem. Phys.* **104** 2043. (1996).; DOI:10.1063/1.470961

129. G. S. Fulcher, Analysis of Recent Measurements of the Viscosity of Glasses, *J. Am. Ceram. Soc.* **8** 339–355. (1925).; DOI:10.1111/j.1151-2916.1925.tb16731.x

130. L. Zhu, C. W. Brian, S. F. Swallen, P. T. Straus, M. D. Ediger and L. Yu, Surface Self-Diffusion of an Organic Glass, *Phys. Rev. Lett.* **106** 256103. (2011).; DOI:10.1103/PhysRevLett.106.256103

131. S. Butler and P. Harrowell, Glassy relaxation at surfaces: The correlation length of cooperative motion in the facilitated kinetic Ising model, *J. Chem. Phys.* **95** 4466. (1991).; DOI:10.1063/1.461769

132. V. V. Hoang and T. Q. Dong, Free surface effects on thermodynamics and glass formation in simple monatomic supercooled liquids, *Phys. Rev. B* **84** 174204. (2011).; DOI:10.1103/PhysRevB.84.174204

133. K. L. Kearns, S. F. Swallen, M. D. Ediger, T. Wu and L. Yu, Influence of substrate temperature on the stability of glasses prepared by vapor deposition., *J. Chem. Phys.* **127** 154702. (2007).; DOI:10.1063/1.2789438

134. S. Ruan, W. Zhang, Y. Sun, M. D. Ediger and L. Yu, Surface Diffusion and Surface Crystal Growth of tris-Napthyl Benzene Glasses, *J. Chem. Phys.* **145** 64503. (2016).; DOI:10.1063/1.4960301

135. P. Sillrén, J. Bielecki, J. Mattsson, L. Börjesson and A. Matic, A statistical model of hydrogen bond networks in liquid alcohols, *J. Chem. Phys.* **136** 94514. (2012).; DOI:10.1063/1.3690137

136. J. Swenson, I. Köper and M. T. F. Telling, Dynamics of propylene glycol and its 7-mer by neutron scattering, *J. Chem. Phys.* **116** 5073. (2002).; DOI:10.1063/1.1453400

137. R. Bergman, C. Svanberg, D. Andersson, A. Brodin and L. M. Torell, Relaxational and vibrational dynamics of poly(propylene glycol), *J. Non. Cryst. Solids* **235** 225–228. (1998).; DOI:10.1016/S0022-3093(98)00638-3

138. L. Saiz, J. A. Padró and E. Guàrdia, Structure of liquid ethylene glycol: A molecular dynamics simulation study with different force fields, *J. Chem. Phys.* **114** 3187. (2001).; DOI:10.1063/1.1340605

139. A. Kaiser, O. Ismailova, A. Koskela, S. E. Huber, M. Ritter, B. Cosenza, W. Benger, R. Nazmutdinov and M. Probst, Ethylene glycol revisited: Molecular dynamics simulations and visualization of the liquid and its hydrogen-bond network, *J. Mol. Liq.* **189** 20–29. (2014).; DOI:10.1016/j.molliq.2013.05.033

140. D. K. Belashchenko, M. N. Rodnikova, N. K. Balabaev and I. A. Solonina, Investigating hydrogen bonds in liquid ethylene glycol structure by means of molecular dynamics, *Russ. J. Phys. Chem. A* **88** 94–102. (2014).; DOI:10.1134/S0036024414010063

141. R. Böhmer, C. Gainaru and R. Richert, Structure and dynamics of monohydroxy alcohols—Milestones towards their microscopic understanding, 100 years after Debye, *Phys. Rep.* **545** 125–195. (2014).; DOI:10.1016/j.physrep.2014.07.005

142. K. S. Vahvaselkä, R. Serimaa and M. Torkkeli, Determination of Liquid Structures of the Primary Alcohols Methanol, Ethanol, 1-Propanol, 1-Butanol and 1-Octanol by X-ray Scattering, *J. Appl. Crystallogr.* **28** 189–195. (1995).; DOI:10.1107/S0021889894010149

143. D. Fragiadakis, C. M. Roland and R. Casalini, Insights on the origin of the Debye process in monoalcohols from dielectric spectroscopy under extreme pressure conditions, *J. Chem. Phys.* **132** 144505. (2010).; DOI:10.1063/1.3374820

144. L. P. Singh, A. Raihane, C. Alba-Simionesco and R. Richert, Dopant effects on 2-ethyl-1-

hexanol: A dual-channel impedance spectroscopy and neutron scattering study, *J. Chem. Phys.* **142** 14501. (2015).; DOI:10.1063/1.4904908

145. A. Vrhovsek, O. Gereben, A. Jamnik and L. Pusztai, Hydrogen bonding and molecular aggregates in liquid methanol, ethanol, and 1-propanol, *J. Phys. Chem. B* **115** 13473–13488. (2011).; DOI:10.1021/jp206665w

146. M. P. Balanay, D. H. Kim and H. Fan, Revisiting the formation of cyclic clusters in liquid ethanol, *J. Chem. Phys.* **144** 154302. (2016).; DOI:10.1063/1.4945809

147. P. Bezot, C. Brot and G. M. Searby, Light scattering evidence for fast relaxation of hydrogen-bonded structures in liquid benzyl alcohol, *Chem. Phys.* **31** 363–367. (1978).; DOI:10.1016/0301-0104(78)85129-5

148. M. Huelsekopf and R. Ludwig, Temperature dependence of hydrogen bonding in alcohols, *J. Mol. Liq.* **85** 105–125. (2000).; DOI:10.1016/S0167-7322(99)00168-3

149. A. Mikusińska-Planner, Structure of liquid benzyl alcohol at 293 K, *Acta Crystallogr. Sect. B Struct. Sci.* **48** 37–41. (1992).; DOI:10.1107/S0108768191010972

150. D. A. Prystupa, A. Anderson and B. H. Torrie, Raman and infrared study of solid benzyl alcohol, *J. Raman Spectrosc.* **25** 175–182. (1994).; DOI:10.1002/jrs.1250250206

151. R. P. Singh and C. P. Sinha, Viscosities and activation energies of viscous flow of the ternary mixtures of toluene, chlorobenzene, 1-hexanol, and benzyl alcohol, *J. Chem. Eng. Data* **30** 470–474. (1985).; DOI:10.1021/je00042a031

152. P. S. Nikam and S. J. Kharat, Densities and Viscosities of Binary Mixtures of N , N - Dimethylformamide with Benzyl Alcohol and Acetophenone at (298.15, 303.15, 308.15, and 313.15) K, *J. Chem. Eng. Data* **48** 1291–1295. (2003).; DOI:10.1021/je030163d

153. J. N. Nayak, M. I. Aralaguppi and T. M. Aminabhavi, Density, Viscosity, Refractive Index, and Speed of Sound in the Binary Mixtures of Ethyl Chloroacetate + Cyclohexanone, + Chlorobenzene, + Bromobenzene, or + Benzyl Alcohol at (298.15, 303.15, and 308.15) K, *J. Chem. Eng. Data* **48** 628–631. (2003).; DOI:10.1021/je0201828

154. A. Mandanici, W. Huang, M. Cutroni and R. Richert, On the features of the dielectric response of supercooled ethylcyclohexane, *Philos. Mag.* **88** 3961–3971. (2008).; DOI:10.1080/14786430802537753

155. M. R. Carpenter, D. B. Davies and A. J. Matheson, Measurement of the Glass-Transition Temperature of Simple Liquids, *J. Chem. Phys.* **46** 2451. (1967).; DOI:10.1063/1.1841068

156. R. Richert, On the dielectric susceptibility spectra of supercooled o-terphenyl., *J. Chem. Phys.* **123** 154502. (2005).; DOI:10.1063/1.2064667

157. R. Richert and C. A. Angell, Dynamics of glass-forming liquids. V. On the link between molecular dynamics and configurational entropy, *J. Chem. Phys.* **108** 9016. (1998).; DOI:10.1063/1.476348

158. Z. Wojnarowska, K. Adrjanowicz, P. Wlodarczyk, E. Kaminska, K. Kaminski, K. Grzybowska, R. Wrzalik, M. Paluch and K. L. Ngai, Broadband dielectric relaxation study at ambient and elevated pressure of molecular dynamics of pharmaceutical:

indomethacin., *J. Phys. Chem. B* **113** 12536–45. (2009).; DOI:10.1021/jp905162r

159. J. A. Baird, D. Santiago-Quinonez, C. Rinaldi and L. S. Taylor, Role of viscosity in influencing the glass-forming ability of organic molecules from the undercooled melt state., *Pharm. Res.* **29** 271–84. (2012).; DOI:10.1007/s11095-011-0540-4

160. R. Richert, K. Duvvuri and L.-T. Duong, Dynamics of glass-forming liquids. VII. Dielectric relaxation of supercooled tris-naphthylbenzene, squalane, and decahydroisoquinoline, *J. Chem. Phys.* **118** 1828–1836. (2003).; DOI:10.1063/1.1531587

161. D. J. Plazek, Physical Properties of Aromatic Hydrocarbons. I. Viscous and Viscoelastic Behavior of 1:3:5-Tri-α-Naphthyl Benzene, *J. Chem. Phys.* **45** 3038. (1966).; DOI:10.1063/1.1728059

162. A. J. Barlow, J. Lamb and A. J. Matheson, Viscous Behaviour of Supercooled Liquids, *Proc. R. Soc. A Math. Phys. Eng. Sci.* **292** 322–342. (1966).; DOI:10.1098/rspa.1966.0138

163. A. Kudlik, C. Tschirwitz, T. Blochowicz, S. Benkhof and E. Rössler, Slow secondary relaxation in simple glass formers, *J. Non. Cryst. Solids* **235**–**237** 406–411. (1998).; DOI:10.1016/S0022-3093(98)00510-9

164. E. Rössler and H. Sillescu, 2H NMR Study of supercooled toluene, *Chem. Phys. Lett.* **112** 94–98. (1984).; DOI:10.1016/0009-2614(84)87048-7

165. J. L. Green, K. Ito, K. Xu and C. A. Angell, Fragility in Liquids and Polymers: New, Simple Quantifications and Interpretations, *J. Phys. Chem. B* **103** 3991–3996. (1999).; DOI:10.1021/jp983927i

166. G. B. McKenna and J. Zhao, Accumulating evidence for non-diverging time-scales in glass-forming fluids, *J. Non. Cryst. Solids* **407** 3–13. (2015).; DOI:10.1016/j.jnoncrysol.2014.08.012

167. H. Wagner and R. Richert, Dielectric relaxation of the electric field in poly(vinyl acetate): a time domain study in the range 10^{-3}–10^{6} s, *Polymer* **38** 255–261. (1997).; DOI:10.1016/S0032-3861(96)00524-1

168. H. Hikawa, M. Oguni and H. Suga, Construction of an adiabatic calorimeter for a vapor-deposited sample and thermal characterization of amorphous butyronitrile, *J. Non. Cryst. Solids* **101** 90–100. (1988).; DOI:10.1016/0022-3093(88)90373-0

169. K. Takeda, O. Yamamuro, M. Oguni and H. Suga, Calorimetric Study on Structural Relaxation of 1-Pentene in Vapor-Deposited and Liquid-Quenched Glassy States, *J. Phys. Chem.* **99** 1602–1607. (1995).; DOI:10.1021/j100005a035

170. M. D. Ediger and J. A. Forrest, Dynamics near Free Surfaces and the Glass Transition in Thin Polymer Films: A View to the Future, *Macromolecules* **47** 471–478. (2014).; DOI:10.1021/ma4017696

171. C. B. Roth and J. R. Dutcher, Glass transition and chain mobility in thin polymer films, *J. Electroanal. Chem.* **584** 13–22. (2005).; DOI:10.1016/j.jelechem.2004.03.003

172. X. Li and G. B. McKenna, Ultrathin Polymer Films: Rubbery Stiffening, Fragility, and Tg Reduction, *Macromolecules* **48** 6329–6336. (2015).; DOI:10.1021/acs.macromol.5b01263

173. E. C. Glor, R. J. Composto and Z. Fakhraai, Glass Transition Dynamics and Fragility of

Ultrathin Miscible Polymer Blend Films, *Macromolecules* **48** 6682–6689. (2015).; DOI:10.1021/acs.macromol.5b00979

174. J. L. Keddie, R. A. L. Jones and R. A. Cory, Size-Dependent Depression of the Glass Transition Temperature in Polymer Films, *Europhys. Lett.* **27** 59–64. (1994).; DOI:10.1209/0295-5075/27/1/011

175. G. Reiter, Mobility of Polymers in Films Thinner than Their Unperturbed Size, *Europhys. Lett.* **23** 579–584. (1993).; DOI:10.1209/0295-5075/23/8/007

176. J. A. Forrest, K. Dalnoki-Veress and J. R. Dutcher, Interface and chain confinement effects on the glass transition temperature of thin polymer films, *Phys. Rev. E* **56** 5705–5716. (1997).; DOI:10.1103/PhysRevE.56.5705

177. D. Qi, M. Ilton and J. A. Forrest, Measuring surface and bulk relaxation in glassy polymers, *Eur. Phys. J. E* **34** 56. (2011).; DOI:10.1140/epje/i2011-11056-1

178. M. Hasebe, D. Musumeci and L. Yu, Fast Surface Crystallization of Molecular Glasses: Creation of Depletion Zones by Surface Diffusion and Crystallization Flux, *J. Phys. Chem. B* **119** 3304–3311. (2015).; DOI:10.1021/jp512400c

179. K. Ishii and H. Nakayama, Structural relaxation of vapor-deposited molecular glasses and supercooled liquids., *Phys. Chem. Chem. Phys.* **16** 12073–12092. (2014).; DOI:10.1039/c4cp00458b

180. J. A. Torres, P. F. Nealey and J. J. De Pablo, Molecular Simulation of Ultrathin Polymeric Films near the Glass Transition, *Phys. Rev. Lett.* **85** 3221–3224. (2000).;

DOI:10.1103/PhysRevLett.85.3221

181. A. Shavit and R. A. Riggleman, Physical Aging, the Local Dynamics of Glass-Forming Polymers under Nanoscale Confinement, *J. Phys. Chem. B* **118** 9096–9103. (2014).; DOI:10.1021/jp502952n

182. P. Z. Hanakata, J. F. Douglas and F. W. Starr, Local variation of fragility and glass transition temperature of ultra-thin supported polymer films, *J. Chem. Phys.* **137** 244901. (2012).; DOI:10.1063/1.4772402

183. S. Peter, H. Meyer and J. Baschnagel, Thickness-dependent reduction of the glass-transition temperature in thin polymer films with a free surface, *J. Polym. Sci. Part B Polym. Phys.* **44** 2951–2967. (2006).; DOI:10.1002/polb.20924

184. P. Scheidler, W. Kob, K. Binder and G. Parisi, Growing length scales in a supercooled liquid close to an interface, *Philos. Mag. Part B* **82** 283–290. (2002).; DOI:10.1080/13642810208221307

185. J.-L. Barrat, J. Baschnagel and A. Lyulin, Molecular dynamics simulations of glassy polymers, *Soft Matter* **6** 3430–3446. (2010).; DOI:10.1039/b927044b

186. R. P. White, C. C. Price and J. E. G. Lipson, Effect of Interfaces on the Glass Transition of Supported and Freestanding Polymer Thin Films, *Macromolecules* **48** 4132–4141. (2015).; DOI:10.1021/acs.macromol.5b00510

187. E. Leon-Gutierrez, A. Sepúlveda, G. Garcia, M. T. Clavaguera-Mora and J. Rodríguez-Viejo, Stability of thin film glasses of toluene and ethylbenzene formed by vapor

deposition: an in situ nanocalorimetric study., *Phys. Chem. Chem. Phys.* **12** 14693–14698. (2010).; DOI:10.1039/c0cp00208a

188. E. A. Di Marzio and A. J. M. Yang, Configurational Entropy Approach to the Kinetics of Glasses, *J. Res. Natl. Inst. Stand. Technol.* **102** 135–157. (1997).; DOI:10.6028/jres.102.011

189. P. A. O'Connell and G. B. McKenna, Arrhenius-type temperature dependence of the segmental relaxation below Tg, *J. Chem. Phys.* **110** 11054. (1999).; DOI:10.1063/1.479046

190. J. P. Garrahan and D. Chandler, Coarse-grained microscopic model of glass formers., *Proc. Natl. Acad. Sci. U. S. A.* **100** 9710–9714. (2003).; DOI:10.1073/pnas.1233719100

191. J. Zhao, S. L. Simon and G. B. McKenna, Using 20-million-year-old amber to test the super-Arrhenius behaviour of glass-forming systems, *Nat. Commun.* **4** 1783. (2013).; DOI:10.1038/ncomms2809

192. H. Huth, L.-M. Wang, C. Schick and R. Richert, Comparing calorimetric and dielectric polarization modes in viscous 2-ethyl-1-hexanol, *J. Chem. Phys.* **126** 104503. (2007).; DOI:10.1063/1.2539105

193. A. Mandanici, W. Huang, M. Cutroni and R. Richert, On the features of the dielectric response of supercooled ethylcyclohexane, *Philos. Mag.* **88** 3961–3971. (2008).; DOI:10.1080/14786430802537753

194. Z. Fakhraai and J. A. Forrest, Probing Slow Dynamics in Supported Thin Polymer Films,

Phys. Rev. Lett. **95** 25701. (2005).; DOI:10.1103/PhysRevLett.95.025701

195. Y. Zhang, E. C. Glor, M. Li, T. Liu, K. Wahid, W. Zhang, R. A. Riggleman and Z. Fakhraai, Long-range correlated dynamics in ultra-thin molecular glass films, *J. Chem. Phys.* **145** 114502. (2016).; DOI:10.1063/1.4962734

196. K. Paeng, S. F. Swallen and M. D. Ediger, Direct Measurement of Molecular Motion in Freestanding Polystyrene Thin Films, *J. Am. Chem. Soc.* **133** 8444–8447. (2011).; DOI:10.1021/ja2022834

197. E. C. Glor and Z. Fakhraai, Facilitation of interfacial dynamics in entangled polymer films, *J. Chem. Phys.* **141** 194505. (2014).; DOI:10.1063/1.4901512

198. L. Berthier, G. Biroli, J.-P. Bouchaud, L. Cipelletti, D. El Masri, D. L'Hôte, F. Ladieu and M. Pierno, Direct Experimental Evidence of a Growing Length Scale Accompanying the Glass Transition, *Science* **310** 1797–1800. (2005).; DOI:10.1126/science.1120714

199. C. Dalle-Ferrier, C. Thibierge, C. Alba-Simionesco, L. Berthier, G. Biroli, J.-P. Bouchaud, F. Ladieu, D. L'Hôte and G. Tarjus, Spatial correlations in the dynamics of glassforming liquids: Experimental determination of their temperature dependence, *Phys. Rev. E* **76** 41510. (2007).; DOI:10.1103/PhysRevE.76.041510

200. A. Cavagna, Supercooled liquids for pedestrians, *Phys. Rep.* **476** 51–124. (2009).; DOI:10.1016/j.physrep.2009.03.003

201. A. Laventure, A. Gujral, O. Lebel, C. Pellerin and M. D. Ediger, Influence of Hydrogen Bonding on the Kinetic Stability of Vapor-Deposited Glasses of Triazine Derivatives,

Prep. (2016).

202. G. P. Johari and W. Dannhauser, Dielectric properties of isomeric phenyl propanols, *Phys. Chem. Liq.* **3** 1–11. (1972).; DOI:10.1080/00319107208084084

203. G. P. Johari, O. E. Kalinovskaya and J. K. Vij, Effects of induced steric hindrance on the dielectric behavior and H bonding in the supercooled liquid and vitreous alcohol, *J. Chem. Phys.* **114** 4634. (2001).; DOI:10.1063/1.1346635

204. O. E. Kalinovskaya, J. K. Vij and G. P. Johari, Mechanism of the Major Orientation Polarization in Alcohols, and the Effects of Steric Hindrance-, and Dilution-Induced Decrease on H-Bonding, *J. Phys. Chem. A* **105** 5061–5070. (2001).; DOI:10.1021/JP0040695

205. R. Böhmer, C. Gainaru and R. Richert, Structure and dynamics of monohydroxy alcohols—Milestones towards their microscopic understanding, 100 years after Debye, *Phys. Rep.* **545** 125–195. (2014).; DOI:10.1016/j.physrep.2014.07.005

206. Z. Rappoport, *CRC Handbook of tables for Organic Compound Identification* 3rd ed. (1967), Boca Raton, Florida: CRC Press Inc.

207. J. Buckingham and C. M. Cooper (Eds.), *Dictionary of Organic Compounds 5th Edition 2nd Supplement* 5th ed. (1984), New York: Chapman and Hall.

208. A. Laventure, G. De Grandpré, A. Soldera, O. Lebel and C. Pellerin, Unraveling the interplay between hydrogen bonding and rotational energy barrier to fine-tune the properties of triazine molecular glasses, *Phys. Chem. Chem. Phys.* **18** 1681–1692. (2016).;

DOI:10.1039/C5CP06630A

209. A. Bondi and D. J. Simkin, On the Hydrogen Bond Contribution to the Heat of Vaporization of Aliphatic Alcohols, *J. Chem. Phys.* **25** 1073. (1956).; DOI:10.1063/1.1743102

210. A. Bondi and D. J. Simkin, Heats of vaporization of hydrogen-bonded substances, *AIChE J.* **3** 473–479. (1957).; DOI:10.1002/aic.690030410

211. M. Preuß, C. Gainaru, T. Hecksher, S. Bauer, J. C. Dyre, R. Richert and R. Böhmer, Experimental studies of Debye-like process and structural relaxation in mixtures of 2-ethyl-1-hexanol and 2-ethyl-1-hexyl bromide, *J. Chem. Phys.* **137** 144502. (2012).; DOI:10.1063/1.4755754

212. W. Zhang and L. Yu, Surface Diffusion of Polymer Glasses. (2016).

213. C. A. Angell, Entropy and Fragility in Supercooling Liquids., *J. Res. Natl. Inst. Stand. Technol.* **102** 171–185. (1997).; DOI:10.6028/jres.102.013

214. H. Tanaka, Relation between Thermodynamics and Kinetics of Glass-Forming Liquids, *Phys. Rev. Lett.* **90** 55701. (2003).; DOI:10.1103/PhysRevLett.90.055701

215. K. Duvvuri and R. Richert, Dynamics of glass-forming liquids. VI. Dielectric relaxation study of neat decahydro-naphthalene, *J. Chem. Phys.* **117** 4414. (2002).; DOI:10.1063/1.1497158